DOCTOR OF PHILOSOPHY

Establishing and Maintaining Cortical Asymmetry in Drosophila Neural Stem Cells

Hannaford, Matthew

Award date:
2017

Establishing and Maintaining Cortical Asymmetry in *Drosophila* Neural Stem Cells

Matthew Hannaford

Supervisor: Dr. Jens Januschke

Division of Cell and Developmental Biology

Submitted for the degree of Doctor of Philosophy

School of Life Sciences

University of Dundee

August 2017

Contents

List of Figures

List of tables

Abbreviations

A/P	Anterior/Posterior
aa	amino acid
ACD	Asymmetric Cell Division
aPAR	Anterior Par complex
aPKC	atypical protein kinase C
ATP	Adenosine Tri-Phosphate
BAC	Bacterial artificial chromosome
Baz	Bazooka
BDM	2,3-Butanedione monoxime
BH	Basic and Hydrophobic
Brat	Brain tumour
CBD	Cargo Binding Domain
CNS	Central Nervous System
C. elegans	*Caenorhabditis elegans*
DAMID	DNA adenine methyltransferase idenitifcation
D-Box	Destruction Box
DNA	Deoxyribonucleic acid
Dpn	Deadpan
Egl	Egg laying failure
F-actin	Filamentous Actin
Flfl	Falafel
FRAP	Fluorescence Recovery after Photobleaching
GBP	GFP binding protein
GFP	Green Fluorescent Protein
GLC	Germ line clone
GMC	Ganglion Mother Cell
hph	hours post hatching
HSC	Hematopoietic Stem Cell
IPC	Intermediate Progenitor Cell
Jar	Jaguar - Myosin VI
Lat-A	Latrunculin A
Lgl	Lethal Giant Larvae
MARCM	Mosaic Analysis with a repressible cell marker
MaSC	Mammary Stem Cell
Mira	Miranda
MLCK	Myosin Light Chain Kinase
MLCP	Myosin Light Chain Phosphatase
MRLC	Myosin Regulatory Light Chain
mRNA	Messenger Ribonucleic Acid
MS	Mammosphere
Mts	Microtubule Star - PP2A subunit
NB	Neuroblast
NEB	Nuclear Envelope Breakdown
NLS	Nuclear Localisation Signal
PAR	Partitioning defective
PBS	Phosphate buffered saline
PCR	Polymerase Chain Reaction
P-Granules	Polar Granules
PI	Phospho-inositide
Pins	Partner of Inscuteable
PM	Plasma Membrane
Pon	Partner of numb
PP4	Protein Phosphatase 4
pPAR	Posterior Par complex.
Pros	Prospero
PTPA	Phospho-tyrosol phosphatase activator
RHAMM	receptor for hyaluronan-mediated motility
RNAi	Ribonucleic acid interference
Rock	Rho Kinase
rod	rough deal
ROI	Region of Interest
Sqh	Spaghetti Squash - Myosin regulatory light chain
Stau	Staufen
Tws	Twins - PP2A subunit
VNC	Ventral Nerve Cord
WT	Wild type
Zip	Zipper - Myosin II

Declaration

I declare that I am the author of the thesis; that all references cited have been consulted by me; that the work of which the thesis is a record has been done by me alone or in collaboration with researchers named in the text. This work has not been previously accepted for a higher degree.

Some data in this thesis can has been published in the following articles:

Ramat, A., Hannaford, M. and Januschke, J. (2017). Maintenance of Miranda Localization in Drosophila Neuroblasts Involves Interaction with the Cognate mRNA. *Curr Biol*.

Hannaford, M., Ramat, A., Loyer, N. and Januschke, J. (2017). aPKC-mediated displacement and actomyosin-mediated retention polarize Miranda in Drosophila neuroblasts. *BioRxiv*. doi: 10.1101/148213

Matthew Hannaford

Acknowledgements

I would like to thank my supervisor Dr. Jens Januschke for allowing me to undertake my PhD project in his lab. I am particularly grateful for the discussions we had that drove the project forward, as well as his patience when things inevitably went awry. I hope I can do his training justice as I move forward in my scientific career.

Furthermore, I would like to thank the rest of the JJ Lab, Dr. Anne Ramat and Dr. Nicolas Loyer for their helpful advice and assistance as well as mindless chatter over a coffee.

Throughout the project my fellow members of the division of cell and developmental biology have been extremely helpful, both in providing advice, feedback, aliquots of antibodies and making the lab a fun place to work. Particularly I would like to thank the members of the Muller lab and members of the Storey lab who have shared the lab with us. I would also like to thank my Thesis committee, Prof. Jason Swedlow and Prof. Tracy Palmer for their advice both throughout the project, and on my future career.

Much of this work would not have been possible without all those who have shared reagents and fly stocks with us throughout the *Drosophila* community and beyond, they are referred to individually in the appropriate sections of this thesis. Furthermore, I would like to acknowledge the Dundee imaging facility and the Central technical services for their help.

Finally I would like to thank the Medical Research Council and the University of Dundee for funding my studentship which allowed me to undertake this work.

Summary

The asymmetric segregation of fate determinants is a conserved process by which differential cell fate can be acquired upon cell division. In this thesis we investigate how the asymmetric localisation of fate determinants is achieved in *Drosophila* neuroblasts (NBs, Neural Stem Cells). In particular we focus on the localisation of the fate determinant Miranda, which is segregated to the basal pole of the NB cell cortex in mitosis and carries a series of signalling molecules into one of the two daughter cells, promoting differentiation. The most widely accepted model for how Miranda becomes polarised at mitosis is based on its phosphorylation by the apically localised kinase, aPKC (atypical protein kinase C). This model proposes that aPKC localises to the apical cortex and phosphorylates Miranda, excluding it from the apical domain by phosphorylation of Miranda's membrane binding motif. However, earlier work demonstrated that the acto-myosin cell cortex is essential for asymmetric Miranda localisation. Thus far these two models have not been successfully integrated.

In this thesis we generated flies carrying fluorescent reporters for apical and basal polarity proteins and imaged their localisation live. We reveal that localisation appears to happen in two stages. Firstly, Miranda is localised uniformly to the plasma membrane, from where it is cleared by aPKC at the onset of prophase in an actin independent manner. After NEB, Miranda returns to the cell cortex, localising to a basal crescent in an acto-myosin dependent manner. Furthermore, the size of the basal domain to which Miranda localises appears to be under the control of Rho kinase, and linked to cell size asymmetry. Together these data suggest that in mitosis, Miranda localisation is under structural control.

Therefore, we reveal that aPKC and Actin-myosin activity contribute to Miranda localisation at distinct time points in the cell cycle.

1. Introduction

1.1. Asymmetric Cell Division

1.1.1. Self-renewing asymmetric cell division

Typically, cell division is viewed as a symmetrical process in which one cell duplicates its genetic information and divides into two cells of equal cell identity and cytoplasmic content. However, cell division is frequently observed to be an asymmetric process in which as the cell divides, the two daughter cells inherit different characteristics. These can be differences in mRNA, protein or organelle content, as well as differences in cell size or signalling. Therefore, this asymmetry produces two cells of a different identity, which frequently differ in developmental potential. This has implications for developmental biology, ageing and disease (Knoblich, 2010).

During development, the generation of a wide array of cells of different functions is essential. This process is frequently conducted by the activity of stem cells. Stem cells are able to generate multiple different cell types, while being able to renew themselves. A hallmark of many stem cell populations is a process known as self-renewing asymmetric cell division (ACD). During ACD, the stem cell divides, producing two daughter cells. One of these daughter cells retains the stem cell identity, the other is fated to differentiate (**Fig. 1-1**). This mode of cell division is beneficial as it enables tight regulation of the number of stem cells within a population, while producing the differentiated cells which go on to perform important functions.

Other mechanisms to control the number of stem cells within a population do exist (Stine and Matunis, 2013). In some cases, stem cell number is maintained

through a process known as neutral competition. In neutral competition the stochastic loss and replacement of stem cells results in a balance in population size. The mechanisms controlling this are not clear, however in some systems this appears to depend on the limited size of the niche available for stem cells to reside.

An example of a stem cell regulated in this manner are the stem cells of the intestinal crypt. Between villi of the intestinal epithelium lies crypts, at the base of these lies the stem cells which produce mitotic daughter cells that migrate out of the crypt region (Stine and Matunis, 2013). Within this crypt is a second cell type known as Paneth cells which function as a niche for the stem cells. Decreasing the number of Paneth cells results in a loss of stem cells (Sato et al., 2011). A similar phenomena has also been observed in the hematopoietic niche (Zhang et al., 2003). It is likely therefore that by restricting niche signals, the potential of stem cells within the population is also limited.

Non-neutral cell competition can also control stem cell number. This occurs when some cells within the niche have a competitive advantage over others (stine and Matunis, 2013). The factors inducing this kind of cell competition are still being elucidated, however one appears to be DNA damage. Irradiated hematopoetic stem cells are outcompeted by those which have not been irradiated (Bodnar and Medzhitov, 2010). Competitive cell number control is beneficial as it enables the loss of damaged cells from the population. However, when cells become “too competitive” they can over proliferate and cause cancer.

Asymmetric cell division is an advantageous method to control stem cell number as it directly links cell number to cell fate. Furthermore, this can often be achieved through intrinsic signalling, removing the requirement for niche maintenance.

It is important to understand how signals are propagated that instruct differential cell fate. These signals can be propagated in two main ways, intrinsic fate commitment, or extrinsic fate cues (**Fig 1-2**).

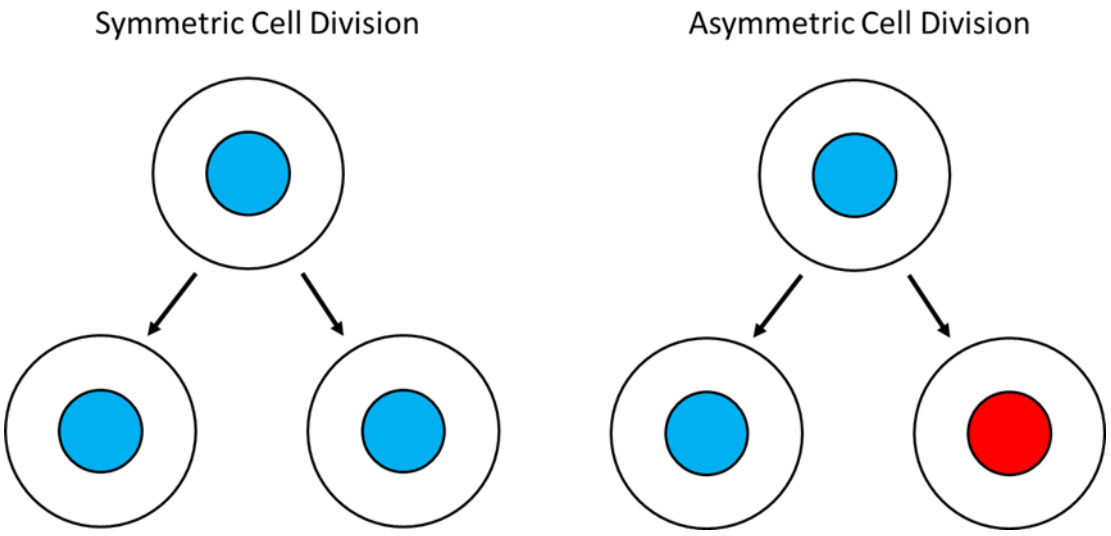

Figure 1-1 - Asymmetric Cell Division – Cell division typically maintains the fate of the mother cell in a symmetrical manner (Left panel). However, sometimes cell division can be asymmetric, generating cells of two different fates. In the example shown in the right panel the mother cell (blue) performs a self-renewing asymmetric cell division. This replenishes the blue cell while generating a cell of a different identity (red).

1.1.2. Intrinsic vs. Extrinsic

When extrinsic fate cues are utilised, the stem cell is maintained by signals coming from an adjoining niche. As the stem cell divides it orients the mitotic spindle such that the spindle forms perpendicular to the niche contact. Upon

mitosis, one daughter cell therefore remains in contact with the niche, maintaining its stem cell fate, while the other daughter cell loses its contact with the niche and begins to differentiate (Yamashita et al., 2010).

Secondly, there is intrinsic asymmetry. In this circumstance cells polarise at mitosis, unequally segregating mRNA, proteins and even organelles to one side of the cell. Once the mitotic spindle aligns with the axis of polarity, these factors are preferentially segregated into one of the two daughter cells. These then cause a change in daughter cell fate, while the cell that does not inherit these factors retains the identity of the mother cell (Neumüller and Knoblich, 2009).

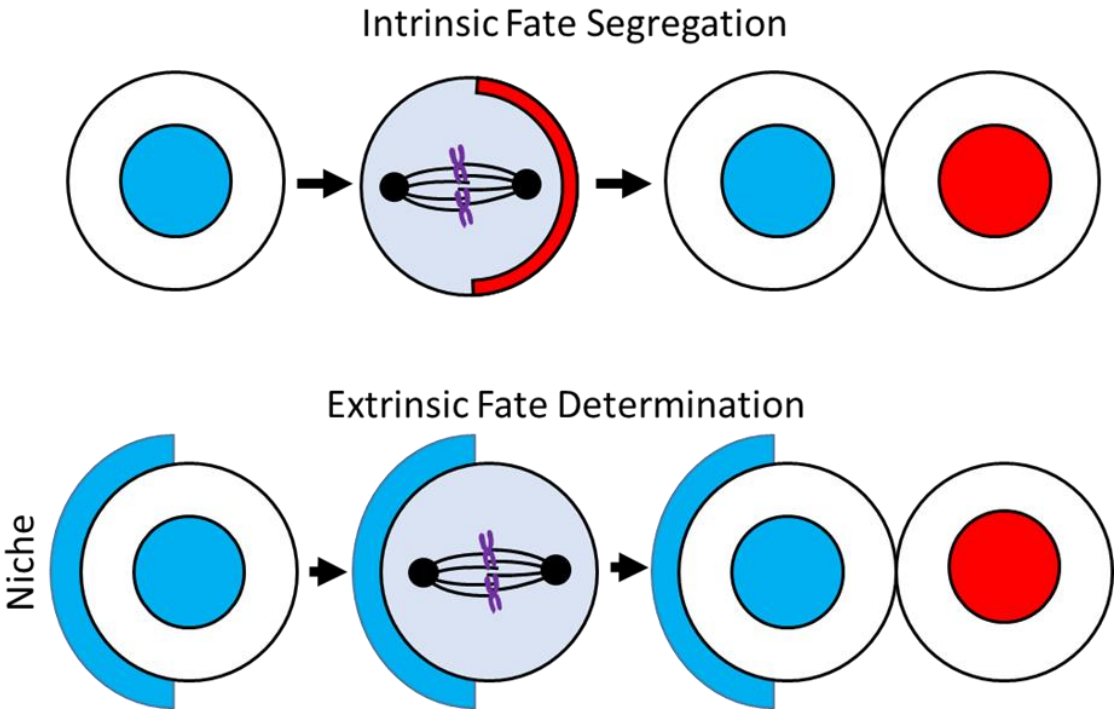

Figure 1-2 - Intrinsic vs. Extrinsic Fate Determination – The signal that generates this fate asymmetry after ACD can be considered intrinsic or extrinsic. In intrinsic ACD, the cell polarises fate determinants to one side of the cell cortex in mitosis. These are then aligned with the mitotic spindle and segregated into one daughter cell, which then acts upon these signals and changes identitiy. In Extrinsic ACD, one cell typically is in contact with a Niche (blue) that provides the fate cue. To divide asymmetrically, that cell then aligns the mitotic spindle perpendicular to the niche resulting in one daughter cell not being in contact with the signal, this cell then differentiates (red).

1.1.3. Asymmetric Cell division in Mammalian Development

Asymmetric cell division is a conserved, essential feature of development. Studies conducted in multiple stem cell compartments have revealed that asymmetric cell division is utilised by stem cells in the gut, brain, lung, mammary gland, blood and skeletal muscle. This has predominantly been studied in mice (Casali and Batlle, 2009; El-Hashash and Warburton, 2012; Huttner and Kosodo, 2005; Kuang et al., 2007; Santoro et al., 2016; Wu et al., 2008).

To determine whether intrinsic asymmetric cell division occurred in the developing mammalian cortex, neural progenitors expressing Green Fluorescent Protein (GFP) were dissociated and imaged by time-lapse microscopy through multiple rounds of division. Interestingly, some cells exhibited asymmetric lineages, with some daughter cells dividing more than others. This is indicative of intrinsic asymmetric cell division, as at this point these cells had been removed from their niche (Qian et al., 1998).

Later work utilised the retroviral transfection of GFP to generate rat cortical sections which expressed GFP in a mosaic fashion *in situ*. This enabled tracking of individual cells and their corresponding lineages. In this work, multiple modes of division were observed, however the most common (65%) was an asymmetric, self-renewing division in which the progenitor produced one neuron, which then migrated away from the ventricle. A second, smaller population generate intermediate progenitor cells which then divided symmetrically in the sub-ventricular zone, producing two cells which differentiate (Noctor et al., 2004).

How is this switch in fate regulated? Notch signalling is a key developmental signalling pathway involved in cell fate commitment. Notch signalling focusses upon the transmembrane receptor Notch which consists of an extra-cellular and intra-cellular domain. Upon binding of the extra-cellular domain with a Notch ligand (in mammals these are Jagged and Delta-like, in *Drosophila* they are Serrate and Delta), Notch is cleaved and the intra-cellular domain translocates into the nucleus where it initiates a transcription programme. The Notch regulator Numb inhibits this translocation of Notch into the nucleus (Bray, 2016).

It had been described previously that asymmetry of Notch reactivity was observed in the developing brain of the ferret in dividing neuronal progenitors (Chenn and McConnell, 1995). Furthermore, Numb (first identified in Drosophila, (Uemura et al., 1989)) was shown to be asymmetrically localised in mitotic progenitors in the developing mouse cortex (Zhong et al., 1996). It further was shown that it was likely that the conserved, polarity regulating, apical Par complex was directing this Notch asymmetry. Par-3 – a key component of the Par complex is also asymmetrically segregated in the developing cortex and its knock down led to an increase in symmetric, terminal divisions generating two differentiating cells (Bultje et al., 2009). Interestingly, this phenotype could be suppressed by the co-depletion of Numb.

Numb is not the only fate determinant which is asymmetrically segregated in the mammalian brain. The RNA binding protein Staufen (Stau, first described in *Drosophila*, (Johnston et al., 1991)) is also asymmetrically localised in mouse cortical progenitors. Stau preferentially segregates into differentiating intermediate progenitor cells (IPC) and its knockdown promotes the differentiation of both daughter cells into an IPC suggesting that Stau inheritance

promotes differentiation. Interestingly, two RNA molecules which interact with Stau are *TRIM32* and *PROX1*, both homologues of key fate determinants in other systems (Kusek et al., 2012; Schwamborn et al., 2009; Vessey et al., 2012).

Many of these components for ACD are present in other stem cell compartments in mammals. A second widely studied population of stem cells is the hematopoietic stem cell (HSC), responsible for the generation of diverse blood cell types (Orkin and Zon, 2008). Similar to the mammalian neocortex, a Notch reporting GFP cell line was found to be frequently asymmetric after HSC mitosis. Importantly Notch+ cells were found to be less mature than Notch-. Furthermore, evidence for intrinsic control of self-renewal came from the observation that Numb was once again asymmetrically inherited (Wu et al., 2008).

However, the regulation of Numb asymmetric localisation is not well understood. (Sengupta et al., 2011); (Hope et al., 2010). Mutation of the Dynein adaptor Lissencephaly-1 (Lis1) led to the loss of HSC number through accelerated differentiation. Though Lis-1 mutation did not affect Numb polarity, it did affect the asymmetric inheritance of Numb due to misalignment of the mitotic spindle with the polarity axis (Zimdahl et al., 2014). It is clear that asymmetric inheritance of Numb in the HSC niche is important. But how it is orchestrated is not understood.

Intrinsic ACD is also key to the development of the mammary gland. The mammary gland is a branched epithelium which is organised into ducts and alveoli growing into a fat pad. At the end of each branch are the cells responsible for secretion, known as luminal cells. This tissue is continuously remodelled from puberty onwards as the branches expand at each reproductive cycle (Joshi et al., 2010), with increased progesterone activating the stem cells. It has been under

some debate whether each mammary stem cell (MaSC) is able to produce multiple different cell types, or whether multiple types of MaSC account for the cellular diversity in the mammary gland (Santoro et al., 2016). What is accepted to be important though, is that asymmetric cell division is key to gland development.

When mammary cells from mice are isolated and cultured, some are able to form a cluster of mammary cells, termed mammospheres (MS). Interestingly, these MS contain a small number of cells which divide very slowly compared to other cells within the MS. Isolating these cells demonstrated that these predominantly divided asymmetrically ~80% of the time. Furthermore, in ~80% of cases, these cells asymmetrically segregate Numb (Cicalese et al., 2009). Later work demonstrated that Numb was in fact doing two jobs in this tissue. Although Numb antagonises Notch, and elevated Notch levels were observed in cells mutant for Numb, Numb was also found to regulate the levels of p53. In mammary cells mutant for Numb, p53 levels decreased. Furthermore, the MS forming ability of these cells increase and compared to the wild type these MSs did not lose self-renewal potential over time. Interestingly, pharmacological prevention of p53 degradation rescued the MS growth phenotype (Tosoni et al., 2015).

It is apparent that in multiple tissues, ACD is integral for organ development and homeostasis. Furthermore, intrinsic segregation of fate determinants seems to be a key mechanism by which the balance of self-renewal and differentiation is maintained. Therefore, it is unsurprising that the ACD machinery has been implicated in various cancers.

1.1.4. Clinical Importance of Asymmetric Cell Division Research

It is established that ACD is a key feature of stem cell homeostasis in a range of different tissue contexts. Furthermore, its dysregulation causes defects related to growth and differentiation. It is unsurprising therefore that it has been linked to tumorigenesis. Statistical work has demonstrated that organs with the highest numbers of stem cell divisions, also have the highest likelihood of tumorigenesis (Tomasetti and Vogelstein, 2015). Recent work by the same authors propose that a large fraction of cancers are generated by DNA replication errors, rather than inherited mutation or environmental factors. Therefore, the more stem cell divisions, the more DNA replication, the higher the chance of tumorigenesis (Tomasetti et al., 2017).

There are clear similarities between tumorigenesis and development. Tumours are heterogeneous structures which display self-renewing properties (Reya et al., 2001). It is these properties that make many cancers resistant to traditional chemotherapy and radiotherapy which target the cancers ability to proliferate. ACD is a clear mechanism which cancer cells could utilise to self-renew while building a heterogeneous tumour mass. A switch to rapid, symmetrical divisions could then cause a more rapid accumulation of tumour mass more commonly associated with the acute phase of cancer progression (Bajaj et al., 2015).

The key proteins involved in ACD have been implicated in multiple cancers. In mammary tumour cells, Numb and p53 signalling were found to be depleted. Expression of Numb in these cells was able to rescue the over proliferation of these cell populations (Pece et al., 2004). Disease progression and loss of life was found to occur much faster in patients whose tumour had reduced, or

completely lost Numb expression (Rennstam et al., 2009). Interestingly, in mouse mammary cancer models Numb asymmetry was significantly reduced in MaSCs (Cicalese et al., 2009). The loss of Numb itself was also shown to be tumorigenic in a mouse model in a p53-dependent manner (Tosoni et al., 2015). This is likely to be due to Numbs role in preventing the degradation of p53 (Colaluca et al., 2008).

ACD is also involved in myeloid leukemia progression. A mouse model of chronic myeloid leukemia found that as the leukemia entered the acute phase, numb levels were reduced. The expression of Numb in these cells reduced the number of mice which entered the acute phase. There was also an increase in the levels of differentiated cells, which could be inhibiting disease progression (Ito et al., 2010). A similar model led to a shift away from asymmetric fate commitment upon cell division, instead hematopoietic precursors underwent more symmetric renewal, increasing the pool of progenitor cells (Wu et al., 2008). Deleting Lis-1 also rescued blood count and Numb levels, suggesting that asymmetric Numb segregation is closely related to the progression of leukemia to the acute phase (Zimdahl et al., 2014).

These data as well as others demonstrate a clear link between the balance of symmetric and asymmetric divisions and the progression of cancer, as well as the severity of cancer prognosis. However, it is not yet understood whether defective ACD actually initiates tumours in patients, or whether subversion of asymmetric cell division in stem cells within the tumour just enhances disease progression. Importantly, the regulators of ACD present themselves as interesting candidates to explore in treating human cancers.

Unfortunately, although more and more regulators of asymmetric cell division are being identified in mammalian models, these organisms are challenging, both to access the organs of interest as well as genetically manipulate the cells *in situ.* Therefore, to gain mechanistic insight into how ACD is regulated it is important that we utilise invertebrate model organisms, in which much of the asymmetric cell division machinery in mammals were first described. The use of model organisms is much less challenging, both financially and experimentally.

1.2. Models of Cortical Asymmetry

Due to the difficulty of researching ACD in vertebrate models, two main model organisms have emerged for studying the mechanisms regulating the polarised differentiation of signalling molecules. These are the nematode worm, *Caenorhabditis elegans* (*C.elegans*) and the fruit-fly, *Drosophila melanogaster* (*Drosophila*).

1.2.1. C. elegans

In the early *C.elegans* embryo the worm must divide from a single cell to form the founder cells that make up the main tissue types in the mature worm. This takes place through asymmetric cell divisions which generate the body plan. Early immunofluorescence conducted in these first divisions demonstrated that granules, termed polar granules (P-Granules) were asymmetrically apportioned in these cells. However, very little was known about how these granules became asymmetrically segregated (Updike and Strome, 2009). The identification of genes involved in segregating these P-granules was daunting due to the large number of worms that would need to be screened in order to find a mutant. A trick was therefore found using a mutant strain in which the female worms failed egg

laying (*Egl,* (Horvitz et al., 1983)). *Egl* worms would then be killed by their offspring feeding after hatching inside the mother. Therefore, by mutagenesis of *Egl* worms, it would be possible to identify genes required for early embryogenesis due to the survival of the mothers, as the eggs would not hatch. Six mutant strains were found, including one in which the embryos had abnormal cell divisions which suggested that partitioning of P-granules could be defective (Cheng, 1988). This was named *par-1*. A further series of *par* genes were then found from similar screens (Goldstein and Macara, 2007).

These par genes encode proteins which enrich at the cell cortex and are asymmetrically segregated to the anterior or posterior pole at the one cell embryonic stage, creating two polarised domains. The anterior pole is occupied by a complex consisting of the PDZ proteins PAR-3 and PAR-6 as well as the serine/threonine kinase atypical protein kinase C (aPKC) (Hung and Kemphues, 1998; Tabuse et al., 1998). The posterior compartment is occupied by another kinase, PAR-1, RING finger protein PAR-2, and the cytoskeletal protein Lethal Giant Larvae (LGL) (Beatty et al., 2010; Guo and Kemphues, 1995; Tabuse et al., 1998).

Interestingly, the polarised localisation of these complexes can be divided into distinguishable establishment and maintenance phases (Cuenca et al., 2003). At the end of meiosis, these complexes are not polarised. The anterior Par complex (aPAR) localises uniformly around the cell membrane. Polarisation occurs as the zygotes enter the mitotic cell cycle. Actomyosin contractions begin and become reduced locally by the sperm centrosome. This change in actomyosin contractility drives the redistribution of the aPAR complex to the anterior pole. Meanwhile, in

the region of low contractility vacated by the aPAR complex, the posterior PAR-complex (pPAR) is able to localise (Munro et al., 2004).

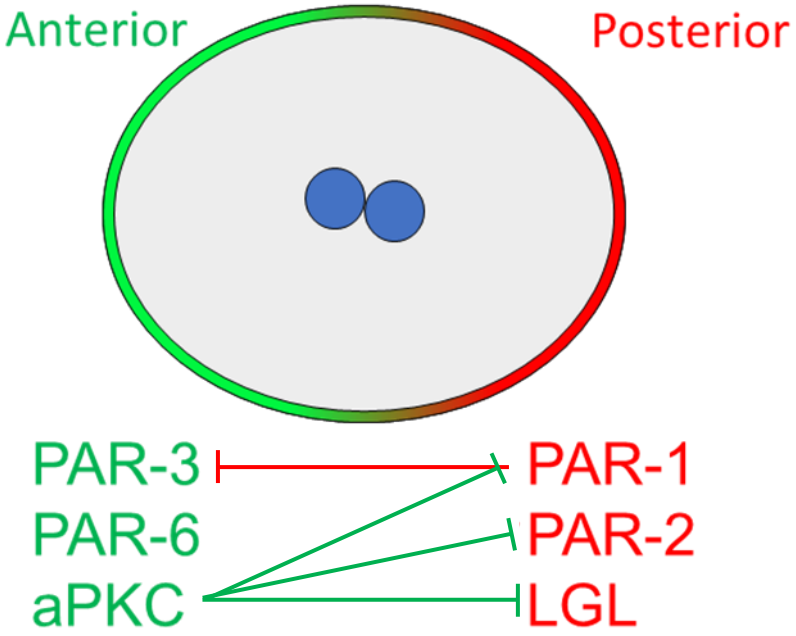

Figure 1-3 - Phosphorylation mediated mutual exclusion maintains the polarised cell cortex in C. elegans. The early C.elegans embryo polarises its cell cortex along the Anterior Posterior (A/P) axis. This is maintained by phosphorylation mediated mutual exclusion. The anterior complex contains the kinase aPKC which phosphorylates the posterior PAR proteins PAR-1, PAR-2 and LGL. The Posterior Complex contains the kinase PAR-1 which phosphorylates PAR-3. This phosphorylation excludes proteins from the respective domains by regulating plasma membrane interaction. This process is independent of the acto-myosin network.

Once these PAR complexes are polarised, the polarised distribution needs to be maintained. Early genetic work demonstrated that this is achieved by a series of antagonistic interactions. Mutagenesis experiments demonstrated that mutation of either aPAR or pPAR components resulted in an expansion of the other domain. Later biochemical work identified that this depends upon protein phosphorylation. aPKC maintains the anterior complex, by phosphorylating PAR-

2; excluding it from localising to the anterior pole. Similarly, PAR-1 maintains the integrity of the posterior pole by phosphorylating PAR-3 therefore excluding it from localising to the posterior pole. This therefore creates a stable boundary by means of mutual exclusion (Hao et al., 2006; Motegi et al., 2011).

Importantly, this is not due to structural compartmentalisation. Inhibition of the Filamentous Actin (F-Actin) network by inhibition by Latrunculin A (Lat-A) or Cytochalasin D did not result in loss of PAR polarity. Further quantitative imaging demonstrated that long range directed transport or diffusion barriers were not present. Instead both aPAR and pPAR components are able to diffuse across the A/P boundary. Thereby a reaction diffusion model has emerged for A/P Polarity (Goehring et al., 2011a).

The reaction diffusion model depends on a fixed pool of maternally contributed PAR proteins in the cell. These proteins can exist in two states: 1) a quickly diffusing cytoplasmic state, 2) a slower diffusing membrane bound state. Growth of the anterior or posterior domain relies upon the availability of quickly diffusing aPAR or pPAR proteins respectively. As the PAR domains grow, the cytoplasmic pool becomes reduced, restricting the growth potential of either domain. Therefore, aPAR proteins localise at the anterior pole, where they are not excluded by pPAR proteins which are not present, they then slowly diffuse down the concentration gradient at the membrane to the A/P boundary. At the boundary they are then phosphorylated and removed to the cytoplasm where they rapidly diffuse, eventually replenishing the diffusing proteins at the anterior pole. The posterior proteins do the same at the posterior pole, resulting in a stable boundary (Goehring et al., 2011b).

C. elegans provides an elegant demonstration of how opposing Par-complexes can form a polarised cell cortex, and maintain that throughout mitosis.

1.2.2. Drosophila Neuroblasts

A second widely studied model for ACD and the focus of this is the *Drosophila* neural stem cells (Neuroblasts; NBs). NBs are progenitor cells which delaminate from the neuro-ectoderm of the *Drosophila* embryo and begin a series of asymmetric cell divisions to generate the central nervous system (CNS) required for the larval stage (**Fig. 1-4**). At the end of embryogenesis a series of NBs undergo apoptosis while a subset enter a period of quiescence. After the embryo hatches towards the end of the first instar larval stage, the NBs reactivate and begin another series of asymmetric cell divisions, preparing the CNS for pupation and generation of the CNS required for adult function (Campos-Ortega and Hartenstein, 1997).

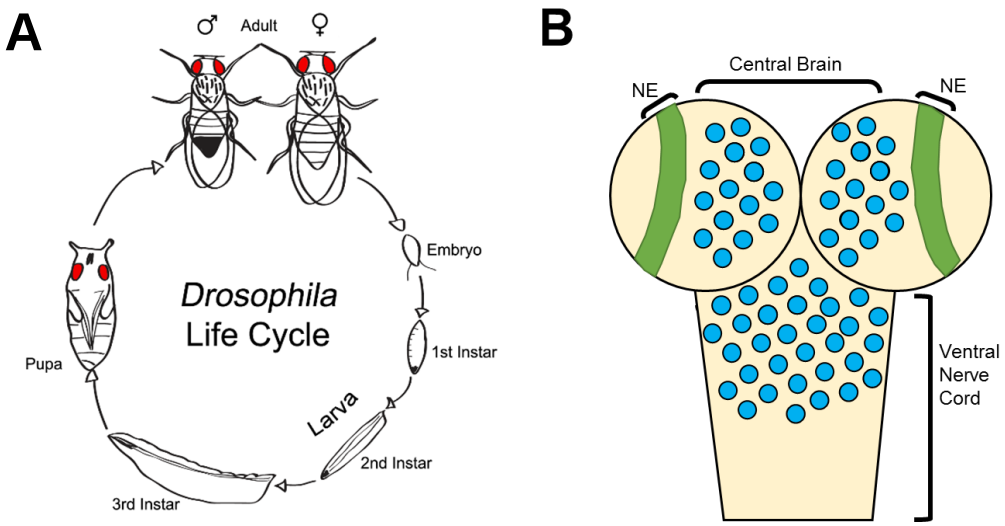

Figure 1-4 - Activity of *Drosophila* Neuroblasts. A) *Drosophila* life cycle. NBs are active in the embryo to generate the CNS required for larval function. They then enter quiescence until the end of the 1st instar larval stage when they reactivity, generating the neurons and glia which will be required for more complex functions. At the onset of the pupal stage the neuroblasts either terminally differentiate or undergo apoptosis. **B)** Schematic of a larval brain. NBs (Blue) are predominantly found in the central brain and the ventral nerve cord (VNC). New NBs arise from the neuroepithelium (Green).

The asymmetric cell division of NBs allows NB self-renewal while at the same time the production of a ganglion mother cell (GMC). It is this GMC which divides once more to generate the neurons and glial cells which constitute the CNS. This differential cell fate is achieved by the asymmetric segregation of fate determinants to the cell cortex in metaphase (**Fig. 1-5**). In the NB this segregation occurs along the apical basal axis. The apical domain contains complexes which are retained by the self-renewed NB, while the basal domain contains a series of fate determinants which direct GMC differentiation. The polarisation of these complexes is an intrinsic mechanism as isolating NBs in culture does not prevent the formation of polarised cortical domains in mitosis (Broadus and Doe, 1998).

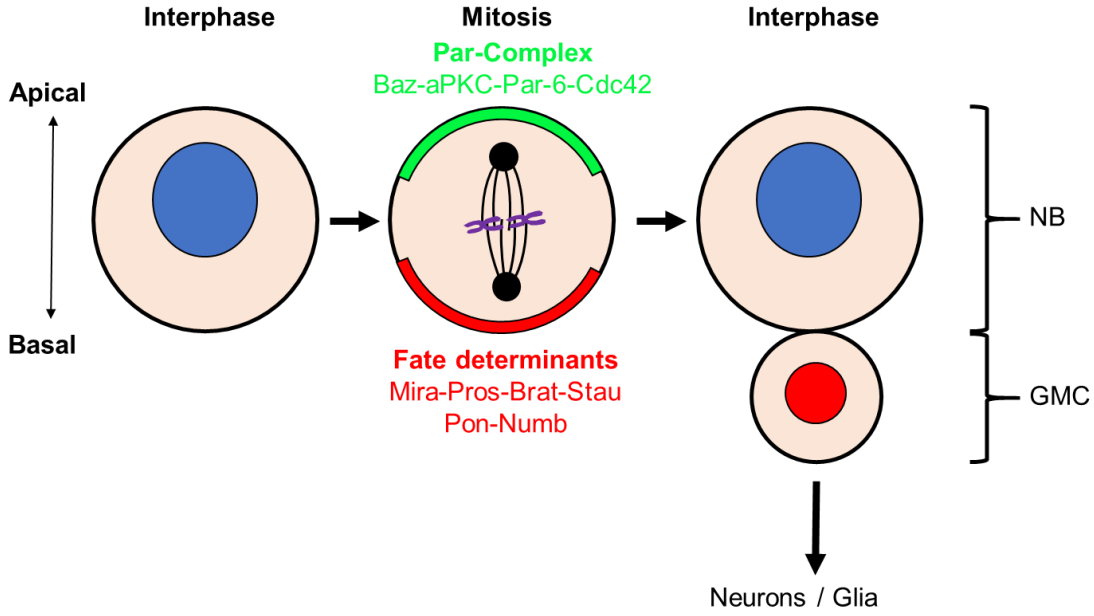

Figure 1-5- Asymmetric Cell Division of *Drosophila* Neuroblasts – Drosophila neuroblasts polarise the cell cortex in mitosis. At the apical cell cortex localises the conserved Par polarity complex consisting of Bazooka (Baz), aPKC and Par-6. Downstream of the Par complex, a series of fate determinants localise to the basal cell cortex. This consists of two complexes: 1) Miranda complex – Miranda is an adaptor protein which carries the cargo Prospero, Brat and Staufen, 2) Numb Complex – Numb localises with its adaptor protein Pon. Upon mitosis, these basally localised factors segregate into the ganglion mother cell (GMC), promoting differentiation.

1.2.2.1. The apical domain

The primary protein complex involved in cortical compartmentalisation is the apically localised Par-complex. Similar to the complex which localises to the anterior pole of the *C. elegans* single cell embryo, this complex contains the proteins Bazooka (Baz, Par-3), aPKC and Par-6. *baz* is a gene encoding a 161kDa PDZ domain containing protein which localises apically in epithelia and neuroblasts (Kuchinke et al., 1999). Mutations in *baz* led to disorganisation of the epithelium and loss of adherens junction integrity (Muller and Wieschaus, 1996). Due to a clear role in cell polarity, the function of Baz was investigated in NBs. *baz* mutations resulted in the mislocalisation of the basal fate determinants, causing their uniform localisation around the cell cortex (Wodarz et al., 1999). This loss of cortical polarity phenotype has since been attributed to the loss of aPKC from the apical domain in *baz* mutants (Rolls et al., 2003; Wodarz et al., 2000). Over-expression of Baz has been shown to result in the reversal of polarity, or the ectopic localisation of the par-complex to the basal pole in embryonic NBs (Petronczki and Knoblich, 2001; Wodarz et al., 1999).

Drosophila atypical protein kinase C (*apkc*) was identified by searching the *Drosophila* genome for sequence homology with Mouse PKCλ and *C. elegans* PKC-3. It is a ~70kDa protein with a 68% homology to the mouse PKCλ and 63% homology to rat PKCζ (Wodarz et al., 2000). Immunoprecipitation experiments revealed a direct interaction with Bazooka, while immuno-fluorescence identified that aPKC forms an apical crescent in mitotic NBs as part of the Par-complex. Interestingly, *apkc* mutants also resulted in the mislocalisation of Baz suggesting that these two proteins co-operate to maintain the apical domain. *apkc* mutants

fail to localise Par-6 to the cortex as well as to localise the fate determinants to the basal pole (Rolls et al., 2003).

par-6 was also identified by looking for sequence homology with the protein found in *C. elegans* (Hung and Kemphues, 1998). Par-6 localisation to the apical pole is dependent upon Baz and interestingly, *par-6* mutations resulted in mislocalisation of Baz to the cytoplasm (73% of cases), suggesting that Par-Complex integrity is essential for maintaining apical localisation of these proteins. Furthermore, mutations for Par-6 also phenocopied those of aPKC in terms of basal fate determinant localisation (Petronczki and Knoblich, 2001). This is probably due to the recent finding that Par-6 activates aPKC. aPKC contains a pseudo substrate motif which inhibits the active site of the kinase. Par-6 was found to activate aPKC by displacing the pseudo substrate and relieving aPKC of its auto inhibition (Graybill et al., 2012).

A fourth core component of the Par-complex in NBs is the Rho GTPase Cdc42. In epithelia the interaction between active Cdc42 and Par-6 is required for the establishment of polarity (Hutterer et al., 2004). Cdc42 - Par-6 interaction was then shown to be important for NB polarity. Overexpression of Cd42 revealed that it exhibits and apical bias in localisation (Atwood et al., 2007). Loss of function mutation for *cdc42* was shown to result in a failure to polarise the NB cell cortex. This was shown to be, similar to epithelia, dependent upon the direct interaction between Cdc42 and Par-6. Further *in vitro* analysis suggested that this Par-6 Cdc42 interaction was important for aPKC kinase activity *in vitro* (Atwood et al., 2007).

How these complexes fit together in the NB is not clear, recent work in *C.elegans* suggests that the Par-complex can exist in two forms. One dependent on bazooka which provides the spatial information consisting of Baz-Par6-aPKC. aPKC and Par-6 then transition to a Cdc42 dependent complex in which the kinase is then active (Rodriguez et al., 2017). In the absence of Cdc42, the active complex does not form therefore resulting in a breakdown of the polarity network, similar to *cdc42* mutant neuroblasts.

A final key conserved regulator of the Par-complex is the cytoskeletal protein Lethal giant larvae (Lgl). Lgl was found to be important for NB polarity by genetic screening. Mutation for *lgl* was found to result in Miranda localising uniformly to the cell cortex in mitosis as well as to the spindle microtubules (Ohshiro et al., 2000). Later work proposed that Lgl localises to the apical cell cortex (Albertson and Doe, 2003) and interacted directly with the Par complex (Betschinger et al., 2003).

Lgl is an aPKC substrate and is phosphorylated by aPKC on three serine residues *in vitro*. Interestingly, the overexpression of a mutant in which these serines cannot be phosphorylated (Lgl3A) resulted in a phenotype similar to aPKC loss of function suggesting that overexpressing an inactive substrate could inhibit aPKC activity (Betschinger et al., 2003). The authors therefore proposed that Lgl was inactive at the apical pole of the cell, but was active at the basal side, promoting asymmetric Miranda localisation. However, recent work has questioned this model for Lgl function in neuroblasts. Although Lgl is present at the cell cortex throughout interphase, in mitosis Lgl is displaced into the cytoplasm due to phosphorylation by Aurora-A (Bell et al., 2015).

In many systems Lgl has shown to have a negative interaction with aPKC (Chalmers et al., 2005; Raman et al., 2016). In neuroblasts it has been proposed that Lgl holds aPKC-Par-6 in an inactive state, phosphorylation then displaces Lgl from this complex resulting in the activation of the Par-complex (Wirtz-Peitz et al., 2008). It is possible therefore that the cytoplasmic localisation of Lgl in mitosis contributes to the restriction of aPKC activity to the apical cell cortex.

1.2.2.2. Basal fate determinants

Basal fate determinants localise as two main complexes. The first complex consists of the adaptor protein Miranda (Mira), the transcription factor Prospero (Doe et al., 1991), the translational regulator Brat (Brain tumour, (Gateff, 1978)) and the mRNA binding protein Staufen (St. Johnston et al., 1991). I shall refer to this as the Miranda complex. The second complex consists of the adaptor protein Partner of Numb (Pon, (Lu et al., 1998)) and the Notch signalling regulator Numb (Uemura et al., 1989).

Mira is an 830 amino acid adaptor protein that was discovered in a yeast-hybrid screen searching for proteins which interact with Prospero (Ikeshima-Kataoka et al., 1997; Ikeshima-Kataoka et al., 1997; Shen et al., 1997). Mutants for *mira* were shown to fail to localise Prospero (Matsuzaki et al., 1998), as well as *mira* embryos exhibiting a decrease in the well characterised aCC/pCC and RP2 neurons which are known to be identified through *even skipped (eve)* expression.

Structure and function analysis revealed that Mira contains three main regions (Fuerstenberg et al., 1999). The first region consisting the amino terminal (N-terminal) 1-290aa is required for cortical asymmetry (Shen et al., 1997). This region was also shown to contain a conserved basic and hydrophobic (BH) motif

allowing for direct interaction with the cell membrane (Bailey and Prehoda, 2015). This first region is also predicted to form a coiled coil (150-290aa, (Shen et al., 1997)). The second region consists of the Mira cargo binding domain (CBD). This region dimerises through cysteine di-sulfide bridges forming a parallel coiled coil (Jia et al., 2015; Yousef et al., 2008). It is unknown how regulation of Miranda dimerisation effects protein function. The third and final region of Miranda is the carboxy terminal (C-terminal) 727-830aa which is required for cargo release and Miranda protein degradation. It has been hypothesised that this region may be required for the “unzipping” of the cargo binding region, facilitating cargo release. The release of cargo would then uncover destruction boxes localised in the cargo binding domain facilitating the degradation of Mira in the GMC, though this has not been formally shown.

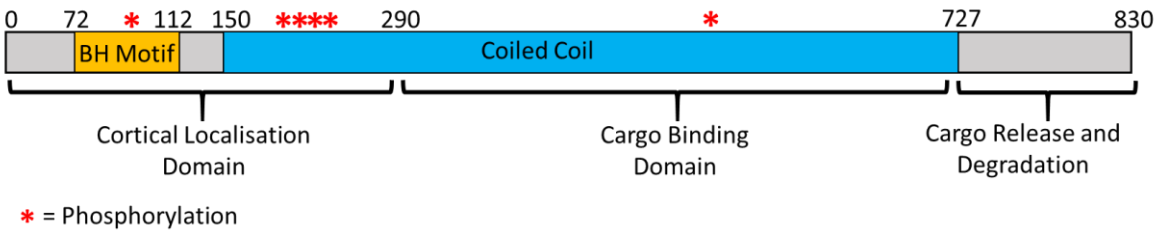

Figure 1-6 - Miranda Protein Domains – Miranda is an 830aa rod shaped adaptor protein consisting of three main regions. N terminal region contains the domain required for cortical localisation (0-290aa). In the centre of the protein is a large region required for carrying the cargo consisting of three cell fate determinants. This region also forms a coiled coil and is predicted to dimerise via disulphide bridges (150-727aa). The Third region is the domain required for timely cargo release and protein degradation at the C terminus (727-830aa). Miranda can be phosphorylated on a series of sites denoted by an asterisk (*). 5 sites are found in the cortical localisation domain (amino acid: 96, 194,195,205,206) and one site within the cortical binding domain (amino acid 591).

Multiple post-translational modifications have been identified upon Miranda. It can be phosphorylated on 5 residues in the N-terminus of the protein (residue: 96, 194, 195, 205, 206 (Atwood and Prehoda, 2009)) and one in the cargo binding domain (residue 591, (Zhang et al., 2015)). Furthermore, the C-terminus of Miranda has been shown to be ubiquitinated, which appears to be required for the localisation as replacing the C-terminal fragment of Miranda with ubiquitin was sufficient to rescue truncation of the C-terminus (Slack et al., 2007). There are multiple destruction boxes (D-boxes) in the C-terminus of Miranda which could be ubiquitinated, though detailed analysis of these sites has not been conducted (Shen et al., 1997).

Miranda has been shown to be able to interact directly with the membrane (Bailey and Prehoda, 2015), with Myosin II and Myosin VI (Petritsch et al., 2003) and directly with filamentous actin (Sousa-Nunes et al., 2009). Furthermore, Mira is able to interact with microtubules (Mollinari and Lange, 2002) and this is likely to be due to conservation between the N-terminus of Miranda and the microtubule binding protein RHAMM (receptor for hyaluronan-mediated motility, (Chang et al., 2011)). However, microtubules are not required for asymmetric localisation (Broadus and Doe, 1998). How these interactions co-operate to result in basal localisation is not clear. Mira carries three identified cargo proteins which act as fate determinants. The first of these described was Prospero.

Prospero is a key transcription factor asymmetrically segregated through its interaction with Miranda (Doe et al., 1991; Ikeshima-Kataoka et al., 1997; Spana and Doe, 1995). It is evolutionarily conserved with the mammalian Prox family of transcription factors which are required for differentiation in a number of tissues (Elsir et al., 2012). Identified in a screen for genes resulting in embryonic lethality,

pros was found to be expressed in NBs and mutation resulted in an ectopic number of cells expressing the NBs marker *deadpan* (*dpn)* demonstrating that *pros* was a key regulator of neuronal cell fate (hence the gene name) (Lu et al., 1998). Shortly afterwards, it was shown that Prospero was asymmetrically segregated in NBs and following mitosis translocated to the nucleus of the GMC (Spana and Doe, 1995).

Later work (Choksi et al., 2006) sought to identify Prospero binding sites on the DNA using a technique known as DNA adenine methyltransferase identiificiation (DamID). DamID is a method used to identify where on the DNA, DNA binding proteins localise. It works by the expression of a DNA-binding protein of interest, fused to DNA methyltransferase. Adenosine methylation then occurs at the region the protein of interest binds which can be detected by cutting the methylated DNA sequences with DpnI and then amplifying these regions by PCR (Aughey and Southall, 2015). These experiments found that Prospero binds overwhelmingly to sites of the genome linked to genes regulating CNS development. More specifically Prospero bound to both genes involved in ACD (*miranda, inscuteable, bazooka, apkc*) as well as genes involved in NB identity (*deadpan, asense*). *prospero* mutants resulted in loss of differentiation in the GMC, leading to excessive NBs and lack of the terminal divisions that GMCs normally undergo (Choksi et al., 2006). This work clearly positioned Prospero as a key transcription factor involved in the repression of NB genes and the activation of differentiation genes.

Prospero also plays a role in the regulation of NB proliferative potential. It was shown that late in larval development (120hours post hatching, hph) Prospero was detected in the NB nucleus, coincident with NBs becoming smaller and the

delocalisation of Miranda from the cell cortex. Transient overexpression of a Prospero fusion protein before the 120 hour timepoint resulted in Prospero observed in the nucleus of the NB and the premature loss of NBs resulting in an early end to neurogenesis (Maurange et al., 2008).

Intriguingly, although high levels of nuclear Prospero trigger early differentiation of the NB, a transient low burst of nuclear Prospero at the end of embryogenesis is required to drive NBs into quiescence. Furthermore, in *prospero* mutants parental NBs (not the de-differentiated progeny) remain proliferative even at the end of the embryonic stage. Finally, transient over-expression of Prospero drives some NBs to enter a period of quiescence rather than terminally differentiate (Lai and Doe, 2014). The regulation of Prospero entry into the nucleus is therefore an interesting problem. This depends somewhat on a RAN-GTPase gradient, with mutants in the RanGEF Bj1 causing a progressive loss of NBs and ectopic Prospero localisation in the nucleus (Joy et al., 2014). Presumably, the over-expression of Prospero results in the RAN-GTPase gradient being insufficient to export Prospero from the nucleus. However, there is more work to be done to fully understand the mechanisms involved in ensuring Prospero is retained in the cytoplasm.

The second key fate determinant which relies upon Miranda for its asymmetric segregation is Brain Tumour (Brat). Brat is a conserved NHL domain protein which acts as a translational repressor (Sonoda and Wharton, 2001). Mutants for Brat are lethal by the pupal stage with larvae exhibiting overgrowth of the brain (Arama et al., 2000; Gateff, 1978). In a screen for regulators of NB self-renewal, mutants for *brat* were found to have a vast increase in NB number (>10 fold increase) 120 hours after larval hatching compared to wild type. Intriguingly this

increase in NB number was shown to be at the expense of neurons with many GMCs continuing to express the neuroblast markers *dpn* and *miranda*. Furthermore, it was shown that Miranda directly interacts with the NHL domain of Brat and that Brat is required for the asymmetric partitioning of Prospero upon mitosis (Lee et al., 2006b).

In *brat* mutants 72 hours after clone induction cell size is deregulated with many daughter cells growing to NB like size. This is potentially due to a misregulation of dMyc translation. *brat* mutant clones showed an increase in dMyc expression but not transcription. It is possible that this loss of dMyc regulation is sufficient to induce these changes in cell growth though the inability to misexpress dMyc alone in the GMC without mutating Brat meant it was impossible to directly show this (Betschinger et al., 2006).

To summarise Brat is a key regulator of asymmetric cell division regulating the proliferation, size and identity of the GMC. Intriguingly this occurs upstream of Prospero, presumably this is due to the loss of Pros asymmetry and reduced Pros in *Brat* mutants (Bello et al., 2006; Betschinger et al., 2006). Furthermore, the function of Brat as a post-transcriptional regulator (translational repressor) remains understudied in the brain. It would be interesting to investigate the other RNA molecules that Brat is able to interact with and therefore identify potential novel regulators of *Drosophila* neurogenesis.

The third and final protein known to be asymmetrically segregated by Miranda is the RNA binding protein Staufen (Stau, (Johnston et al., 1991; Matsuzaki et al., 1998). Stau is required to localise *prospero* mRNA to the basal cortex of the NB ensuring that it is segregated into the GMC (Broadus et al., 1998; Li et al., 1997).

Interestingly, there was no phenotype when *stau* was mutated alone. However, in double mutants of *stau* and *prospero* an enhancement of the *prospero* phenotype was observed (Broadus et al., 1998). This data suggests that the localisation of the mRNA is a redundant pathway to Prospero protein localisation which may play a protective function if the protein is mislocalised, thereby, ensuring differentiation of the GMC and protecting brain homeostasis (Li et al., 1997; Schuldt et al., 1998). It is not yet comprehensively shown however that this enhancement of the *pros* phenotype is not due to a role *stau* plays in the asymmetric localisation of a thus far unknown mRNA, which contributes to differentiation of the GMC.

The second basal complex consists of Numb (Uemura et al., 1989) and Partner of Numb (Pon, (Lu et al., 1998)). Numb is a 557aa membrane binding protein that is required for correct cell fate generation in the NB lineages of the CNS and the sensory organ precursor cell lineages of the peripheral nervous system. Similarly to Miranda, its asymmetric localisation depends upon the Actin cytoskeleton as well as the localisation of the Par-complex (Knoblich et al., 1995; Smith et al., 2007). Its role is to control binary cell fate required for neuronal diversity (Spana and Doe, 1995) as well to suppress ectopic NB production by suppressing Notch in the GMC (Wang et al., 2006).

Interestingly, despite the similarities to Miranda, Numb relies upon the 672 amino acid protein Pon for its asymmetric localisation in metaphase, however, in *pon* mutants, Numb is still asymmetrically segregated into the daughter cell (Lu et al., 1998). Pon and Numb directly interact *in vitro* and co-localise throughout mitosis. In *numb* mutants Pon is still asymmetrically localised. Little more is known about the regulation of Pon localisation, though separate to the regulation of the

Miranda complex Pon is phosphorylated by Polo kinase and mutating the site phosphorylated by Polo results in the mislocalisation of Pon (Wang et al., 2007).

The asymmetric segregation of these basal proteins is essential for balancing self-renewal with differentiation. Mutations for many of the basal proteins result in ectopic neuroblast number and overproliferation of the tissue resulting in a tumour like state. Indeed, the implantation of adult fly abdomen with GFP expressing fate determinant mutant brains resulted in the GFP expressing tissue expanding until it occupied vast quantities of the abdomen, compared to the implantation of GFP expressing, otherwise wild type, brains in which case this did not occur (Caussinus and Gonzalez, 2005).

1.2.2.3. Cortical Polarity and Cell size asymmetry

An interesting feature of *Drosophila* NBs is that as well as the fate determinant asymmetry at mitosis, they also divide asymmetrically in cell size. The NB being over two times larger than the GMC (Fuse et al., 2003). Live imaging of NBs during mitosis revealed that cell size asymmetry could potentially be explained by a shift in spindle position towards the basal pole in anaphase (Kaltschmidt et al., 2000). This was seen to be due to the astral microtubules being longer in the presumptive NB than the GMC.

It was not long before mutagenesis screens identified the genes regulating this process. G protein signalling was implicated when mutant analyses revealed that the Gβγ complex appeared to suppress microtubule growth (overexpression of members of this complex resulted in short disorganised spindles), while the Gαi

subunit was localised apically and suppressed the activity of Gβγ (Schaefer et al., 2001). In mutants for the apically localised protein Partner of Inscuteable (Pins) the spindle became symmetric, this was thought to be due to the mislocalisation of Gαi form the apical pole and loss of apical Gβγ suppression (Cai et al., 2003; Yu et al., 2003). Importantly, mutation in the G protein subunits alone was not enough to generate total size symmetry, with the spindle shifted slightly towards the basal pole at anaphase. This was shown to be due to a separate pathway involved in size asymmetry downstream of the apical Par complex, mutation in the Par complex on top of the G protein subunit genes resulted in symmetric divisions (Fuse et al., 2003).

An interesting observation led to a challenge to this model of size asymmetry. NBs depleted of the centriolar protein Sas4 do not have astral microtubules, yet the NBs still divide asymmetrically, both in fate and size (Cabernard et al., 2010). Imaging of Myosin II dynamics revealed that Myosin became asymmetric at anaphase. In NBs in which the microtubules had been depolymerised with Colcemid, but the metaphase arrest checkpoint had been silenced by *rough deal (rod)* mutation, Myosin still became asymmetric in mitosis and a cleavage furrow formed. Importantly, microtubules are still required for cytokinesis (Roth et al., 2015). In an attempt to find out what regulates the asymmetric localisation of Myosin, a small screen was conducted. Interestingly, *pins* mutation resulted in mislocalisation of Myosin regulatory light chain (Spaghetti squash, Sqh) in anaphase (Cabernard et al., 2010).

How does asymmetric Myosin lead to a shift of the cleavage furrow position? Detailed live imaging of NBs revealed that at anaphase the apical cell cortex extends asymmetrically relative to its size at metaphase. Interestingly, this is

independent of microtubules but dependent upon Pins. It is further sensitive to overexpression of Gαi (Connell et al., 2011). The current model therefore proposes that Gβγ promotes formation of a basal Myosin domain at anaphase. This is in part a result of its apical inhibition by Gαi. In *pins* mutants, Gβγ is able to interact with Gαi, resulting in the inactive heterotrimer. Thus far it is not known whether microtubule asymmetry can rescue defective Myosin II localisation as in mutant conditions which have been found to effect Myosin II localisation in anaphase, the microtubules are also effected.

1.3. Polarising the *Drosophila* Neuroblast

Two main models have emerged to explain how the basal fate determinants become polarised at the cell cortex. The first model was known as the “repressive cascade model” which focussed on a series of genetic interactions between different proteins inhibiting one another, eventually leading to basal localisation. A second simplified model, known as the “phospho-relay model” focussed on the direct phosphorylation of fate determinants by the kinase aPKC. Neither of these models is yet sufficient to explain how polarity is established and maintained.

1.3.1. The Repressive Cascade Model

The repressive cascade model focuses on the inter-relationship between aPKC, Lgl and the acto-myosin cytoskeleton leading to Miranda localisation (**Fig. 1-7**).

This model was predominantly based on early genetic interaction screens which showed that *zipper* (*zip,* Myosin II) negatively interacts with the tumour suppressor *lethal (2) giant larvae* (*lgl)* to promote neuroblast polarity. In summary, zygotic *zip* mutants exhibited normal Miranda localisation in embryonic neuroblasts (Ohshiro et al., 2000; Peng et al., 2000), though this is possibly due to the maternal contribution of Zipper protein or mRNA obscuring any phenotype from being observed. Mutating *lgl* resulted in a severe defect in the basal localisation of Miranda (being localised uniformly to the cell cortex and on the mitotic spindle). Interestingly, reducing the copy number of *zip* rescued the *lgl* phenotype, restoring basal Miranda crescents. This suggested that *lgl* mutants were in part causing the over activation of Myosin II which was preventing asymmetric Miranda localisation. Interestingly, inhibition of Myosins by 2,3-Butanedione monoxime (BDM) treatment resulted in Mira and Pon no longer localising to the cell cortex (Lu et al., 2000; Peng et al., 2000). Both, excess or insufficient Myosin results in Miranda localisation defects.

So what of aPKC? aPKC was shown to form a complex with Lgl and to phosphorylate Lgl *in vitro* and *in vivo* on three residues (Betschinger et al., 2003). The over-expression of non-phosphorylateable Lgl (Lgl^{3A}) resulted in loss of Mira asymmetry. Thereby, the authors concluded that the role of the Par-complex was likely to inhibit Lgl at the apical cortex resulting in the loss of Lgl inhibition of Myosin II.

Later work investigated the role of Myosin II in more detail. In this work germ-line clones for the myosin regulatory light chain (*spaghetti squash, sqh)* were generated. Germ-line clones were used to prevent the clouding of any phenotype by maternal contribution. Interestingly, sqh^{GLC} neuroblasts phenocopied the

neuroblasts in embryos injected with BDM. Namely, Mira was mislocalised from the basal cortex to the mitotic spindle. Microscopy suggested that Zip normally localises to the apical pole of the neuroblasts, however in *sqh*^{GLC} neuroblasts Zip and Lgl were both localised predominantly to the cytoplasm (Barros et al., 2003).

A second important piece of evidence for the role of Myosin was the injection of the Rho-kinase inhibitor Y-27632. This resulted in the uniform cortical localisation of Mira and the mislocalisation of Numb. Furthermore, this inhibitor also prevented the cortical localisation of Myosin II in NBs (Barros et al., 2003). A final interesting observation was that in neuroblasts ectopically expressing active Lgl (Lgl3A), Zipper was also mislocalised into the cytoplasm. This led to the proposed model that Lgl inhibits Myosin II which in turn inhibits Miranda localisation. Therefore, in *lgl* mutant neuroblasts Myosin II is active all around the cortex, excluding Mira from the cortex. However, when over-expressing Lgl3A (Active) Myosin II filaments were unable to form, thereby resulting in Mira being able to localise uniformly to the cortex. At the time the authors proposed that the apical accumulation of Myosin II in prophase was “pushing” Miranda to the basal pole (Barros et al., 2003).

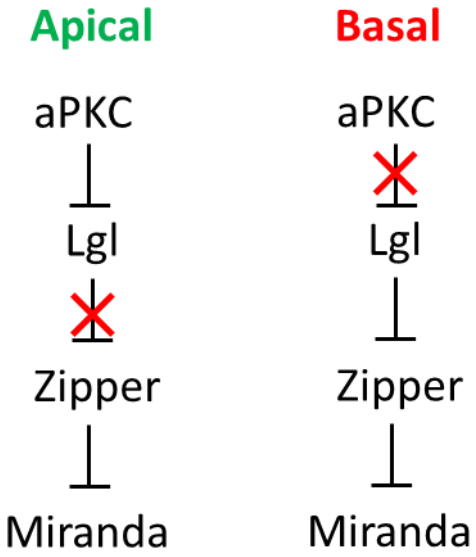

Figure 1-7 - Repressive Cascade Model – aPKC by localising apically inhibits Lgl specifically in the apical domain. This results in Lgl no longer suppressing Myosin II filament formation. These then inhibit Miranda localising to the apical pole. In the basal domain where aPKC is not present, Lgl is active. Lgl therefore inhibits Myosin II filament formation, allowing Miranda to localise.

Work on another Myosin (Myosin VI, *jaguar, jar*) at the same time suggested that *jar* is also required for asymmetric Mira localisation. In neuroblasts mutant for *jar* or in embryos injected with *jar* RNAi, Mira was mislocalised to the cytoplasm and mitotic spindle (Petritsch et al., 2003). A follow up study using fluorescence recovery after photobleaching (FRAP) analysis demonstrated that Miranda was not being pushed laterally by the activation of Myosin II. Instead, Mira exchanged directly between the cytoplasm and the basal crescent. The authors therefore proposed a model that while Zipper was inhibiting Mira from localising to the apical pole, it was Jar that was required to localise Mira to the basal pole, through an unknown mechanism (Erben et al., 2008).

The Myosin dependent repressive cascade model has come under some criticism and has since largely been discarded. This was largely due to the observation that the Rho kinase inhibitor used also inhibited aPKC at a much lower concentration than that injected into the embryos (Atwood and Prehoda,

2009). Furthermore, analysis of *jar* mutants revealed that the mutations used also encoded for a deletion in essential neighbouring tRNA synthase enzyme resulting in the possibility that the phenotypes observed were unspecific. However, this was not tested. Finally, recent work has demonstrated that Zip is not apical for very long in mitosis (Cabernard et al., 2010) and that Lgl is also not normally localised to the cortex in mitosis (Bell et al., 2015). Therefore, it seems unlikely that Lgl specifically inhibits Myosin II filament formation at the basal pole to maintain basal domain integrity.

However, the evidence for the involvement of the acto-myosin cytoskeleton has been observed on multiple occasions by different laboratories and it is important that any model for Miranda localisation to the basal cortex takes this into account. Instead, a simpler model referred to as the phospho-relay model has been adopted.

1.3.2. The Phosphorylation Relay Model

The most widely accepted model for how the *Drosophila* NB establishes and maintains cortical asymmetry is a model based on the phospho-exclusion of cell fate determinants (**Fig. 1-8**). This is largely based on the observation that in mutants for *par-3, apkc* or *par-6,* Miranda was localised uniformly around the cell cortex. Interestingly, Mira and Numb are both directly phosphorylated by aPKC (Atwood and Prehoda, 2009; Smith et al., 2007; Wirtz-Peitz et al., 2008). Mira contains five residues which are phosphorylated by aPKC *in vitro* within its N-terminal region. When Drosophila S2 cells were transiently transfected with Mira they observed that it was localised at the cell cortex (symmetrically). Interestingly, upon co-expression with aPKC, Mira was no longer cortical but instead was found

in the cytoplasm. To show this was a direct effect of aPKC phosphorylation, Miranda mutant for the five identified aPKC phosphorylation sites (*mira*^{5A}) was expressed in S2 cells and was found to be resistant to co-transfection with aPKC. Furthermore, “phospho-mimetic” mutation of Miranda decreased the cortical accumulation in S2 cells (Atwood and Prehoda, 2009).

To demonstrate the role of aPKC phosphorylation of Mira in the NB, Mira^{5A} was overexpressed and was shown to localise uniformly to the cortex even through metaphase (Atwood and Prehoda, 2009). This was in agreement with previous results that showed the expression of a truncated, constitutively active aPKC allele (aPKC$^{\Delta N}$, (Betschinger et al., 2003)) and an allele of aPKC targeted to the entire cell cortex (aPKC^{CAAX}, (Sotillos et al., 2004)) also resulted in displacement of Miranda from the cell cortex (Lee et al., 2005).

A question not answered was how the phosphorylation excludes Mira from the cell cortex? Recent work has shed light on this. Bioinformatics analysis identified a conserved membrane binding basic and hydrophobic motif (BH motif) in Mira as well as Numb and Lgl (Bailey and Prehoda, 2015; Dong et al., 2015). The BH motif coincided with the location of one of the key aPKC phosphorylation sites in Miranda (Serine 96) and a deletion of the BH motif removed the ability of Miranda to bind to the membrane of S2 cells. Furthermore, phospho-mimetic version of Mira S96D and 2RD in which aspartic acids were introduced instead of the serine, or flanking the serine, decreased affinity to the membrane of S2 cells as well as to phospholipids *in vitro*. This provided a good mechanistic insight into how Mira cortical localisation could be modulated by aPKC activity preventing the electrostatic interaction of Miranda with the cell membrane.

However, although this study provided a detailed description of how aPKC phosphorylation can regulate membrane binding it does not explain how asymmetry is generated. If Mira phosphorylation prevents all cortical association, it must be coupled to a phosphatase to enable dephosphorylation events which would thereby generate a stable boundary of basally localised unphosphorylated Mira and apical aPKC activity. Alternatively, a pool of Mira must not be phosphorylated by aPKC.

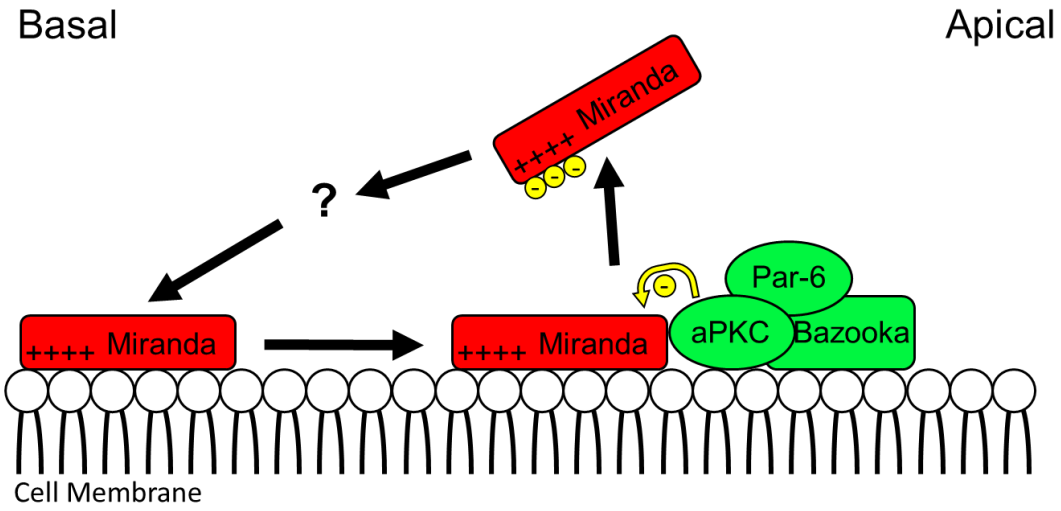

Figure 1-8 - The Phospho-Relay Model. Miranda (Red) associates directly with the plasma membrane through its Basic and Hydrophobic (BH) Motif. In the apical domain the Par-Complex (Green) is active. The Par complex phosphorylates (Yellow) the BH motif of Miranda preventing association with the plasma membrane. This results in the exclusion of Miranda into the cytoplasm. It is not known (?) how Miranda is then able to relocalise to the Basal cell cortex.

A phosphatase proposed to do this was the Protein Phosphatase 4 (PP4) complex (Sousa-Nunes and Somers, 2010). Mutations for the subunit *falafel (flfl)* as well as knockdown by RNAi of the subunits PP4-19C and PP4R2r all resulted in Mira being restricted to the cytoplasm and no longer forming a basal crescent in mitosis (Sousa-Nunes et al., 2009). Unfortunately, when examining the link between PP4 and aPKC they found that when aPKC was knocked down by RNAi

or inhibited by the overexpression of Lgl3A in a *flfl* mutant background, Mira was still cytoplasmic. This demonstrated that PP4 was actually working either upstream or in parallel but more importantly independent to aPKC activity.

More recent work identified another sub-unit of the PP4 complex implicated in the asymmetric localisation of Miranda with the cell cortex; Phospho-tyrosol phosphatase activator (Ptpa) (Zhang et al., 2015). This is another protein, localised to the nucleus in interphase which when absent results in Miranda becoming cytoplasmic in mitosis. Importantly, the phospo-site was identified which is dephosphorylated by the PP4 complex; Threonine 591. T591 is in the centre of the cargo binding domain of Miranda and not implicated in the activity of the BH motif – located almost 500 amino acids away. When this phospho site was mutated to a phospho-mimetic aspartic acid (591D), the authors reported that Miranda was cytoplasmic in metaphase, phenocopying Miranda localisation in *flfl* and *ptpa* mutants (Zhang et al., 2015). Therefore, to establish asymmetry there must either be another phosphatase involved which removes the phosphates which aPKC adds to Miranda, or Miranda does not need to be dephosphorylated to achieve asymmetric localisation. It is not known which kinase phosphorylates this site of Miranda.

A second phosphatase has also been implicated in the regulation of asymmetric cell division; PP2A. PP2A is a heterotrimeric complex composing of the subunits Microtubule star (Mts) which serves as the catalytic subunit, PP2A-29B which serves as a scaffolding subunit and finally Twins (Tws) which serves as a regulatory subunit. A potential role for PP2A was bought to light when *mts* mutants enhanced the *apkc* phenotype in a genetic screen for *Drosophila* eye

phenotypes (Ogawa et al., 2009). In the brain itself, perturbing PP2A function resulted in over proliferation and NB overgrowth.

The cause of this and the role of PP2A in asymmetric cell division was subject to some debate. Three papers in the same year demonstrated that perturbing PP2A resulted in uniformly cortical aPKC. Either in *mts* mutants (Wang et al., 2009), overexpression of a dominant negative *mts* (Ogawa et al. 2009) or in *tws* mutants (Chabu and Doe, 2009). Interestingly, in *mts* mutants Miranda was shown to localise asymmetrically despite the mislocalisation of aPKC, however Numb was no longer localised to the basal pole. In *tws* mutants, Miranda was reported to be no longer basally localised in mitosis. The *tws* and *mts* mutant phenotypes can be rescued by decreasing *aPKC* copy number and it is thought that PP2A inhibits aPKC activity through an interaction with Par-6. However, *mts* mutants could also be rescued by the expression of Polo kinase suggesting there are multiple roles for PP2A in the neuroblast, hence explaining the phenotypic variation observed. Importantly, PP2A has not yet been shown to regulate the phospho-serines and threonines in the N-terminus of Miranda.

If not dephosphorylation, how could the basal domain be established? Two other possibilities exist. One is that phosphorylated Miranda is degraded and replaced by newly folded Miranda (Bailey and Prehoda, 2015) this is unlikely due to the rapid nature of NB mitosis (Savoian and Rieder, 2002) although has not been formally tested. A second option is the existence of other interactions which stabilise the basal complex at the basal side of the cell. This has been shown in other contexts, in yeast the pheromone signalling protein ste5 interacts directly with phospho-lipids. However, this as well as its interaction with the G-protein Gβγ are required for stable membrane localisation (Winters et al., 2005).

It is possible that the genetic evidence presented as part of the repressive cascade model provides the answer to how Miranda is stabilised at the basal pole. The main criticism of the phospho-relay model currently is that it does not take into account the described role for acto-myosin in regulating asymmetric Miranda localisation. A second criticism is that the phospho-relay model has largely been conducted using unpolarised, *Drosophila* S2 cells as a paradigm for asymmetrically dividing cells. The model has not yet been robustly challenged in the system it seeks to explain.

1.4. Aims of this thesis

This study aims to re-examine *in vivo* how polarity proteins become asymmetrically segregated in mitosis. In the *C. elegans* zygote, polarity is first established by the activity of the acto-myosin cytoskeleton and then maintained by the inhibitory actions of the opposing par-proteins. In *Drosophila* NBs this is more complex. The basal proteins are not par-proteins and there has been no described inhibitory mechanism from these proteins onto the apical pole. Furthermore, cell size asymmetry requires a structural component to ensure the basal domain is segregated into the smaller GMC. The acto-myosin cytoskeleton has been implicated in *Drosophila* NBs for a long time, however the Phospho-relay model has yet to take this into account. We propose that NB polarity may be a multi-stage process in which both phosphorylation of substrates by aPKC and the activity of the acto-myosin cytoskeleton could be required to co-ordinate polarity establishment and maintenance.

In *Drosophila* NBs much of the current model has been inferred from the phenotypes observed in metaphase cells in either a mutant genetic context or

following RNAi expression. This has led to a detailed understanding of the genetic networks underlying cortical polarity. However, thus far the temporal dynamics of how these proteins localise has not been taken into account, blurring which components could be required for establishing polarity, which for maintaining it, or indeed both.

This study aimed to use live cell imaging of endogenously expressed, fluorescently tagged alleles of polarity proteins to understand the dynamics of how they become polarised at the cell cortex. Then to utilise genetic perturbation with pharmacological inhibition of known polarity regulators to understand which factors are required for the initial establishment of polarity and which are required to maintain it throughout mitosis in the *Drosophila* NB.

2. Materials and Methods

2.1. Fly husbandry

Flies were raised on molasses-based food and crossed at 25^{0}C unless otherwise stated. For heatshock experiments, L2 larvae were heat-shocked for 1 hour at 30^{0}C. Stocks were maintained at 18^{0}C.

2.1.1. Lines used in this study

Table 2-1 – *Drosophila* lines used in this study

Name	Description	Supplier	Stock Number/Reference
Baz::GFP (protein trap)	Bazooka endogenously tagged with GFP from the Carnegie protein trap project.	Bloomington	51572
*wor*GAL4	GAL4 under the control of the Worniu promoter for expression in neuroblasts.	Chris Doe	(Albertson et al., 2004)
UAS-Lifeact::Ruby	Life Act- F-Actin reporter fused to mRuby fluorescent protein.	Bloomington	35545
Mz1061-GAL4	Neuroblast GAL-4 driver	Cayetano gonzalez	(Ito et al., 1995)
UAS-Myr::EOS	A Myristoylation sequence tagged with the photo convertible protein tdEOS.	Bloomington	32226
ZipperGFP	Zipper endogenously tagged with GFP from the Carnegie Protein trap project	Bloomington	51564
UAS-aPKC^{RNAi}	UAS driven aPKC RNAi line from the Trip line database	Bloomington	34332
UAS-Lgl^{3A}::GFP	Non-Phosphorylateable form of Lgl3A which is known to inhibit aPKC	Gift from J.Knoblich	(Wirtz-Peitz et al., 2008)
aPKC::GFP^{BAC}	Bac Rescue construct for aPKC tagged with GFP	Francois Schweisguth	(Besson et al., 2015)
UAS-aPKC$^{\Delta N}$	Consitutively active aPKC overexpressed under UAS control.	J. Knoblich	(Betschinger et al., 2003)
UAS-GBP::Pon	GFP binding protein fused to the Pon localisation Domain	Marcos Gonzalez Gaitin	(Derivery et al., 2015)
L-3-3-3 GAL4	Neuroblast specific GAL4 Driver.	Bloomington	5820
Jar^{322}, β-Phers^{322}	Mutant containing a deletion of Jaguar (Myosin VI) and the neighbouring gene β-Phers.	Bloomington	8776
Df (3R) Crb 87-5	Deficiency on the third chromosome deleting a series of genes including Jaguar (Myosin VI) .	Bloomington	2363
UAS::Sqh^{EE}	Phospho-mimetic spaghetti squash (Myosin Regulatory Light Chain) Under UAS control.	Bloomington	64411
UAS-aPKC::CAAX	aPKC fused to CAAX prenylation motif	Andreas Wodarz	(Sotillos et al., 2004)
UAS-GBP::CAAX	GFP binding protein fused to the CAAX prenylation motif.	Daniel St. Johnston.	Unpub.

Miranda::mCherry^{BAC}	Bac Rescue construct tagged with mCherry and Miranda stem loops	JJ Lab	(Ramat et al., 2017)
UAS-Miranda::GFP	C-terminal GFP fusion for Miranda	Cayetano Gonzalez	(Mollinari and Lange, 2002)
aPKC^{K06403}	Null mutation for aPKC	Andreas Wodarz	(Wodarz et al., 2000)
Df(3R)I9	Third Chromosome deficiency covering the Miranda locus.	Bloomington	(Shen et al., 1997)
hsflipAct-FRT-STOP-FRT-GAL4 UASGFP	Stock for generating flip out clones.	Michel Gho	
hsflp, tubgal4UASNLSGFP; ;FRT82BtubGAL80	Stock for generating MARCM clones	Liqun Luo	(Lee and Luo, 1999)
W1118	Wild Type.	Bloomington	3605

2.1.2. Lines generated in this study

Table 2-2 – *Drosophila* lines generated in this study

Name	Description
Miranda::mCherryHA	Miranda tagged with mCherry and HA at the C-terminus
Miranda$^{\Delta BH}$::mCherryHA	Miranda tagged with mCherry and HA at the C-terminus. The BH motif has been deleted.
Miranda^{S96A}::mCherryHA	Miranda tagged with mCherry and HA at the C-terminus. Serine 96 mutated to alanine.
Miranda^{S96D}::mCherryHA	Miranda tagged with mCherry and HA at the C-terminus. Serine 96 mutated to aspartic acid
Mira^{194195DD}::mCherryHA	Miranda tagged with mCherry and HA at the C-terminus. Threnine 194 and Serine 195 mutated to aspartic acid.
Mira^{205206DD}::mCherryHA	Miranda tagged with mCherry and HA at the C-terminus. Threnine 204 and Serine 205 mutated to aspartic acid.
Mira^{5D}::mCherryHA	Miranda tagged with mCherry and HA at the C-terminus. Serine 96, Threonine 194, Serine 195, Threonine 204 and Serine 205 mutated to aspartic acid
Miranda^{591A}::mCherryHA	Miranda tagged with mCherry and HA on the C terminus. Threonine 591 mutated to alanine.
Miranda^{591D}::mCherryHA	Miranda tagged with mCherry and HA on the C terminus. Threonine 591 mutated to aspartic acid.

2.2. Generation of Knock-in Miranda alleles

2.2.1. Materials

Table 2-3 - Cloning Reagents

Reagent	Supplier	Cat #/Reference
Q5 DNA polymerase	New England Biolabs	M0491S
Gibson Assembly Master Mix	New England Biolabs	E2611
Fast Digest NotI	Thermo-Fisher Scientific	FD0593
Fast Digest XbaI	Thermo-Fisher Scientific	FD0684
Fast Digest EcoR1	Thermo-Fisher Scientific	FD0274
Neb 5-alpha competent E.Coli	New England Biolabs	C2987I
Qiagen Gel Extraction Kit	Qiagen	28704
Qiaprep-spin Miniprep kit	Qiagen	27104
Qiagen Midi-Prep kit	Qiagen	12143
invitrogen	Ultra-pure agarose	16500500

Table 2-4 - Plasmids

Reagent	Supplier	Cat #/Reference
BAC CH322-11P04	BAC clone containing Genomic Miranda DNA Sequence	BAC PAC resources/ CH322 11P04
pTriEx-mCherry::LANS4	Plasmid containing MCherry coding sequence	Addgene/ #60785
RIV^{white}	Plasmid for integrating new Miranda alleles into the endogenous locus via the attpko fly line.	(Baena-Lopez et al., 2013)

Table 2-5 - Oligonucleotides

Name	Sequence (5'-3')
MiramChHAF1Fwd	CGAATTCTCCGGAGCGAGGGTTGTTTTCTTTGC
MiramChHAF1Rev	GCACGTCGTAGGGGTACTTGTACAGCTCGTCCATG
MiramChHAF2Fwd	GTACAAGTACCCCTACGACGTGCCCGACTACGCCTAGGCTATTCCTTTGTAACAACTA
MiramChHAF2Rev	GTACCGGCGCGCCACTAATAAATGGAAAAAATAATTGATGCATTC
MiramChHAF3Fwd	GAATGCATCAATTATTTTTTCCATTTATTAGTGGCGCGCCGGTAC
MiramChHAF3Rev	CAAGGGTTTCCACTGGGC
MiraS96DmChHAF1Fwd	GCGTACTCCACGAATTCTC
MiraS96DmCHHAF1Rev	CAAGTCAGGAGTAGTCAGGAGTACGGAACAG
MiraS96DmChHAF2Fwd	CCGTACTCCTGACTACTCCTGACTTGCCGCA
MiraS96DmCHHAF2Rev	GTACCGGCGCGCCACTAA
MiraS96AmChHAF1Fwd	GGGCGTGCCCTTGGGCTC
MiraS96AmCHHAF1Rev	CGTAGGCGCTGCGGCAACGCAGGAGTACGGAACAGAC
MiraS96AmChHAF2Fwd	ACTCCTGCGTTGCCGCAGCGCCTACGCTTCC
MiraS96AmCHHAF2Rev	CGAAGTTATGGTACCGGCGC
MiraΔBHmChHAF1Fwd	CGAATTCTCCGGAGCGAGGGTTGTTTTCTTTGCCTC
MiraΔBHmChHAF1Rev	GCCGTATCCTTCGAGCTGGACGCGAA
MiraΔBHmChHAF2Fwd	GCTCGAAGGATACGGCCACCGGAAGC
MiraΔBHmChHAF2Rev	CAAGGGTTTCCACTGGGC
Mira194195DDmChHAF1Fwd	CACGAATTCTCCGGAGCG
Mira194195DDmChHAF1Rev	CTGTCTTGTCGTCAGCCAAC
Mira194195DDmChHAF2Fwd	TGGCTGACGACAAGACAG
Mira194195DDmChHAF2Rev	TACGAAGTTATGGTACCGG
Mira205206DDmChHAF1Fwd	CGAATTCTCCGGAGCGAG
Mira205206DDmChHAF1Rev	ATTCTCATCGTCCAGGGC

Mira205206DDmChHAF2Fwd	TGGACGATGAGAATTTATCGCACAAAG
Mira205206DDmChHAF2Rev	GTTATGGTACCGGCGCGC
Mira5DmChHAF1Fwd	GCGTACTCCACGAATTCTC
Mira5DmChHAF1Rev	CAAGTCAGGAGTAGTCAGGAGTACGGAACAG
Mira5DmChHAF2Fwd	CCGTACTCCTGACTACTCCTGACTTGCCGCA
Mira5DmChHAF2Rev	CAGGGCTTCGATGTGCCGATCTGTCTTGTCGTC
Mira5DmChHAF3Fwd	AAGACAGATCGGCTCATCGAAGCCCTGGACGATG
Mira5DmChHAF3Rev	GTACCGGCGCGCCACTAA
Mira591AmChHAF1Fwd	CGAATTCTCCGGAGCGGCCGCGAGGGTTGTTTTCTTTGC
Mira591AmChHAF1Rev	TCTGCAGCGCCTGGGAGGAGGATCTCAG
Mira591AmChHAF2Fwd	CTCCTCCCAGGCGCTGCAGAGCGAGGTATCGTTG
Mira591AmChHAF2Rev	GTACCGGCGCGCCACGCCGCGCGCCCTCGAG
Mira591DmChHAF1Fwd	CGAATTCTCCGGAGCGGCCGCGAGGGTTGTTTTCTTTGC
Mira591DmChHAF1Rev	TGCAGATCCTGGGAGAGATCTCAG
Mira591DmChHAF2Fwd	CCTCCCAGGATCTGCAGAGCGAGGTATCGTTGAAGGAG
Mira591DmChHAF2Rev	GTACCGGCGCGCCACGCCGCGCGCCCTCGAG

2.2.2. Molecular Cloning

Miranda::mCherry fusion constructs for the generation of knock in mutations were cloned into the RIV white vector (Baena-Lopez et al., 2013) by Gibson assembly. This involves the digest of the plasmid, and PCR amplification of overlapping fragments which are then ligated together by Gibson assembly (Gibson et al., 2009).

Plasmid Digest

RIV white vector was digested using the fast digest XhoI and NotI enzymes. The reaction was set up as detailed in table **2-6**.

Table 2-6 - Restriction Enzyme digestion

Component	Quantity
Riv White vector	1µg
Fast Digest XhoI	1µl
Fast Digest Not I	1µl
Fast Digest Buffer	2µl
dH_2O	To 20µl

Reaction was then incubated at 37ºC for 30 minutes.

Reaction mix was then loaded onto a 1% agarose gel containing gel red DNA stain (Biotium) in 1xTAE buffer (40mM Tris, 20mM Acetate and 1mM EDTA) and run for half an hour by electrophoresis alongside 1Kb+ DNA ladder (invitrogen) for size identification.

DNA bands were exposed using a UV transilluminator and excised with a scalpel blade. DNA was then purified using the gel extraction kit (Qiagen). DNA concentration was measured using a thermofisher nanodrop.

Preparation of Overlapping Fragments

Overlapping fragments were amplified by PCR using High fidelity Q5 DNA polymerase (New England Biolabs). To generate the overlaps, primers were designed that overlapped one another using the NEBuilder online tool.

Reaction was prepared as described in table **2-7**.

Table 2-7 - PCR mix recipe

Component	**Quantity**
Template	50ng
Forward Primer	0.5µl of 100µM stock
Reverse Primer	0.5µl of 100µM stock
10mM DNTP	1µl
Reaction Buffer	10µl
GC Enhancer	10µl
dH_2O	To 50µl

PCR reactions were performed using a G-storm thermocycler (GS4822). Cycling conditions were as described in table **2-8**.

Table 2-8 - PCR cycling conditions

Step	Duration	Temperature
Initial denaturation	1minute	95ºC
30x Cycles		
Denaturation	20 Seconds	95ºC
Primer Annealing	30 Seconds	55 ºC
Extension	2 minutes	72 ºC
End cycles		
Final Extenstion	5 minutes	72 ºC

PCR was visualised by running the reaction on a 1% agarose gel with Gel red in 1X TAE. Bands of the correct size for each amplicon were then excised from the gel under the trans-illuminator and purified using the gel extraction kit (Qiagen).

Gibson Assembly Reaction

To generate the final plasmids, the purified digested vector and PCR amplified overlapping fragments were combined with the Gibson assembly master enzyme mix (NEB). The mix contains the enzymes required for the protocol:

1. Exonuclease removes bases from the 5’ ends of each fragment.
2. Overlapping fragments anneal and the polymerase extends the DNA from the 3’ ends.
3. DNA ligase then seals gaps.

To assemble the fragments, the reaction mix was incubated at 50ºC for 30 minutes before being transformed into competent *E. coli*. Negative control

reactions were performed that did not contain the digested backbone and did not contain the enzyme master mix.

Transformation of competent *E.coli*

For each transformation reaction 50µl of competent NEB-5-alpha E-coli were thawed on ice. 2µl of the assembly reaction is mixed with the bacteria by gentle pipetting before being incubated on ice for 30 minutes. Bacteria were then heat-shocked for 30 seconds at 42ºC. Bacteria were then left on ice for 2 minutes before being mixed with 950µl of room temperature SOC (Super Optimal broth with Catabolite repression, NEB) media. Bacteria were then incubated at 37ºC for 60 minutes while shaking. 100µl of the bacteria were then spread by glass beads onto LB-Agar plates containing ampicillin (School of Life Sciences, Central Technical Services). Plates were incubated overnight at 37ºC.

Screening clones for successful assembly of plasmid

If assembly reaction plates had many more colonies than negative control plates, 5 colonies were picked and used to inoculate 3ml LB broth (Luria-Bertani Broth; School of Life sciences, Central Technical Services) containing ampicillin. Bacteria were then left to grow over night at 37ºC while shaking.

The following morning, bacteria were centrifuged for 3 minutes at 8000x rpm and plasmids were purified by Miniprep (Qiagen). 2µl of the purified plasmid was then digested using Fast Digest EcoR1 to screen for successful integration of the Miranda allele of interest by agarose gel electrophoresis.

Positive clones were then sequenced. DNA sequencing was performed by DNA Sequencing & Services (MRC I PPU, School of Life Sciences, University of Dundee, Scotland, www.dnaseq.co.uk) using Applied Biosystems Big-Dye Ver 3.1 chemistry on an Applied Biosystems model 3730 automated capillary DNA sequencer. Clones of the correct sequence were then re transformed into competent *E. coli* and re-purified using a midiprep kit (Qiagen) for generation of transgenic *Drosophila* lines.

2.2.3. Transgenesis

To generate the Miranda knock-in alleles, we utilised a previously described technique (Baena-Lopez et al., 2013) for PhiC31 mediated integration of Miranda alleles into the endogenous locus. To do this, a section of the 5'UTR and coding sequence of Miranda was deleted by CRISPR/Cas9 and replaced with an attp landing site (**Fig. 2-1**). This work was conducted by *InDroso* (Rennes, France).

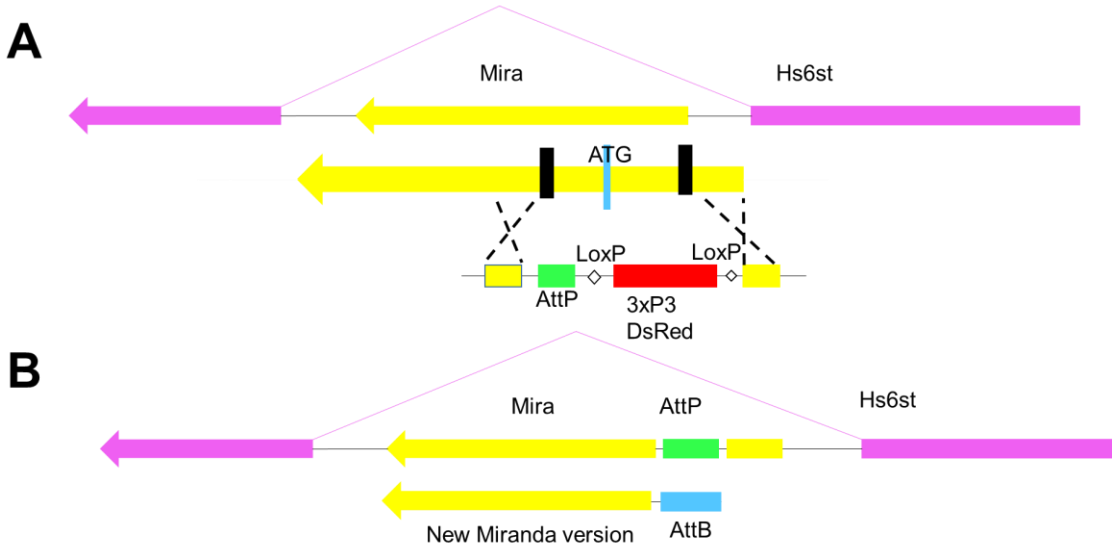

Figure 2-1 – Generation of Miranda Knock-in alleles. A) Miranda^{attpKO}was generated by CRISPR/CAS9. Homology arims in the 5' UTR and coding sequence, inserted the attp site, with Dsred for screening flies, flanked by loxP sites for its removal by cre expression. **B)** Knock in alleles were generated by injection new Miranda alleles with an AttB site into embryos carrying the attpKO allele. The new Miranda allele was then integrated into the endogenous locus.

Embryos were co-injected with the prepared plasmid and PhiC31 integrase by the Fly injection service, University of Cambridge Department of Genetics. Upon receipt of injected flies, they were crossed together. To identify transgenic flies, offspring from this first generation were screened for red eyes, due to the *mini-white* gene being present in the RIV white vector. Red-eyed virgins and males were then crossed together to generate a balanced stock. All lines were not homozygous viable.

2.3. Isolated Culture of Neuroblasts

2.3.1. Materials

Table 2-9 - Isolated Neuroblast Culture Reagents

Reagent	Supplier	Cat #/Reference
Collagenase from *Clostridium histolyticum*	Sigma	C0130
Schneider's Medium	Lonza	04-351Q
Glucose	VWR	101174Y
Fibrinogen from human plasma	Sigma	F3879
Insulin from bovine pancreas	Sigma	I0516
Thrombin from bovine plasma	Sigma	T7513
Foetal Calf Serum	Gibco	12657011
Fly Serum	Prepared in laboratory	n/a

2.3.2. Buffer Recipes

Collagenase Buffer:

800mg NaCl, 20mg KCl, 5mg NaH_2PO_4, 100mg $NaHCO_3$ and 100mg D(+)Glucose. In 100ml MiliQ sterile water

Supplemented Schneider's medium:

3ml Schneider's medium, glucose (1g/l), 300µl FCS,75 µl fly serum,2µl Insulin.

To prepare fly serum:

1.3g flies were added to 7ml of Schneider's medium supplemented with glucose and manually homogenised on ice for about twenty minutes. Solution was then centrifuged for 15 min at 5000x rpm. Supernatant was then transferred into 1.5ml tubes and incubate at 60ºC for 5min. Tubes were then centrifuged at 12000x rpm for 90 minutes at 4ºC then sterile filtered and aliquoted before being stored at -20ºC.

2.3.3. Isolation of Neuroblasts

To generate isolated NBs, third instar larvae were washed twice in water before being dissected in Collagenase Buffer (CB). Collagenase was then added to the buffer and brains were incubated in the dark for 25 minutes. Following incubation, brains were transferred by a tungsten needle into a 4µl drop of fibrinogen in a 35mm glass bottomed dish (World Precision Instruments). The brain lobes were then manually dissociated using tungsten needles. Following dissociation, cells were left to settle for 10 minutes. After 10 minutes, 1µl of thrombin (Sigma) was added to the drop causing it to clot within 10 minutes. After 10 minutes, supplemented Schneider's medium was pipetted on top of the cells. Samples were then left for 30 minutes prior to imaging.

2.3.4. Drug Treatment of isolated NBS

For drug treatment of isolated NBs all inhibitors were diluted to 2x final concentration in the same volume of supplemented Scheniders medium used when isolating the NBs. Drugs were then pipetted into the media on the cells and pipetted up and down to mix. Due to the cells being in the clot of fibrinogen, they rarely moved following drug treatment.

The following drugs and concentrations were used as indicated in table **2:10**.

Table 2-10 - Small Molecule Inhibitors

Drug	Description	Supplier	Stock Number	Concentration
Colcemid	Depolyermises Microtubules	Cambiochem	234109	50µM
Y-27632	Rho-kinase inhibitor	Abcam Biochemicals	Ab120129	25-200µM
Latrunculin-A	Prevents F-Actin polymerisation	Sigma	L5163	1-5µM
ML-7	Myosin Light Chain Kinase inhibitor	Sigma	I2764	10-20µM

2.4. Fixation and immunofluorescene

2.4.1. Materials

Table 2-11 - Primary Antibodies

Antibody Target	Host Species	Supplier	Cat #/Reference	Concentration
Miranda	Rabbit	Cayetano Gonzalez	(Mollinari and Lange, 2002)	1:250 (IF)
PKCζ	Rabbit	Santa cruz-Biotech	SC-216	1:1000 (IF
GFP	Mouse	Life Technologies	A11120	1:400 (IF)
Numb	Guinea Pig	James Skeath	(O'Connor and Skeath, 2003)	1:500 (IF)
HA	Rat	Roche	11867423001	1:500 (IF)
Par-6	Guinea Pig	Andreas Wodarz	(Kim et al., 2009)	1:500 (IF)
Tubulin	Rabbit	Developmental Studies Hybridoma Bank	12G10	1:1000 (W.B)
Jaguar(MyoVI)	Mouse	Kathryn Miller	(Morrison and Miller, 2008)	1:20 (W.B)
Deadpan	Guinea Pig	James Skeath	(O'Connor and Skeath, 2003)	1:500 (IF)

Table 2-12 - Secondary Antibodies and other fluorescent reagents

Name	Host Species	Supplier	Cat #/Reference	Concentration
Rabbit Alexa 647	Donkey	Life Technologies	A21244	1:250 (IF)
Rabbit Alexa 594	Donkey	Life Technologies	A21207	1:1000 (IF
Mouse Alexa 488	Donkey	Life Technologies	A21202	1:400 (IF)
Rat Alexa 647	Donkey	Life Technologies	A21247	1:500 (IF)
Rabbit HRP	Goat	Life Technologies	A24537	1:500 (W.B)
Mouse HRP	Goat	Life Technologies	A24518	1:500 (W.B)
Phalloidin Alexa 488	n/a	Life Technologies	A12379	5:200
DAPI	n/a	Sigma	D8417	1:1000

Table 2-13 - Immuno-fluorescence reagents

Reagent	Supplier	Catalogue Number
Formaldehyde	Sigma	F8775
Triton	Sigma	X100
Tween	VWR	437082Q
Glycerol	Sigma	G5516
Vectashield	Vector Labs	H-1000

2.4.2. Buffer Composition

1x PBS: 137 mM NaCl, 10 mM Na_2HPO_4, 1.8 KH_2PO_4, 2.7 mM KCl, pH of 7.4 in dH_2O.

2.4.3. Fixation and immunofluorescence of isolated NBs

For fixation of isolated NBs, Supplemented Schneider's medium was replaced with 4% Formaldehyde in PBS (Phosphate buffered saline) and incubated in the dark for 10 minutes. Following fixation, cells were washed three times in 1X PBS before being incubated for one hour in PBS-0.1% Tween (PBT). Cells were then incubated overnight in primary antibodies dissolved in PBT while gently rocking at 4ºC.

The following morning, primary antibodies were removed and the cells were washed 3x while gently shaking in PBT. Secondary antibodies diluted in PBT were then added to the cells. Cells were incubated for 90 minutes. Secondary antibodies were then removed and the cells were washed three times in 1xPBT before a further three washed in 1xPBS. PBS was then replaced with vectashield mounting media. Cells were then ready for imaging.

2.4.4. Fixation and immunofluorescence of whole brains

For whole mount brains. 3rd Instar larvae were identified by crawling across the food. They were collected and then rinsed in 1xPBS followed by 70% ethanol. Brains were then dissected out of the larvae in 1x PBS in a nine well glass dish. 1x PBS was then replaced with 4% methanol free para-formaldehyde diluted in 1x PBS. Brains were fixed for twenty minutes. Following fixation, brains were rinsed three times with 1x PBS, before washing in 1x PBS for 10 minutes with

gentle shaking. Brains were permeabilised in blocking solution (1x PBS-0.1%Triton -10%FCS) for three hours. Blocking solution was then replaced with primary antibody diluted to an appropriate concentration in 1xPBS-0.1%Triton and incubated at 4°C overnight. The following morning, brains were rinsed three times in 1x PBS-0.1% Triton before washing for 10 minutes in 1xPBS-0.1% Triton and then undergoing three more rinses. Secondary antibody was then added, diluted in 1xPBS-0.1% Triton. Brains were then incubated in the dark at room temperature for two hours. Two further washes in 1xPBS occurred before PBS was replaced with 1xPBS-50% Glycerol for 2 hours. This was then replaced with 1xPBS-70% Glycerol and left at 4°C overnight. The following morning brains were mounted in Vectashield with the ventral surface facing the coverslip to easily image the NBs.

For drug treatment of whole brains, brains were dissected in Schneiders medium and then incubated in the inhibitor of interest prior to fixation.

2.4.5. Imaging of Fixed samples

Fixed samples were imaged using a Leica SP8 laser scanning confocal microscope, 63X water objective (N.A 1.2).

2.5. Live cell imaging

2.5.1. Time-lapse microscopy of isolated NBs

Isolated NBs were imaged using a 100x OIL objective (N.A. 1.45) on a spinning disk confocal microscope. Typically, 5 z-sections of 0.7µm spacing were acquired every 1-2minutes. NBs were selected for imaging based upon morphology. For

imaging Miranda::Cherry constructs, 30% of a 594nm laser was used and cells were exposed for 100ms at each frame.

2.5.2. Fluorescence Recovery after Photobleaching (FRAP).

FRAP experiments were conducted on a Leica SP8 laser scanning confocal microscope using the 63x water objective (N.A 1.2). Miranda::mCherry was imaged using 2.5% of the 561nm laser. Bleaching was performed with 40% 561nm laser on a 2.5 x 2.5µm spot. Recovery was then monitored every 2s for 30s, then every 5 seconds for 3 minutes.

2.5.3. Photoconversion

Photoconversion experiments were conducted on a Leica SP8 laser scanning confocal microscope using the 63x water objective (N.A 1.2). tdEOS (488, unconverted) was imaged using 0.4% of the 488nm laser. tdEOS (561, converted) was imaged using 1.8% of the 561nm laser. Conversion was performed with 7.5% 405nm laser three times on a 2.5 x 2.5µm spot. Fluorescence was then monitored every 2s for 30s, then every 5 seconds for 3 minutes.

2.5.4. Data Analysis

Images were analysed using the FIJI software platform (Schindelin et al., 2012). For live imaging experiments, background was subtracted and then a 3D-gaussian blur was applied (0.8, 0.8, 1) after any intensity measurements were taken. For 3D volume measurements, nuclei were measured in IMARIS (Bitplane). All statistical analysis was performed using Microsoft Excel and R-

studio. Details of the statistical analysis can be found in the figure legends of the respective experiments. For FRAP experiments, data was normalised using the standard methods described (Goldman et al., 2006). Curves were fitted and t1/2 estimated using the easyFRAP matlab tool (Rapsomaniki et al., 2012).

2.6. Western Blotting

2.6.1. Materials

Table 2-14 - Western Blotting Reagents

Reagent	Manufacturer	Cat. Number
cOmplete Protease Inhibitor	Roche	11697498001
Mini-Protean TGX stain free gel	Bio-Rad	456-8125
ECL Western Blotting substrate	Thermo-fisher	32106
Amersham Protran 0.2µm Nitrocellulose membrane	G.E. healthcare	10600001
X-Ray film	Konica Minolta	A9KN
Sample Buffer 4X	Life Technologies	NP0007
Sample reducing agent 10X	Life Technologies	NP0009

2.6.2. Buffers

RIPA Buffer: 10mM Tris-Cl (pH 8.0), 1mM EDTA, 0.5 mM EGTA, 1% Triton X-100, 0.1% SDS, 140mM NaCl + 1 protease inhibitor tablet per 10ml.

10x transfer buffer: 480mM Tris, 390mM Glycine, 0.01% SDS in dH_2O

1x Running Buffer: 25mM Tris, 192mM Glycine, 0.1% SDS in dH_2O

TBS: 50mM Tris-Cl (pH 7.6), 150mM NaCl, dH_2O, adjust pH with HCl.

2.6.3. Method

5 brains per experiment were homogenised in RIPA buffer for 20 minutes with manual grinding, before being cleared by centrifugation for 10 minutes at 4^0C. 15µg of protein lysate was then mixed with Sample buffer and Reducing agent before being boiled at 95^0C for 5 minutes. Samples were then loaded into the poly-acrylamide gel (Bio-Rad) and run by electrophoresis until the front had reached the bottom of the gel.

Gel was then removed from the tank and placed in the transfer cassette next to the membrane (GE healthcare) between layers of paper and sponge soaked in transfer buffer. Transfer was done at 20V overnight in transfer buffer.

Membrane was then removed from the transfer cassette and washed twice in dH_2O. Membrane was blocked in 5% milk in TBS-0.1%Tween (TBST) for 90 minutes while shaking. Membrane was then rinsed twice in TBST. For primary antibody staining, antibody was diluted in TBST and sealed with membrane in a plastic pocket. It was then left under agitation over night at 4ºC.

Following primary antibody, the membrane was washed while shaking 3 times for 5 minutes each in TBST. Secondary antibody was then diluted in TBST and incubated with the membrane for 2 hours at room temperature under agitation. Following secondary antibody incubation, membrane was washed three times with TBST, twice with TBS and then incubated for 1 minute in ECL mix. Membrane was then developed with X-Ray film and scanned.

3. Results Chapter 1 – Establishing Cortical Asymmetry

3.1. Introduction

The observation that in mitosis the neuroblast (NB) segregates cell fate determinants to a basal crescent in mitosis is not new. In fact for many years genetic screens have identified the key genes required for this process (Sousa-Nunes and Somers, 2013). However, mechanistic understanding has been lacking. This is predominantly due to the majority of studies observing the localisation of fate determinants in mitosis, and then inferring the upstream events based upon genetic or physical interactions. Alternatively, the cortical localisation of fate determinants in unpolarised S2 cells has been used as a proxy (Atwood and Prehoda, 2009; Bailey and Prehoda, 2015; Zhang et al., 2015). This results in the loss of vital information, namely the temporal dynamics of how these elements fit together in NBs.

In this chapter I describe our experiments looking at the dynamics of the cortical polarisation of *Drosophila* larval NBs, focussing on the transition of Miranda from uniform cortical localisation in interphase, to localising to a basal crescent in mitosis

3.2. Characterisation of apical and basal domain size

Although the distribution of proteins at the NB cell cortex has been widely described, accurate measurements of the distribution of the proteins at the cell cortex has not been fully carried out. This can provide a useful basis for understanding how polarity is established and maintained.

Therefore, we decided to use the advantageous system of isolated NB culture (Pampalona et al., 2015) to analyse the fluorescence distribution of antibody labelled or fluorescently tagged proteins at the cell cortex without interference from surrounding cells. A similar experiment was previously carried out examining the fluorescence distribution of polarity proteins in the *C. elegans* embryo. Examination of the fluorescence profiles revealed that there is a clear overlap between the two domains (Goehring et al., 2011a).

In the NB it is proposed that polarity is maintained by the direct phosphorylation of cell fate determinants by the apically localised aPKC (Atwood and Prehoda, 2009; Bailey and Prehoda, 2015). We hypothesised that if this was the mechanism regulating NB polarity, we would observe an overlap in the intensity gradients between aPKC and its substrates.

To this end we performed immunofluorescence comparing aPKC and the basally localised Numb. Contrary to *C. elegans* there was no overlap in the fluorescence distribution. Instead we detected a gap between the two proteins of 7µm ± 2 µm (**Fig. 3-1A, A'**; n=8). Using a line expressing endogenous Bazooka::GFP (Baz GFP), (Buszczak et al., 2006) and a Mira BAC rescue construct (Mira::mCherry^{BAC}) generated in the lab (Ramat et al., 2017) we confirmed this finding. Mira and Baz were separated by a mean gap size of 12µm ± 2.6µm (**Fig. 3-1B, B'**; n=10). Inspection of the fluorescent profiles showed that the intensity of Miranda plateaus at the cortex, suggesting that there is not a diffusion gradient from the centre of the basal crescent, to the edge.

We then asked whether the localisation of Mira and Numb at the basal pole matched. Interestingly, the fluorescence profile of Numb was different to that of Mira (**Fig. 3-1C, C'**; n=7) at the basal cortex. This corresponded with previous

evidence suggesting that there are two different mechanisms responsible for Miranda and Numb localisation (Lee et al., 2006a; Lu et al., 1998; Sousa-Nunes et al., 2009).

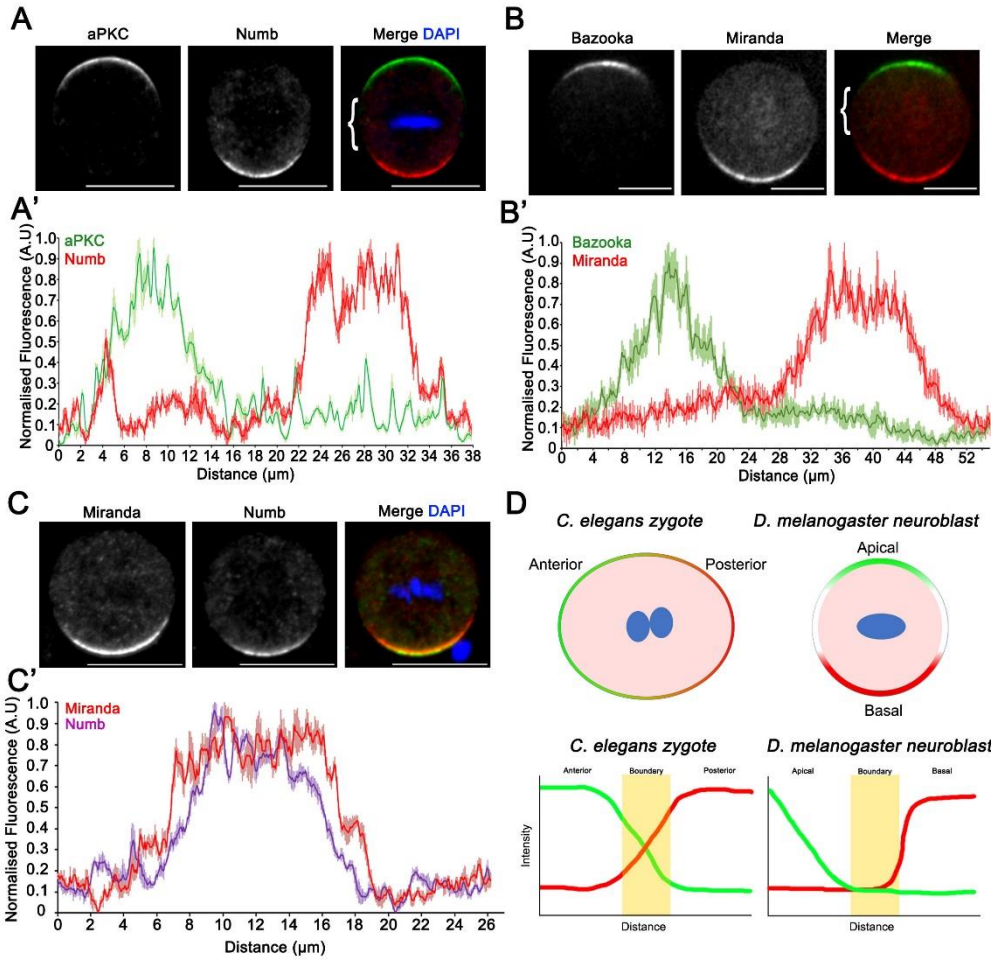

Figure 3-1 - There is a gap between the apical and basal domain. A) Immunofluorescence on a *w*^{1118} isolated NB. aPKC (Green), Numb (Red). Gap labelled with bracket. **A')** Quantification of average fluorescence intensity normalised to min max over 5 z sections. There is a gap between the aPKC and Numb domain of 7µm±2 (n=8). Error bars: Standard deviation**. B)** Representative example of a live, metaphase, isolated NB expressing Baz::GFP and Mira::mCherry^{BAC}. Gap denoted by bracket. **B')** Quantification of Baz and Mira domain size by normalised fluorescence intensity. There was an average gap size of 12µm±2.6 (n=10)**. C)** Immunofluorescence of *w*^{1118} isolated NB. Miranda (red), Numb (Green). **C')** Quantification of Mira and Numb domain size by fluorescence intensity. Mira (red) displays a broader domain than Numb (purple, n=7), **D)** Diagram demonstrating differences between *C.elegans* zygote and *Drosophila* NBs. In *C.elegans* the anterior and posterior domains overlap and mutually exclude one another. In NBs there is a gap between the apical and basal domain. Scale bars: 10µm

We concluded that there appears to be another layer of structural compartmentalisation compared to the *C. elegans* zygote due to the differences in fluorescence intensity profiles (**Fig. 3-1D).**

To fully characterise the domains in both space and time we then decided to perform high resolution time-lapse microscopy to observe the formation of the apical and basal domains as the cell enters mitosis.

3.3. High resolution live cell imaging of cortical polarisation

Mira has been reported to localise in different ways during interphase, with some claims that it localises apically (Shen et al., 1998), while other reports state that it localises uniformly to the cell cortex (Sousa-Nunes et al., 2009). We wanted to clarify the interphase localisation of Miranda and assay the dynamics of how Mira re-localises to form a basal crescent.

Previously, the dynamics of Miranda protein localisation have been analysed through fixed cell analysis (Erben et al., 2008) or through overexpression of fusion proteins using the GAL4/UAS system (Chabu and Doe, 2008). Using the *baz::GFP*; *miranda::mCherry*^{BAC} background we were able to assay protein localisation at endogenous levels through the cell cycle.

We observed that in interphase Mira was localised uniformly to the cell cortex (**Fig. 3-2A**, -33 min pre NEB). Once Baz began to localise apically Mira was cleared from the cortex in an apical to basal direction before being almost completely cleared from the cortex shortly before NEB (**Fig. 3-2A**, -8 to -4 mins pre NEB, n=5). Following NEB Mira re-localised to the cortex and formed a basal crescent (**Fig. 3-2A** +4 after NEB, n=5). The same dynamics were observed in

isolated neuroblasts expressing Miranda::mCherry^{BAC} with an aPKC::GFP BAC construct ((Besson et al., 2015), aPKC::GFP^{BAC}, **Fig 3-2B** n=10).

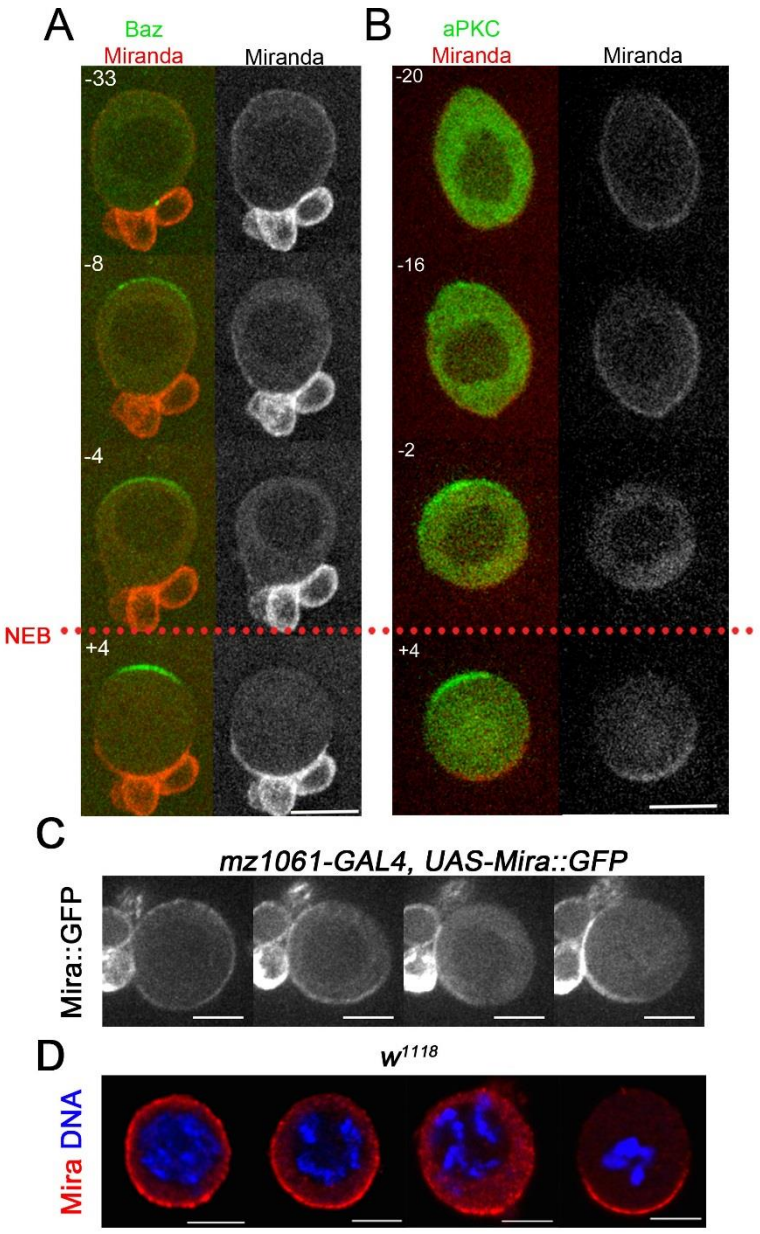

Figure 3-2 - Miranda is cleared from the interphase cortex coincident with the localisation of the Par complex A) Stills from a timelapse series of an isolated NB expressing Baz::GFP, Mira^{BAC}::mCherry. Mira is uniformly cortical in interphase (-33) before being cleared in an apical to basal direction prior to NEB (-8 to-4) after NEB Mira returns to form a basal crescent (+4, n=5). **B)** Stills from an image-series of an isolated NB expressing aPKC::GFP^{BAC}, Mira::mCherry^{BAC}. Mira is cleared in an apical to basal direction coincident with the localisation of aPKC until it is almost completely cleared from the cortex (-2, n=10). After NEB Mira returns to form a basal crescent (+4). **C)** NB in primary culture expressing UAS-GFP::Mira under the control of Mz1061-GAL4. Clearance dynamics are similar to the wild type (n=22). **D)** Fixed *w^{1118}* NBs showing Miranda clearance from the cell cortex by immunofluorescence against Miranda (n=8). Scale bars: 10µm. Time is minutes relative to NEB.

Given that the *miranda::mCherry*^{BAC} flies were not homozygous viable and could have an effect on protein stability or localisation, the experiment was repeated with a Miranda::GFP fusion protein overexpressed under UAS control ((Mollinari and Lange, 2002), **Fig. 3-2C**, n=22). We also were able to correlate our clearance localisation of Miranda with fixed, wild type (WT) cultured NBs (**Fig. 3-2D**, n=8).

We concluded that Miranda is uniformly cortical in interphase and is then almost completely removed from the cell cortex prior to NEB. Following NEB, Mira returns to form a basal crescent.

Previously the actin cytoskeleton has been shown to be required for Miranda cortical localisation in mitosis (Broadus and Doe, 1998; Shen et al., 1997). We therefore sought to understand whether the actin cytoskeleton was required for the localisation of Miranda from the interphase cell cortex or its removal prior to NEB.

3.4. F-Actin is not required for the interphase localisation of Miranda

The phospho-relay model explaining Mira asymmetry (phospho-regulated direct binding via Basic and hydrophobic motif to the plasma membrane), does not take into account a previously published role for the Actin cytoskeleton in this process (Atwood and Prehoda, 2009; Bailey and Prehoda, 2015). Previously, two studies have shown that in embryonic NBs *in vivo* and *ex vivo* Miranda is sensitive to treatment by actin depolymerising agents (Broadus and Doe, 1998; Shen et al.,

1997). However, the role of actin in Mira localisation to the interphase cell cortex has not been tested. To address this we treated wild type (*w*^{1118}) larval brains with 5µM Latrunculin -A (Lat-A) or the equivalent amount of DMSO (vehicle control) for 20 minutes prior to fixing and performing immunofluorescence against Miranda (**Fig. 3-3A**).

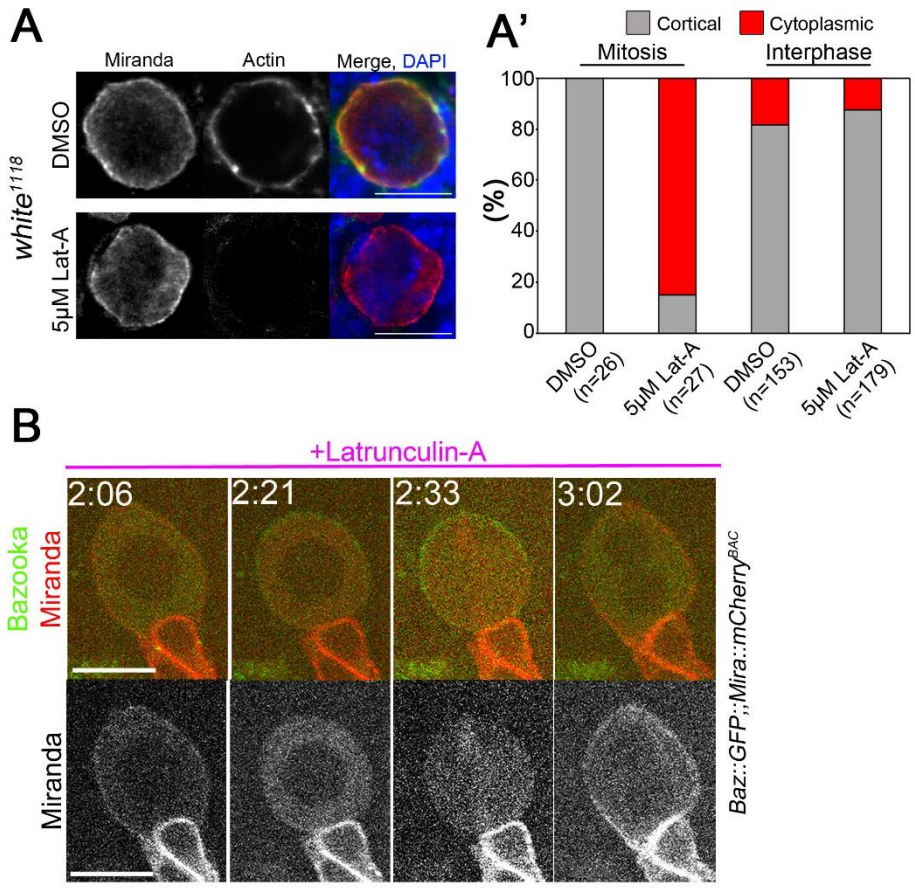

Figure 3-3 – Interphase Miranda localisation is independent of the F-Actin network. **A)** Fixed *w*^{1118} NBs in whole brains. Immunofluorescence against Miranda (red), and Phalloidin (green) labelling of F-Actin demonstrates that Miranda is still at the cell membrane in interphase NBs after F-Actin depletion by Lat-A treatment. **A')** Quantification of the percentage of NBs either showing cortical (gray) or cytoplasmic (red) localisation in interphase and mitosis following DMSO or Lat-A treatment.. **B)** Stills from a timelapse series of an isolated NB expressing Bazooka::GFP (Green) and Miranda::mCherry^{BAC} (Red). F-Actin is depleted by 1µM Lat-A as evidenced by the failure to complete cytokinesis resulting in a multinucleated cell (3:02). Clearance of Miranda from the interphase cortex is still able to occur (2:06-2:21) however after NEB, Miranda is unable to form a basal crescent, instead localising to the microtubules (2:33, n=12). Scale Bar: 10µm. Time: hh:mm

Despite mitotic NBs showing loss of cortical Mira after Lat A treatment (DMSO: 0% cytoplasmic, n=26, Lat-A: 85% cytoplasmic, n=27), interphase NBs retained robust cortical Mira localisation following Lat-A treatment (DMSO: 18% cytoplasmic, n=153, Lat-A: 12% cytoplasmic, n=179). Therefore we concluded that Mira was not dependent on F-actin to localise to the interphase cell cortex.

We then wanted to understand whether Lat-A treatment affected the clearance of Mira from the interphase cell cortex. Previously, it was suggested that Mira was "pushed" to the basal half of the cell by Myosin activity (Barros et al., 2003). To this end we disrupted the F-Actin network in NBs expressing Bazooka::GFP with Miranda::mCherry^{BAC} and observed the dynamics of polarisation. As in the wild type cells (**Fig. 3-2A**), Mira was cleared from the cortex coincident with the localisation of Bazooka to the apical pole. Interestingly, contrary to control cells, Bazooka spread laterally rapidly until it covered the entire cell cortex demonstrating that an intact actin cytoskeleton is required to maintain Bazooka at the apical pole. The clearance of Mira from the apical pole is therefore independent of an intact F-Actin cytoskeleton. However, the formation of a basal crescent is actin dependent (**Fig. 3-3B**; n=12). Therefore, it appears that in interphase Mira is bound directly to the plasma membrane, presumably through its Basic and Hydrophobic motif (Bailey and Prehoda, 2015).

3.5. F-Actin is required to anchor Miranda to the Basal Pole.

Although F-actin is required for Miranda localisation to the basal cell cortex, this does not demonstrate that F-actin is required to maintain basal localisation, instead it may just be required to establish the basal domain. To assess the role of F-Actin in maintaining asymmetric Mira localisation during mitosis we arrested NBs in a metaphase like state by depolymerising the microtubules (C-metaphase) (Kleinfeld and Sisken, 1966). It is known that Miranda localisation is not dependent on an intact microtubule network (Broadus and Doe, 1998).

Isolated NBs expressing Bazooka::GFP and Miranda::mCherry^{BAC} were arrested using 50µM Colcemid then treated with 5µM Lat-A, which causes the uniform loss of cortical F-Actin (**Fig. 3-4B**; n=10). Mira was lost from the cortex (20/20 NBs). At the same time the cells rounded up and Bazooka spread laterally until it covered the entirety of the cell cortex. This raised the interesting question of whether it was the spread of Bazooka and therefore aPKC which was phosphorylating basal Mira and preventing membrane association, or whether F-Actin provides an anchor for Miranda in metaphase.

If the spread of the Par-complex was the cause of Mira loss, Mira should be cleared from the cortex in an apical to basal direction. Instead if F-Actin was providing an anchoring function then we would expect to see Miranda lost uniformly from the cortex (**Fig. 3-4C**). To address this we first confirmed that actin depolymerisation occurred uniformly around the cell cortex (**Fig. 3-4A, A'**; n=10). Then we took high resolution timelapse movies of C-metaphase NBs following Lat-A treatment, straightened the cell cortex at each time point and plotted them as a kymographs to observe the dynamics of Miranda loss. Furthermore, we plotted the Miranda intensity at the centre and periphery of the basal crescent

over time. We found that Miranda basal localisation was always lost homogenously (**Fig. 3-4C', D**; n=13) suggesting that F-Actin is required to anchor Miranda to the cell cortex. The kymographs also revealed that Miranda was lost from the cortex 2.8±1min (n=13) prior to the Par complex being detectable basally.

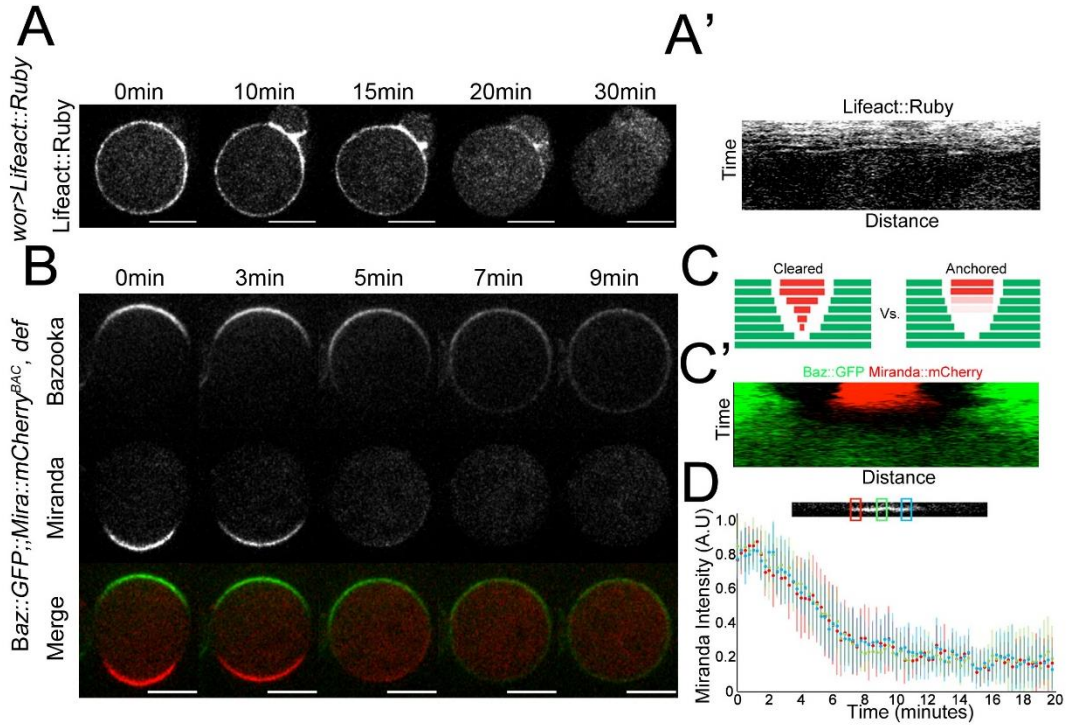

Figure 3-4 – F-Actin is required to maintain basal Miranda crescents. A) Stills of a timelapse of a C-metaphase arrested isolated NB expressing UAS-Lifeact::Ruby under the control of *worniu*-GAL4. F Actin is lost uniformly from the cell cortex after Lat-A treatment (drug added timepoint 0min, n=10) as evidenced by the kymograph (**A'**). **B)** Stills of a timelapse of a C-metaphase arrested isolated NB expressing Baz::GFP and Mira::mCherry^{BAC}. After Lat-A treatment (drug added at time point 0min) Bazooka spreads in an apical to basal direction while Miranda falls off the cortex into the cytoplasm. **C)** Diagram depicting whether Miranda is cleared such as prior to NEB after Lat-A treatment or whether it falls uniformly, suggesting F-Actin is anchoring it to the cell cortex. **C')** Kymograph of NB cell cortex from NB expressing Baz::GFP and Mira::mCherry^{BAC} after Lat-A treatment. Miranda (red) is lost uniformly suggesting it is anchored by F-Actin to the basal pole. **D')** Quantification of average fluorescence intensity from 13 NBs. Fluorescence was measured in 3 regions of interest (ROI). One in the centre (Green) and two on the edge (Red and Blue) of the basal crescent. Fluorescence declines equally between all three ROIs. Error bars: St Deviation. Scale Bars: 10µm.

In summary we conclude it is likely that Mira utilises two different mechanisms to localise to the cell cortex. One, in interphase, which is actin independent and one, in mitosis, which is actin dependent. Given that the clearance of Miranda from the interphase cortex is independent of the actin cytoskeleton and coincident with the localisation of the Par-complex to the apical pole, the direct phosphorylation of Mira by aPKC was likely to be the driving force behind cortical clearance at prophase.

3.6. *aPKC* mutant neuroblasts fail to clear Miranda from the interphase cell cortex

In NBs mutant for *apkc* Miranda is localised uniformly around the cell cortex (Rolls et al., 2003). We hypothesised that this phenotype could arise due to a failure to remove Miranda from the interphase cell cortex. To assess the role for aPKC in clearing Miranda from the interphase cell cortex we analysed the dynamics of Miranda in NBs mutant for *apkc*. Due to *apkc* mutant flies dying at the end of L1/early L2 stages (Rolls et al., 2003), we needed to clonally induce homozygous mutant NBs within the brain. To do this we used the Mosaic analysis with a repressible cell marker (MARCM) technique (Wu and Luo, 2007). This technique utilises recombination in mitosis mediated by FLP-FRT recombination. In short, FRT sites are located on sister chromosomes. Upon expression of the FLP recombinase, recombination occurs at the FRT sites. This results in one daughter cell which will be homozygous for the mutant. These cells will be labelled by GFP for identification (**Fig. 3-5A**).

We utilised this technique to generate mosaic cells expressing GFP coupled to a nuclear localisation signal (NLS::GFP) which were homozygous for the null *apkc*

allele *apkc*^{K0603} (Wodarz et al., 2000) as well as expressing Miranda::mCherry^{BAC}. Live imaging of these cells demonstrated that Miranda::mCherry^{BAC} was never cleared at the onset of mitosis, resulting in mitotic cells with uniformly cortical localisation of Miranda in mitosis (**Fig. 3-5B**, n=12).

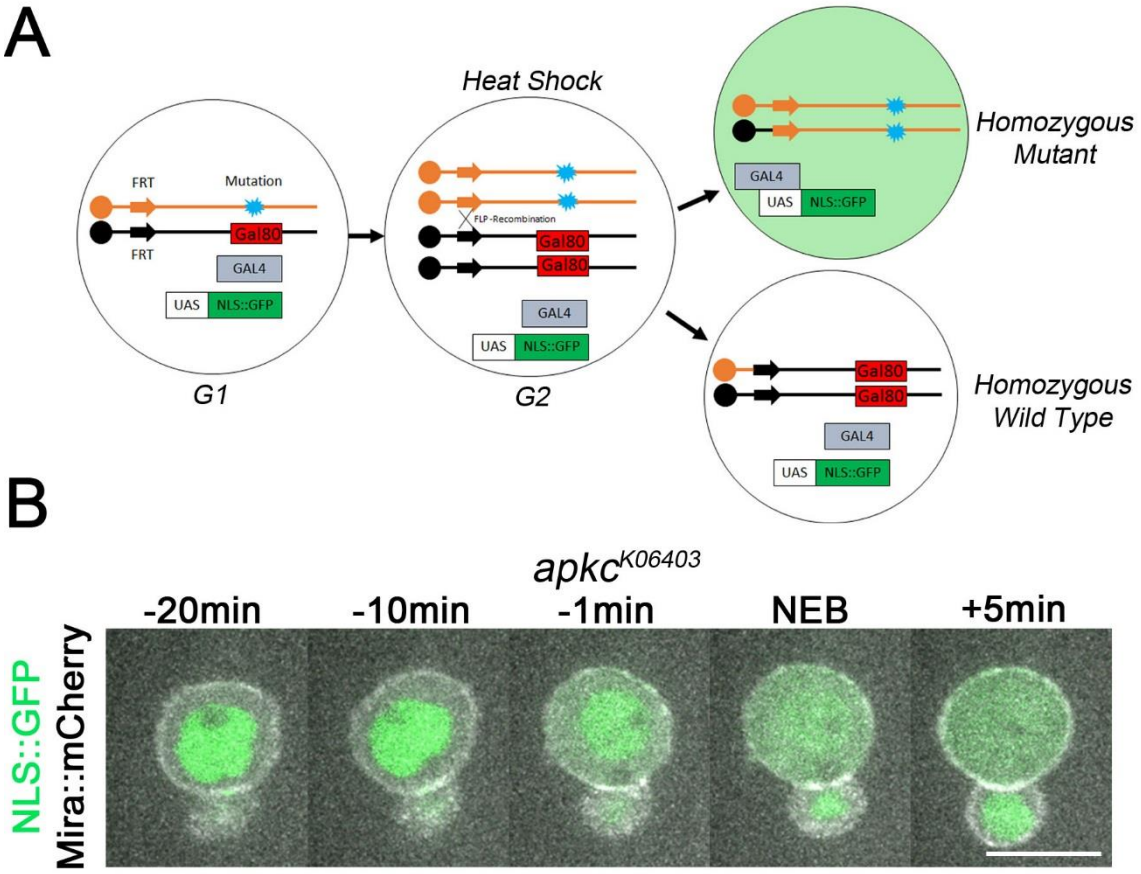

Figure 3-5 - aPKC mutant NBs fail to clear Miranda from the interphase cell cortex. **A)** Diagram depicting the mosaic analysis with repressible cell marker (MARCM) to generate cells homozygous for a mutation through FLP-FRT mediated recombination. These mutants are labelled with GFP. **B)** GFP positive, aPKC null (*apkc*^{k06403}) isolated NB expressing Miranda::mCherry$^{BAC.}$ Miranda is never cleared from the cell cortex, even -1min prior to NEB, this results in uniform cortical Miranda persisting through mitosis (+5min) n=12. Scale bar = 10µm.

Therefore, the uniform localisation of fate determinants previously identified in *apkc* mutants, is likely to arise from a failure to clear Miranda from the plasma membrane at interphase.

3.7. Over-expression of constitutively active aPKC

We predicted that during interphase Mira is bound directly to the plasma membrane via the basic and hydrophobic motif. Therefore, we would predict that the interphase localisation would be sensitive to aPKC over-activation i.e. ectopic phosphorylation of the basic and hydrophobic motif would result in cytoplasmic Miranda. To test this we utilised an *apkc* allele in which the N-terminus has been truncated (*apkc$^{\Delta N}$*) (Betschinger et al., 2003). *apkc$^{\Delta N}$* codes for a protein which is constitutively in the active conformation, allowing for ectopic phosphorylation of aPKC target sites. Over-expressing aPKC$^{\Delta N}$ in NBs was previously described to result in a reduction of cortical Miranda in mitosis (Lee et al., 2005).

In fixed NBs, within whole mount brains expressing aPKC$^{\Delta N}$ and stained for Miranda, Miranda was cytoplasmic in 85% of interphase NBs compared to 12% of control (**Fig. 3-6A, A'**; n=40 and 53 respectively). Furthermore, in 88% of mitotic NBs Miranda did not form a basal crescent compared to 8% in control mitotic NBs (**Fig. 3-6A, A'**; n=15). Interestingly, in both aPKC$^{\Delta N}$ and control telophase NBs Miranda was rescued to the basal cell cortex, a process previously described as telophase rescue (Schober et al., 1999). In cycling NBs in primary cell culture expressing aPKC$^{\Delta N}$ and Miranda::mCherry^{BAC}, the same behaviour was observed (**Fig. 3-6B**; n=20). Miranda was cytoplasmic throughout the cell cycle until late anaphase/telophase when it became localised to the basal pole (15 min).

This demonstrates that interphase Miranda cortical localisation is sensitive to ectopic aPKC activity. Furthermore, Miranda appears to be sensitive to ectopic aPKC phosphorylation in mitosis. However, it is unknown how the over-expression of over-active aPKC affects other proteins which could then impinge upon Miranda localisation.

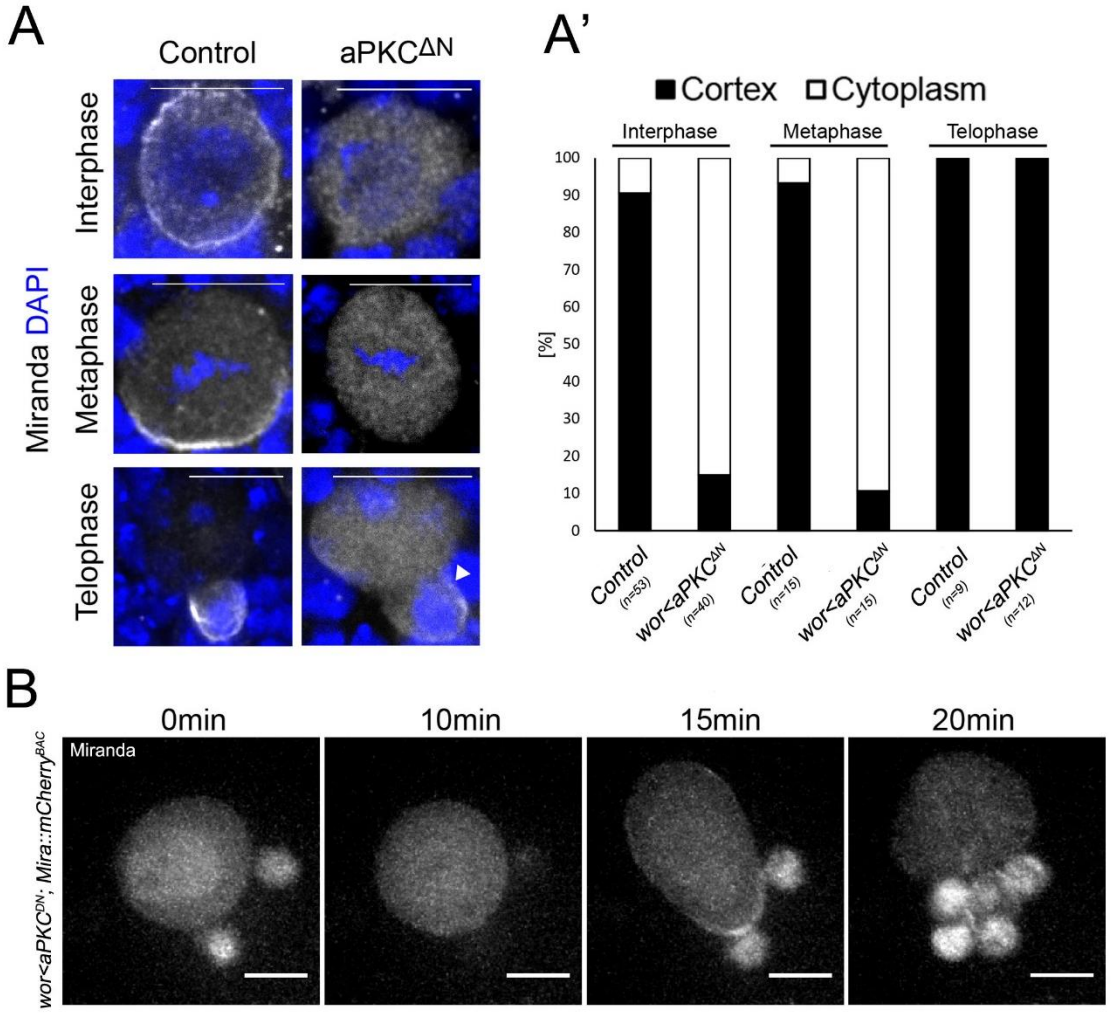

Figure 3-6 – interphase Miranda localisation is sensitive to expression of constitutively active aPKC (aPKC$^{\Delta N}$) A) NBs in fixed *w*^{1118} brains. Miranda (Grey) and DNA (Blue) immunofluorescence shows that in interphase the expression of aPKC$^{\Delta N}$ prevents cortical localisation. Cortical localisation is also prevented in mitosis, until telophase when Miranda is segregated into what will become the GMC. **A')** Quantification of NBs from Panel A. **B)** Stills from an isolated NB expressing aPKC$^{\Delta N}$ and Miranda::mCherry^{BAC}. Miranda only localises to the cortex in late anaphase/telophase (B, 15min) and after NEB Miranda is present in the nucleus, while the Miranda::mCherry^{BAC} normally remains at the cortex of the GMC (n=20). Scale bar: 10um.

3.8. Miranda localisation is actin independent following failure of aPKC to remove Miranda from the cell cortex.

Given that aPKC is required to clear Miranda from the interphase cell membrane, it is probable that the uniform cortical localisation of Miranda observed in aPKC perturbed mitotic cells is due to direct binding to the plasma membrane as observed in interphase. We therefore sought to test whether the localisation of Miranda in aPKC-depleted cells was actin dependent.

To assay this we clonally expressed an aPKC^{RNAi} construct using the FLIP out clones technique (del Valle Rodríguez et al., 2011). In short, heat shock activates the expression of GAL4 which then drives the expression of whichever UAS controlled transgene is present as well as a GFP marker (**Fig. 3-7A)**. FLIP-out expression of UAS-aPKC^{RNAi} significantly reduced aPKC levels and recapitulated the aPKC mutant phenotype (**Fig. 3-7B, B'**; p=0.002, n=8 brains control, 12 brains aPKC^{RNAi}).

Brains expressing aPKC^{RNAi} in a subset of NBs were treated with DMSO or 5µM Lat-A for 20 minutes before being fixed and stained for Miranda and F-Actin. In GFP negative (RNAi negative) mitotic control cells, Miranda is in a crescent (DMSO) or cytoplasmic (Lat-A). However in GFP positive (RNAi positive) cells Miranda was cortical in both DMSO and Lat-A treated NBs (**Fig. 3-7C**; 100%, n=5). Therefore we concluded that in *apkc* mutants Miranda is never cleared from the interphase cell membrane which leads to Lat-A insensitive localisation in mitosis. To corroborate these results we decided to genetically perturb the activity of aPKC by the overexpression of a mutant allele of the aPKC substrate *lgl,* which cannot be phosphorylated ((Betschinger et al., 2003), *lgl*^{3A}).

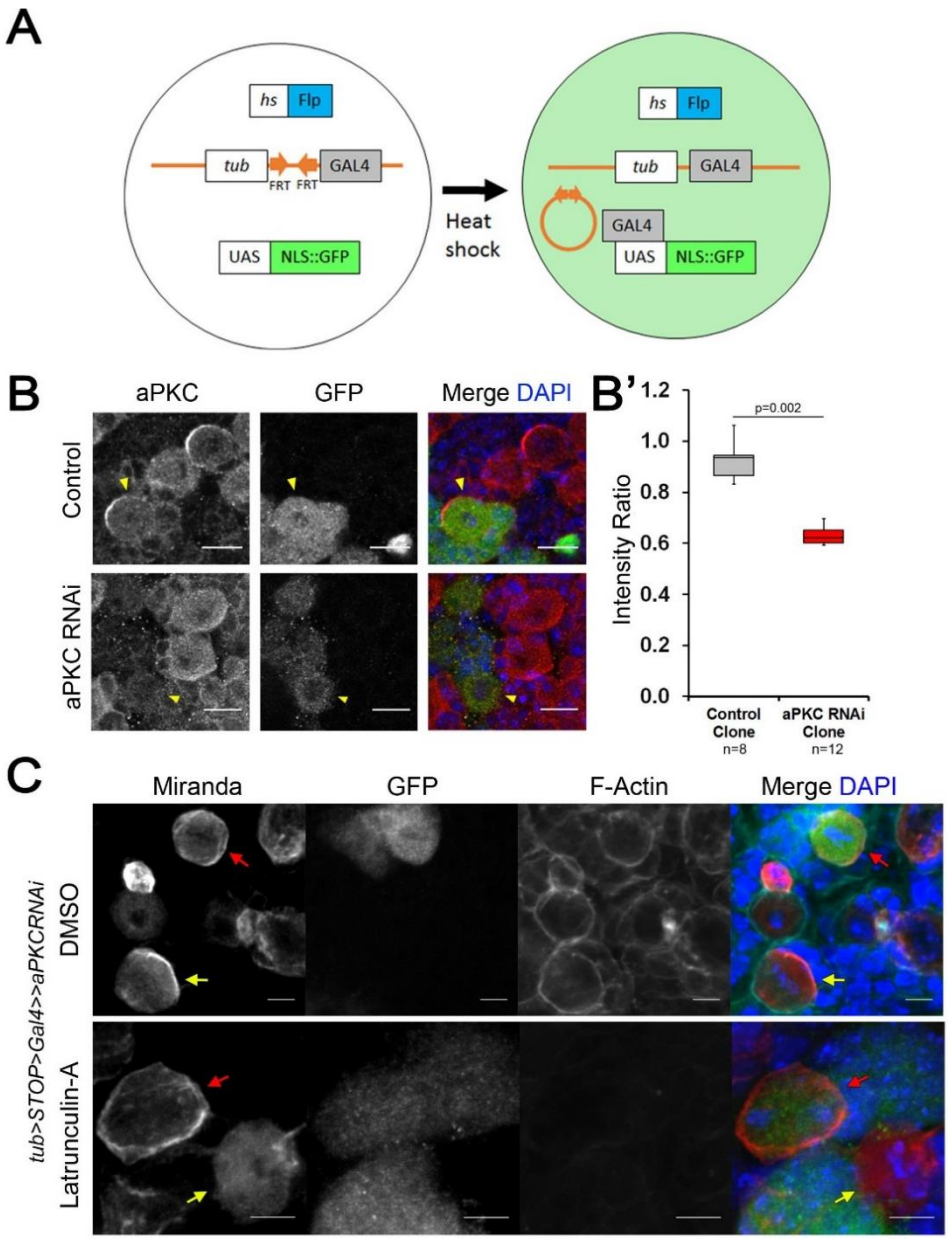

Figure 3-7 - Miranda cortical localisation in aPKC depleted NBs is independent of the F-Actin Network. A) Diagram summarising the flip out clones system. After heatshock a spacer is removed from the GAL4 cassette by FLP/FRT recombination. The UAS/GAL4 system becomes active, expressing a UAS-transgene of choice, in this case aPKC^{RNAi}. **B)** Example clones in fixed brains labelled with GFP (Green). In aPKC^{RNAi} expressing neuroblasts, aPKC expression evaluated by immunofluorescence is significantly lower than in control clones, quantified in **B'**. **C)** Clones in fixed brains expressing aPKC^{RNAi}. In DMSO controls, Miranda (red) is uniformly cortical in the clone (Red arrow) and forms a basal crescent in the control cell (yellow arrow). After 10µM Lat-A treatment, Miranda is uniformly cortical in the aPKC^{RNAi} expressing clone (Red arrow) while in the control cell (yellow arrow) Miranda is mislocalised into the cytoplasm. Scale bars: 10µM.

Lgl^{3A} overexpression is known to result in uniform cortical localisation of Miranda in mitosis (Atwood and Prehoda, 2009). We therefore wanted to test whether in this background Miranda localisation was sensitive to F-Actin depolymerisation. NBs over-expressing Lgl^{3A}::GFP and Miranda::mCherry^{BAC} were Colcemid arrested and then treated with Lat-A. We were able to divide our NBs into three classes. One class expressed Lgl^{3A}::GFP at a low level (determined by low intensity of Lgl3A::GFP). In these NBs, Miranda was asymmetrically localised, and this asymmetric localisation was lost upon treatment with Lat-A (n=4/25, **Fig. 3-8A, I**). The second class of NBs exhibited the anticipated uniformly cortical localisation of Miranda, this was insensitive to Lat-A treatment (n=7/25, **Fig. 3-8A, III**). Interestingly, we also observed a third class of NBs. These NBs had asymmetrically localised Miranda in mitosis, however, upon treatment with Lat-A the asymmetry was lost, Miranda spread laterally until it covered the entire cell cortex (n=14/25, **Fig. 3-8A, II**).

To confirm these findings, brains in which NBs were expressing Lgl3A::GFP were treated with either DMSO or Lat-A prior to fixation. Immunofluorescence against wild type Miranda and Phalloidin staining for F-Actin revealed that in control cells >90% of control NBs showed cytoplasmic Miranda following Lat-A treatment (**Fig. 3-8B, B'**; n=19). In NBs expressing Lgl^{3A}::GFP ~70% exhibited uniform cortical localisation following Lat-A treatment (**Fig. 3-8B, B'**; n=57) compared to only ~50% which were treated with DMSO (**Fig. 3-8B, B'**, n=32). This shows that more NBs expressing Lgl3A have uniformly cortical without an intact F-actin cytoskeleton.

These results demonstrated that even when aPKC is inhibited, Miranda is able to localise to the basal cell cortex, however, this localisation was dependent upon F-Actin. Following F-Actin depletion Miranda is able to bind directly to the plasma membrane, localising uniformly. This therefore is likely to demonstrate a situation in which aPKC activity is reduced but not eliminated.

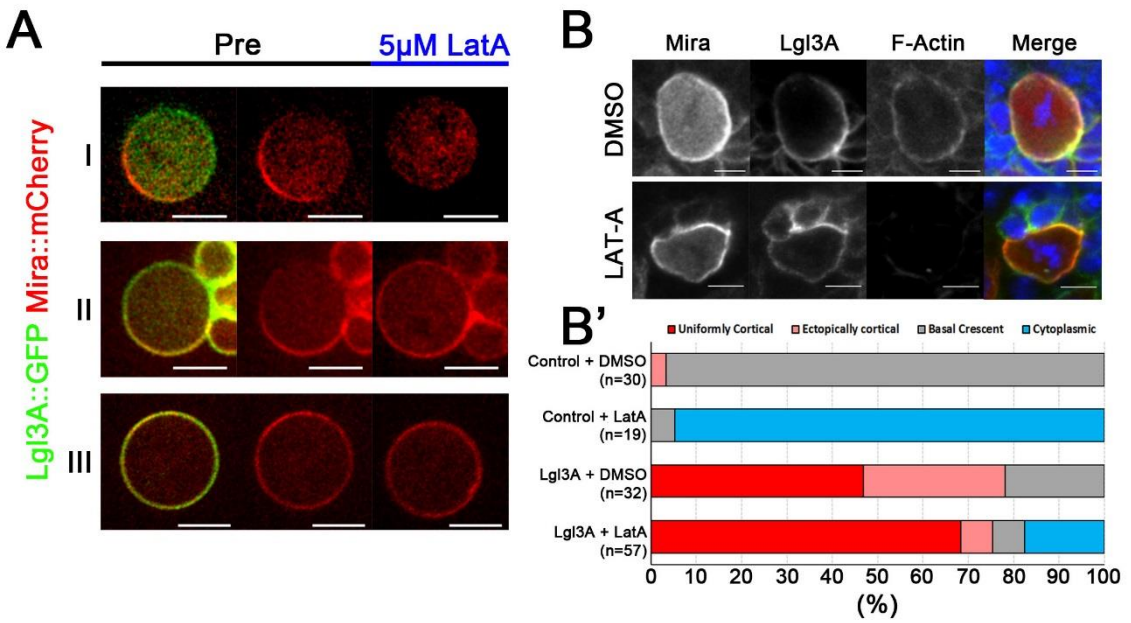

Figure 3-8 – Miranda localisation in mitosis is insensitive to Lat-A treatment in Lgl3A overexpressing NBs. A) Still frames from isolated NBs before and after treatment with 5µM Lat-A. Lgl3A::GFP (green) Mira::mCherry^{BAC} (red). NBs can be divided into three classes. The first expressed Lgl3A at a low level. In these NBs, Miranda falls into the cytoplasm (I). The second, Lgl3A does not prevent Miranda basal localisation, however, treatment with Lat-A results in uniform membrane bound Miranda (II). The third class results in Miranda uniform cortical localisation before and after Lat-A treatment (III) demonstrating that inhibition of aPKC results in Miranda retaining the ability to interact with the plasma membrane, independently of the F-Actin network. **B)** Corroboration of the live imaging in fixed brains. Depletion of the actin network as seen by Phalloidin staining, did not prevent uniformly cortical Miranda localisation in metaphase NBs. **B')** Quantification of Miranda cortical localisation. Lgl3A results in an increase in cells which are uniformly cortical or have enlarged (>50%) coverage of Miranda at the cortex. Treatment with Lat-A results in a decrease in the number of NBs with a basal crescent. Instead an increase of NBs with uniformly cortical Miranda localisation is observed. This likely reflects the three classes of localisation observed in **A.** Scale bars: 10µm.

3.9. Preventing phosphorylation of the Miranda basic and hydrophobic motif blocks clearance from the interphase plasma membrane.

One of the key findings that direct phosphorylation of Miranda was necessary to exclude Miranda from the apical domain was the observation that over expressing a non-phoshorylatable Miranda mutant (*mira*^{5A}) resulted in uniformly cortical Miranda and Prospero in mitosis (Atwood and Prehoda, 2009). We hypothesised that the aPKC dependent clearance of Miranda from the cortex prior to NEB which we have observed (**Fig. 3-2 and 3-5**) is due to the direct phosphorylation of the Basic and Hydrophobic motif by aPKC. To address this we generated a Miranda knock-in allele in which Serine 96 within the Basic and Hydrophobic motif was replaced with an Alanine and Miranda was tagged with mCherry at its C-terminus (*miranda*^{S96A}*::mCherry*, **Fig. 3-9A**) in the endogenous locus (Baena-Lopez et al., 2013), by injection into the *mira*^{attpko} background ((Ramat et al., 2017) See Materials and Methods for details on generation of the knock in allele, **Fig. 2-1**). It is important to note that due to the tagging of Miranda C-terminus these knock in alleles are not homozygous viable. Therefore the localisation of the Miranda::mCherry knock in lines are examined in a heterozygous background. Therefore some rescue of localisation could be observed by the wild type copy.

Isolated NBs heterozygous for this mutation or a control knock-in line, in which Miranda is tagged with mCherry without further mutation, were then imaged. In the control NBs Miranda::mCherry behaved as we had previously observed for the Miranda::mCherry^{BAC} (**Fig. 3-9B**; n=18).

We reasoned if direct phosphorylation of Serine 96 would be sufficient for clearance, Miranda^{S96A}::mCherry would behave as Miranda in *apkc* null NBs.

Instead, we observed something surprising. At the onset of mitosis when clearance would normally take place, Miranda^{S96A} begun to accumulate at the apical cell cortex (**Fig. 3-9C**; n=49/51). After NEB Miranda is then redistributed until it is uniformly cortical (**Fig. 3-9C**; n=51/51), as described following Mira^{5A} overexpression (Atwood and Prehoda, 2009). Later in mitosis at the onset of telophase Miranda appears to be basally biased resulting in a telophase rescue (**Fig. 3-9C**; n=26/36).

Interestingly, the apical accumulation of proteins at prophase has previously been described for Myosin II (Barros et al., 2003; Cabernard et al., 2010). Therefore, it is possible that phosphorylation by aPKC is required to both prevent membrane association of Miranda and its direct association to Myosin II as it begins to accumulate prior to NEB.

To test this idea we imaged Mira^{S96A} in cultured NBs in the presence of either DMSO or Lat-A. In the absence of F-Actin, the accumulation of Mira^{S96A} at the apical pole was significantly reduced. Instead, Miranda^{S96A} remained uniformly cortical throughout the entire cell cycle similar to that observed in *aPKC* mutant NBs (**Fig. 3-9D, D'**; n=17).

To test whether the apical accumulation of Mira^{S96A} was due to Myosin II interaction, we co-expressed Mira^{S96A}::mCherry with a Zipper::GFP (Myosin II heavy chain) endogenous fusion protein. Interestingly in all cells analysed (**Fig. 3-10A**; n=25) Mira^{S96A} accumulated apically before Zipper::GFP was recruited to the cortex. We therefore concluded that it was not through interaction with Myosin II that the apical accumulation occurs. Due to the actin dependency and the timing to the accumulation prior to NEB, it was possible that Miranda^{S96A} was just interacting with the Par-complex. We therefore co-expressed MirandaS96A with

aPKC::GFP^{BAC}. In these NBs Miranda^{S96A}::mCherry and aPKC::GFP^{BAC} both start to accumulate at the apical pole at the same time point (**Fig. 3-10B**; n=15).

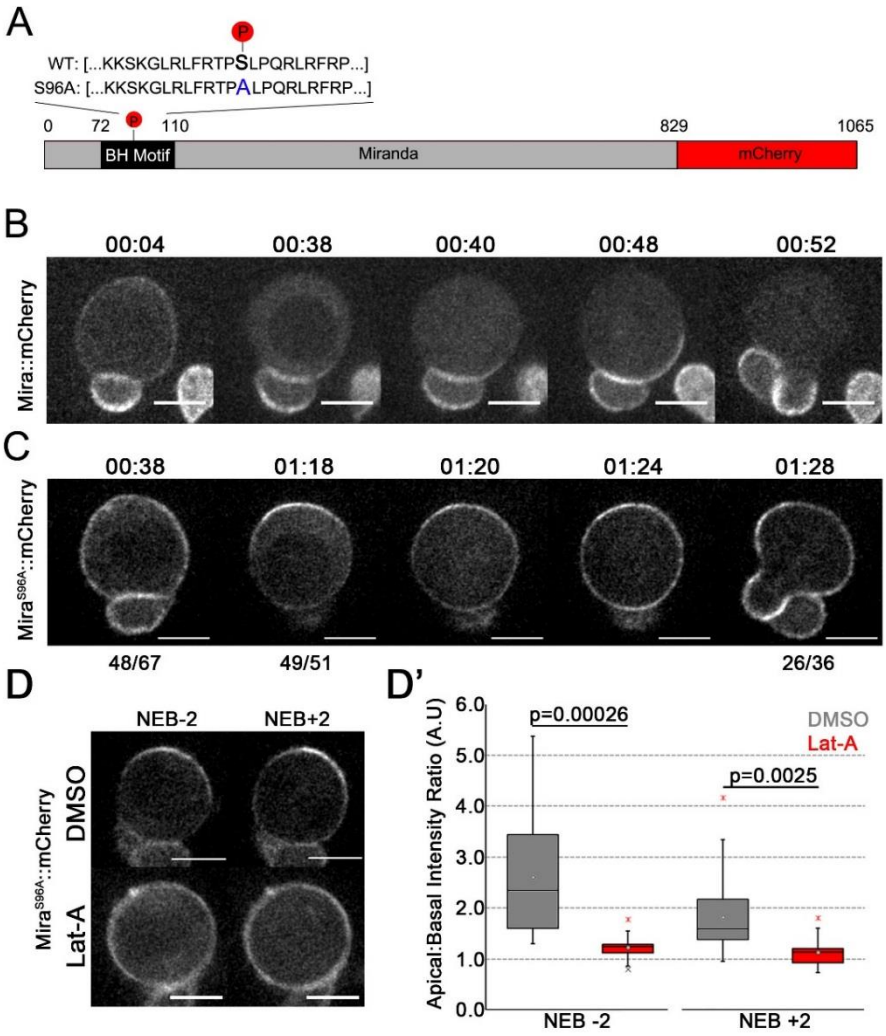

Figure 3-9 - Miranda^{S96A} is not cleared from the interphase cell cortex. A) Diagram showing the position of the S96A substitution in the Miranda protein. **B)** Stills from a timelapse movie of Mira::mCherry control knock in line. Mira::mCherry is cleared from the cortex similarly to Mira::mCherry^{BAC}. **C)** Heterozygous Mira^{S96A}::mCherry is not cleared from the interphase cortex, instead it accumulates apically prior to NEB (01:18) before becoming uniformly cortical in mitosis (01:24). At telophase the majority of cells show a basal bias in Miranda signal (01:28). **D)** 1µM Lat-A treatment does not cause a loss of Miranda from the mitotic cell cortex, but does result in a loss of the apical accumulation prior to NEB. **D')** Quantification of Apical to Basal Mira^{S96A}::mCherry intensity ratio in NBs treated with DMSO (Grey) or Lat-A (Red) prior to and after NEB (n=17). P values originate from a two tailed t.test. Scale bars: 10µm. Time: hh:mm

Therefore, we are able to conclude that Serine 96 phosphorylation is required to clear Miranda from the cell cortex.

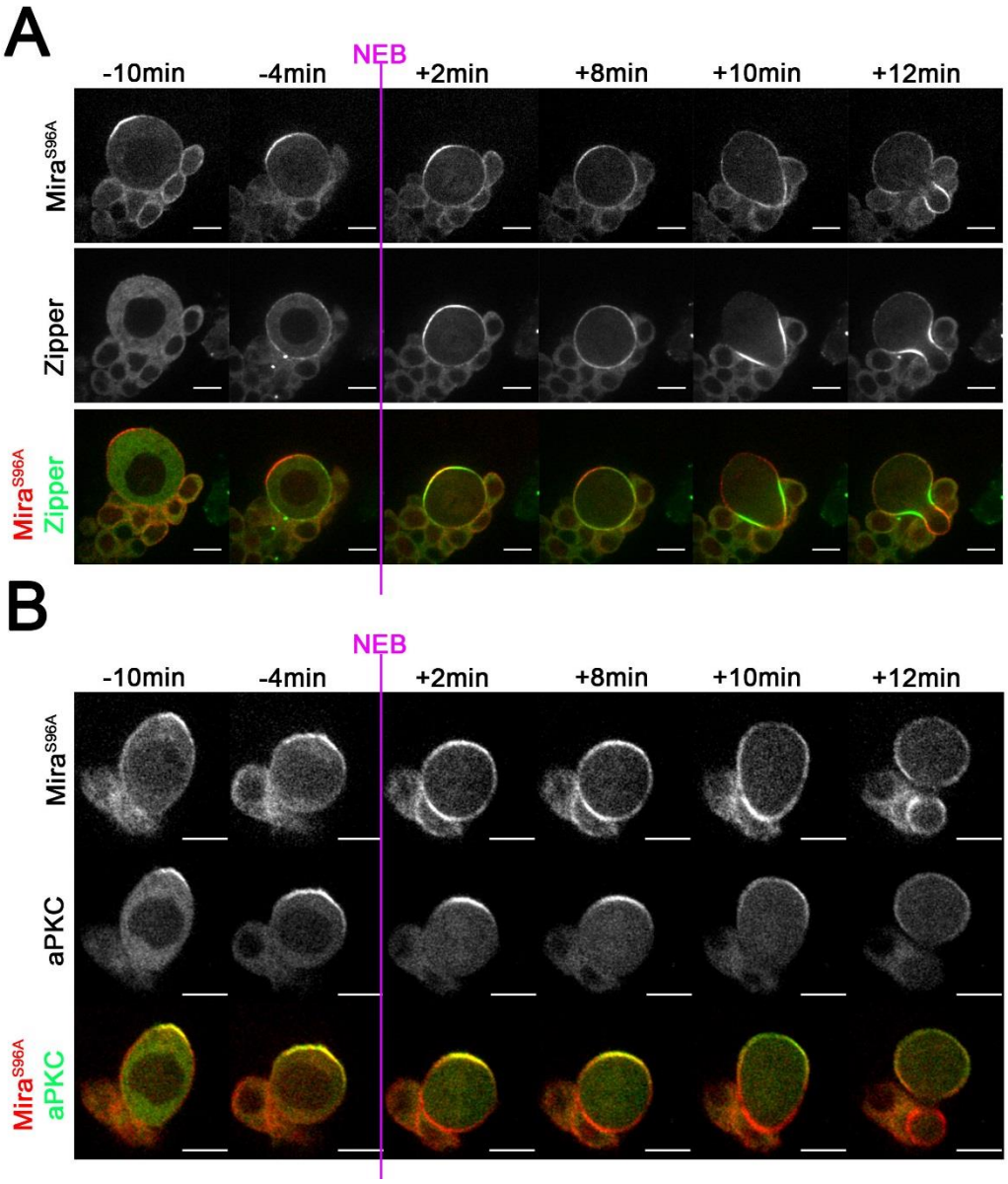

Figure 3-10 – MiraS96A apical accumulation coincides with the localisation of aPKC to the cell cortex. A) Stills from a timelapse of an isolated NB expressing Zip::GFP (green) with Mira^{S96A}::mCherry (red). Mira^{S96A} accumulates apically before Zip::GFP accumulates at the cell cortex (n=25) **B)** Stills from a timelapse of an isolated NB expressing aPKC::GFP^{BAC} (green) with Mira^{S96A}::mCherry (red). Apical accumulation of Mira^{S96A}::mCherry is coincident with the localisation of aPKC::GFP at the apical cell cortex (n=15). Scale bar: 10µm. Time: minutes before/after NEB.

3.10. Assessing the dynamics of Miranda localisation.

We sought to quantitatively measure whether Miranda utilised a different binding mode in interphase to mitosis. To this end we conducted a fluorescence recovery after photo-bleaching (FRAP) experiment. FRAP experiments involve the photo-bleaching of a small region of interest (ROI) of the cell, inactivating the fluorescent protein tagged to your protein of interest (**Fig. 3-11A**). Over time it is possible to monitor recovery of fluorescence into the ROI. This gives a measure of the dynamics of protein turnover in the region, accounted for by differences in binding affinity and rates of diffusion (Axelrod et al., 1976; Sprague et al., 2004).

To understand whether Miranda may be associated with the cortex in different ways, we bleached a ROI at the cell cortex in Mira::mCherry^{BAC} expressing NBs. We hypothesised that in interphase Miranda is bound to the membrane via electrostatic forces, which would exhibit faster dynamics than an actin based anchor in mitosis. Consistently with this Miranda::mCherry^{BAC} fluorescence recovered ~three times faster in interphase NBs (n=21) compared to mitotic NBs (n=20). Importantly, the fluorescence recovery of uniformly cortical Miranda::mCherry^{BAC} in mitotic NBs expressing Lgl^{3A}::GFP (n=26) also exhibited significantly faster recover time than control mitotic NBs, however this was not as fast as in interphase. This could potentially be explained by changes in the F-Actin network between mitosis and interphase limiting lateral diffusion (Heinemann et al., 2013). Therefore, we treated Lgl^{3A}::GFP expressing NBs with Lat-A. Following F-Actin network depletion the recovery of Mira::mCherry^{BAC} was not significantly different to interphase NBs (n=12; **Fig. 3-11BC**).

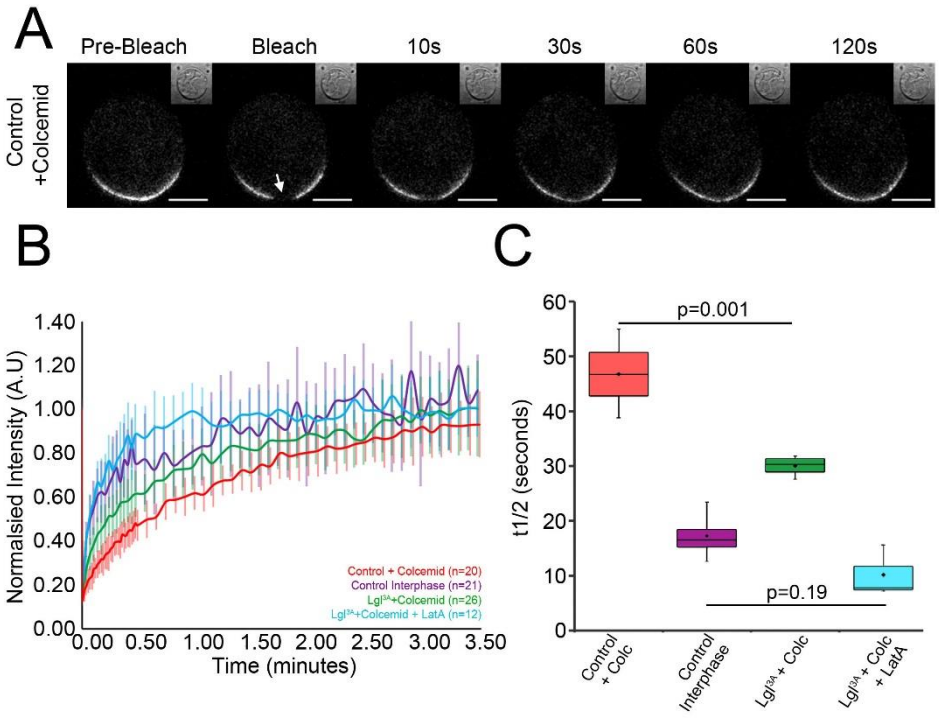

Figure 3-11 – Miranda dynamics are faster in aPKC impaired mitotic cells. A) Representative stills showing example of FRAP experiment. Isolated colcemid arrested neuroblast expressing Miranda::mCherry^{BAC}. Bleach was performed in the basal crescent (white arrow). Scale bar: 5 µm. **B)** Fluorescence recovery curves. Interphase cells (purple) showed much faster recovery compared to control mitotic cells (Red). Lgl^{3A}::GFP expression (green) resulted in faster Miranda recovery, which was made faster by depolymerising the actin cytoskeleton (blue), indicative of membrane interaction. Error bars: Standard deviation. **C)** Measurements of the half time recovery ($t^{1/2}$) demonstrate that Lgl^{3A}::GFP overexpression caused Miranda dynamics to be significantly faster. Miranda dynamics in interphase were not significantly faster than in Lgl^{3A}::GFP expressing NBs following Lat-A treatment. P values are derived from two-tailed t-test. Scale bar: 10µm

To further investigate the role that changes in the F-Actin network could be having on the lateral diffusion of membrane bound proteins we expressed a naïve membrane bound fluorescent protein consisting of a myristoylation signal which binds to the inner leaflet of the plasma membrane and the photoconvertible fluorescent protein tdEOS (**Fig. 3-12A**). Photoconversion experiments are in principle similar to FRAP but instead of bleaching the fluorescent protein the

emission spectrum of the fluorescent protein in the ROI is changed. It is then possible to monitor the dynamics of converted protein out of the ROI ((Mavrakis et al., 2009), **Fig. 3-12A**).

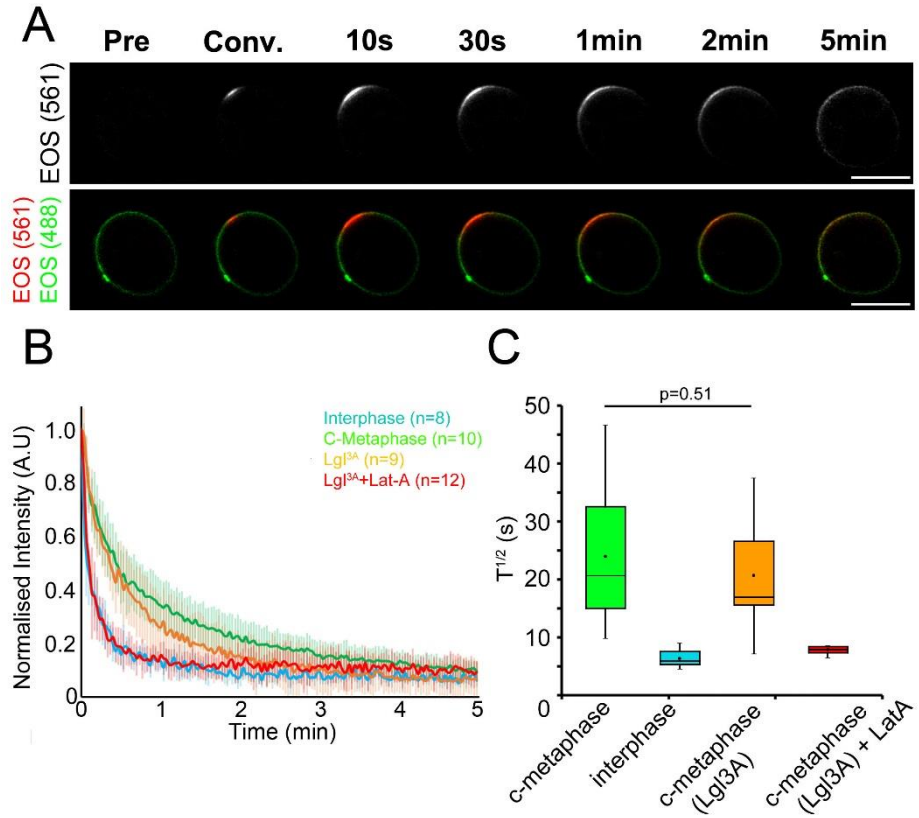

Figure 3-12 – A naïve membrane reporter is sensitive to changes in the actin cytoskeleton and cell cycle stage, but not Lgl3A overexpression. A) Stills from an example photoconversion experiment on a colcemid arrested, isolated NB expressing UAS-Myr::tdEOS by *worniu*-GAL4. Upon UV mediated conversion, the excitation spectrum of tdEOS shifts to excitation at 561nm (Conv, red). Converting a small ROI enables the measurement of diffusion out of the converted ROI. **B)** Quantification of the fluorescence decline of the converted EOS signal within the converted ROI. Interphase (blue) and Lgl3A expressing NBs treated with Lat-A had the faster Myr::Eos Dynamics. C-metaphase control NBs (Green) had the slowest **C)** Measurements of the half time decline ($t^{1/2}$) demonstrate that Lgl^{3A}::GFP overexpression alone (orange) does not cause membrane dynamics to be significantly faster compared to mitotic control NBs. However, depolymerising the F-Actin cytoskeleton, results in membrane dynamics similar to interphase. Scale bar: 10µm. p value derived from two-tailed t-test.

As expected the $t^{1/2}$ of Myr::tdEOS was about four fold faster in interphase (n=8) compared to mitosis (n=10) as well as in Lgl^{3A}::GFP expressing NBs when Lat-A was added (n=12). However, expressing Lgl^{3A}::GFP without Lat-A did not have a significant effect on Myr::tdEOS dynamics (n=9) suggesting that Lgl^{3A}::GFP did indeed affect the binding mode of Miranda and not the dynamics of membrane bound proteins in general (**Fig. 3-12BC**).

In summary these results quantitatively reveal that Miranda can interact with the cortex via two different modes, most likely demonstrating a difference between actin independent association (interphase and aPKC perturbed) and actin dependent binding (mitosis).

3.11. Phosphorylation of Miranda on Threonine 591 does not appear to be sufficient to regulate the switch to actin dependent binding after NEB

The described experiments in this chapter point to a fundamental difference in the dynamics of Miranda before and after NEB. This is reflected in the differential requirement for the F-Actin network for Miranda cortical localisation. Molecular understanding of what happens to Miranda at NEB to trigger its re localisation to the basal domain of the neuroblast is not clear. An enticing possibility focuses upon the activity of the Protein Phosphatase 4 (PP4) complex. PP4 is localised in the nucleus through interphase before being released into the cytoplasm upon NEB (Sousa-Nunes et al., 2009).

Previously, analysis of the phosphatase subunit Phospho-Tyrosol Phosphatase Activator (Ptpa) revealed that in mutants for *ptpa*, Miranda was mislocalised in mitosis, only forming basal crescents later in anaphase. It was demonstrated that

Ptpa deposphorylates Threonine 591 (Thr591) and the over-expression of phosphomimetic Miranda^{T591D} copied the *ptpa* phenotype (Zhang et al., 2015). We therefore wanted to examine this further and knocked Mira^{T591D} and Mira^{T591A} tagged with mCherry and HA (**Fig. 3-13A**) into the endogenous Miranda locus using the *mira^{attpko}* allele (Ramat et al., 2017).

Interestingly, both lines gave homozygous larvae that did not reach adulthood. We anticipated that the Mira^{591D}::mCherryHA would localise normally in interphase, and be mislocalised in metaphase, while the Mira^{591A}::mCherryHA would localise normally throughout the cell cycle. To test this, brains from homozygous larvae were fixed and stained for HA and aPKC. The wild type Miranda::mCherryHA construct behaved as expected, Miranda localised uniformly to the cortex in interphase, and formed a basal crescent in mitosis (Interphase: 30/30 cortical Miranda, aPKC cytoplasmic; Mitosis: 10/10 basal Miranda crescents, aPKC apical; **Fig. 3-13B**). Miranda^{591A}::mCherryHA was interesting. In mitosis it behaved normally, however in interphase Miranda^{591A} was observed in the nucleus, as was aPKC (Interphase: 119/129 nuclear Miranda^{591A} and aPKC; Mitosis: 17/17 Miranda basal crescents, aPKC apical; **Fig. 3-13C**). Miranda^{591D}::mCherryHA was not expected to localise in metaphase, however, we observed basal crescents and interphase cortical localisation indistinguishable from the wild type protein (Interphase: 202/220 cortical Miranda, aPKC cytoplasmic; Mitosis: 50/52 Miranda basal crescent, aPKC apical; **Fig. 3-13D**).

This suggests that the phospho-regulation of threonine 591 might be important for regulating interphase Miranda localisation, however it is not clear the contribution this has in mitosis.

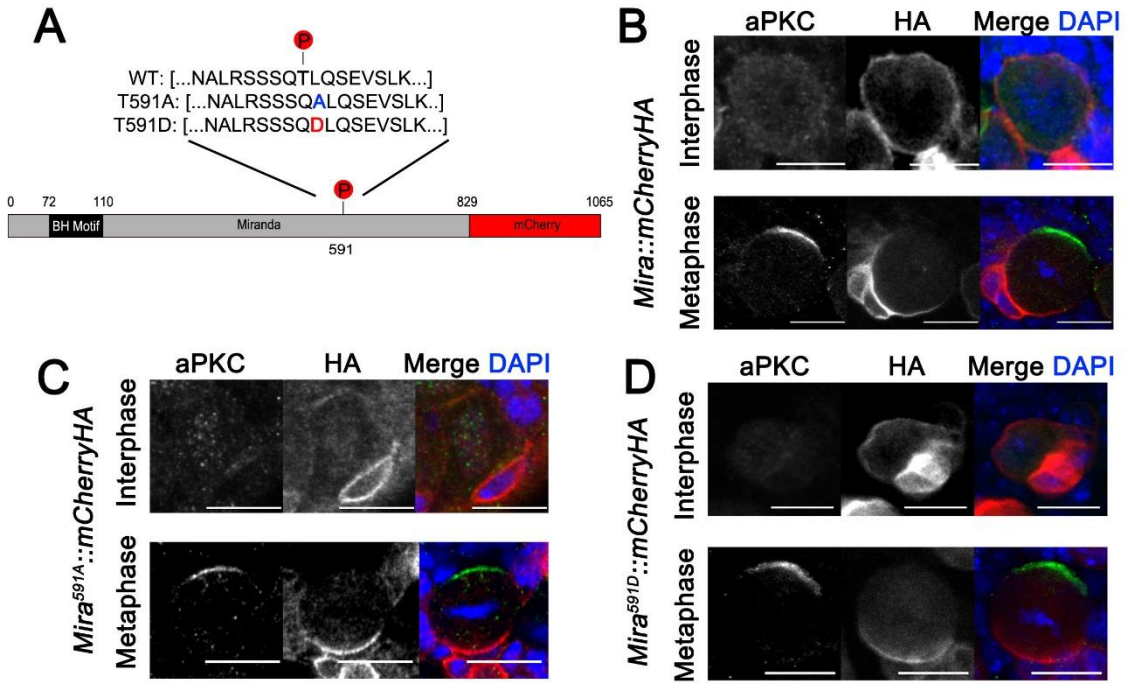

Figure 3-13 - Phospho-mimetic mutation of Miranda at Threonine 591 does not prevent metaphase localisation. A) Schematic showing the sites of the phospho-mutants generated for T591. Mutants were knocked in to the endogenous locus and were double tagged with mCherry and HA. **B)** Representative example NBs from immunofluorescence staining of Miranda (HA, red) and aPKC (green) in interphase and mitosis from WT Mira::mCherryHA knock-in homozygous larvae. Miranda is cortical in interphase and forms a basal crescent in mitosis. aPKC is cytoplasmic in interphase and forms an apical crescent in mitosis. **C)** Representative example of NBs from immunofluorescence staining of Miranda^{591A}::mCherryHA (HA, red) and aPKC (green) in Interphase and mitosis. Miranda^{591A}::mCherry localises to the cortex and the nucleus in interphase NBs, aPKC is also found in the nucleus. In mitosis the 591A mutation does not affect asymmetric protein localisation. **D)** Representative example NBs from immunofluorescence staining of Miranda^{591D}::mCherryHA (HA, red) and aPKC (green) in Interphase and mitosis Miranda and aPKC localise similar to the control localisation (**13B**). Scale bars: 10µm.

3.12. Conclusion

In this section we have described the temporal dynamics of Miranda localisation. During interphase, Miranda is localised to the plasma membrane in a manner which is sensitive to aPKC phosphorylation. When the Par-complex assembles at the apical side of the NB, Miranda is cleared from the membrane in an apical to basal, actin independent, manner which requires the phosphorylation of Serine96 within Miranda's BH motif. Following NEB, Miranda returns to the cell cortex, localising with higher affinity, in an actin dependent manner to the basal cell cortex.

It is unknown what causes the switch in the binding mode between interphase and mitosis. It was previously suggested that de-phosphorylation of Thr591 of Miranda by PP4 was required (Zhang et al., 2015). However, after generating knock-in mutations for this amino acid we were unable to reproduce the previously published results. Nevertheless, this does not mean that the activity of the PP4 complex is not required.

In the next chapter I will analyse in more detail the second stage of Miranda localisation. In particular, I will examine in more detail different elements of the cytoskeleton and investigate in more detail the role of aPKC after NEB.

4. Results Chapter 2 – Maintaining Cortical Asymmetry

4.1. Introduction

In the previous chapter we showed that the establishment of polarity is dependent upon aPKC to remove Mira from the interphase cell cortex, while the binding of Miranda to the basal pole in mitosis is a separate event dependent on an intact actin cytoskeleton. This raises interesting questions. Firstly, what regulates Mira binding to the cortex in mitosis? Previously Myosin II was implicated to “push” Miranda from the apical to the basal pole (Barros et al., 2003). Furthermore, the Myosin VI Jaguar was proposed to localise to the basal half of the cell where it “catches” Mira in the cytoplasm and brings it to the cell cortex (Erben et al., 2008; Petritsch et al., 2003). However, the phospho-exclusion model suggests that polarity is maintained through mitosis by a steady state of apical aPKC activity excluding Miranda from the apical domain, thereby resulting in basal Miranda localisation (Atwood and Prehoda, 2009). These two models have thus far not been integrated. The focus of this chapter will therefore be on re-examining the roles that Myosins and aPKC have in maintaining the basal domain throughout mitosis.

4.2. Inhibition of Myosin Light Chain Kinase prevents Miranda crescent formation and maintenance.

Previously, Myosins were suggested to play a key role in localising Miranda to the neuroblast cell cortex (Barros et al., 2003; Petritsch et al., 2003; Sousa-Nunes et al., 2009). However, more recent work has disputed this due to the use of the small molecule inhibitor Y-27632 to inhibit myosin. Y-27632 was shown to also

inhibit aPKC (Atwood and Prehoda, 2009). We believed our primary neuroblast culture system presented a unique opportunity to re-examine the role of Myosins in localising Miranda to the basal pole.

Blebbistatin, the commonly used inhibitor of non-muscle Myosin II (Zipper in *Drosophila*) does not work in *Drosophila* (Heissler et al., 2015). This is due to a point mutation in the blebbistatin binding region of Myosin II. We attempted to reverse engineer this mutation using CRISPR/CAS9, however it was homozygous lethal. This meant that there was one wild type copy of Myosin which is insensitive to blebbistatin, potentially blocking any Myosin phenotype (Data not shown). Therefore, we had to take an alternative approach to inhibit myosin activity.

Another way to inhibit myosin activity is to inhibit Myosin Light Chain Kinase (MLCK). MLCK phosphorylates the Myosin Regulatory Light Chain (MRLC), activating Myosin contraction (Gallagher et al., 1997). We therefore turned to the specific inhibitor of MLCK, ML-7 (**Fig. 4-1A**, (Bain et al., 2003; Saitoh et al., 1987)). Adding ML-7 to cycling NBs did not affect Miranda localisation during interphase, nor the clearance of Miranda from the cell cortex. However, during mitosis Miranda was unable to localise to the cell cortex, instead localising to the microtubules, similarly to NBs with a depleted F-Actin cytoskeleton (**Fig. 4-1B**; n=8). To separate establishment of the cortical compartments to maintenance, NBs were arrested in metaphase using colcemid and then treated with ML-7. Miranda was rapidly lost from the cell cortex (**Fig. 4-1C**; 10 minutes, n=13). Upon washout of the inhibitor, Miranda recovered to the basal domain (**Fig. 4-1C**; ~30 mins, n=13).

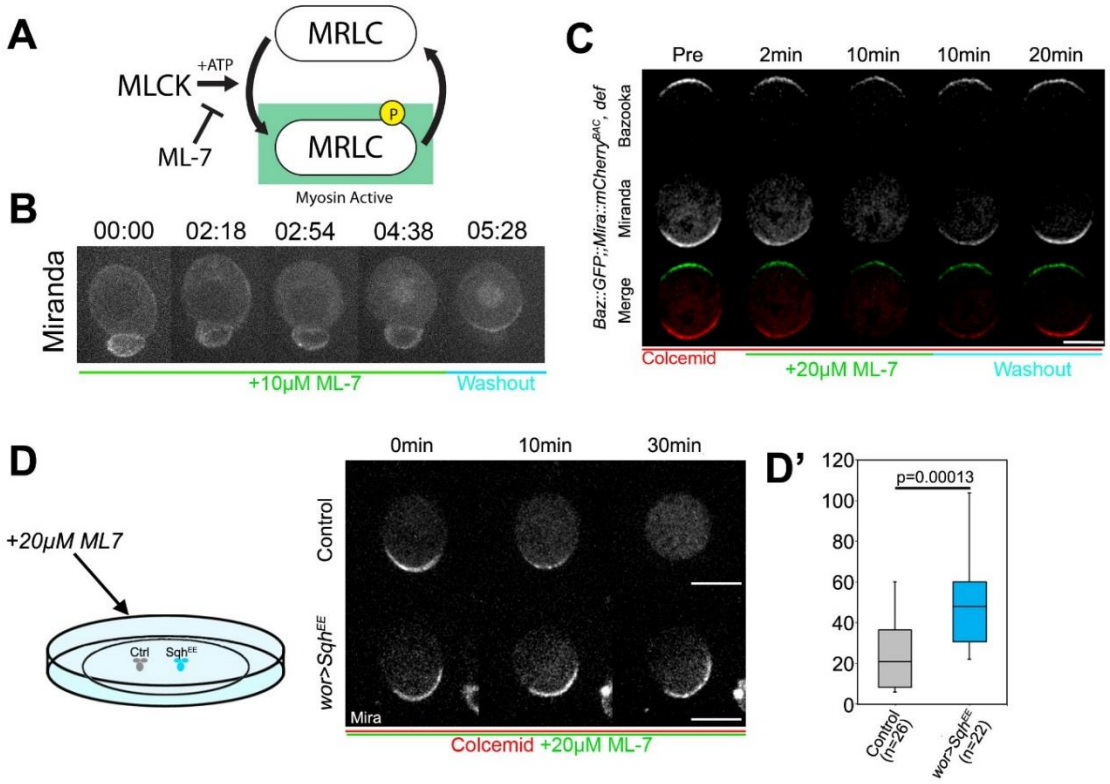

Figure 4-1 - Myosin Regulatory Light Chain Phosphorylation Regulates Miranda localisation. A) Schematic of Myosin light chain kinase activity. MLCK phosphorylates the myosin regulatory light chain, activiating it. The small molecule ML-7 inhibits this phosphorylation, resulting in myosin inhibition. **B)** Stills from a timelapse series of an isolated NB expressing Mira::mCherry^{BAC}, 10µM ML-7 does not inhibit Miranda interphase localisation or cortical clearance (0', 138'). However, Miranda does not form a basal crescent in mitosis (278'). ML-7 also causes mitotic arrest. Washout of ML-7 rescues Miranda localisation but not mitotic arrest (328', n=8/8). **C)** Representative stills from a timelapse movie of a colcemid arrested isolated NB expressing Baz::GFP (green), Mira::mCherry^{BAC} (red). Addition of 20µM ML-7 caused loss of basal Mira crescent while Baz localisation was unaffected (10min). Upon ML-7 washout, Mira crescents recover at the basal pole (n=13/13). **D)** Left Panel: Schematic showing experimental set up. Isolated NBs expressing Mira::mCherry with and without phosphomimetic UAS-Sqh^{EE} were arrested with colcemid and treated with ML-7. Right Panel: Representative isolated NBs from the described experiment. Miranda localisation persists in NB expressing UAS-Sqh^{EE}. **D')** Quantification of the time taken for Miranda to be lost into the cytoplasm. Expression of UAS-Sqh^{EE} caused a significant delay (p=0.00013, two tailed T-test). Scale bars: 10µm.

A weakness of ML-7 is that it is a kinase inhibitor and can therefore cause off target effects. Previously, the effects of ML-7 have been rescued by misexpression of a phospho-mimetic Myosin Regulatory Light Chain (MRLC) (Das and Storey, 2014). *Drosophila* MRLC is encoded by *spaghetti squash* (*sqh*). Neuroblasts over-expressing a UAS-Sqh^{EE} construct and Miranda::mCherry^{BAC} were subjected to ML-7 treatment alongside wild type controls. Strikingly, there was a significant delay in the time taken for Miranda to be lost from the cortex in NBs expressing sqh^{EE} compared to the controls (**Fig. 4-1D D'**; ~2 fold slower, n=26 control, n= 23 Sqh^{EE}, p=0.00013). This suggests the effect we observed on Miranda localisation was due to Myosin perturbation. Previously, both Myosin II (Zipper, (Barros et al., 2003)) and Myosin VI (Jaguar, (Petritsch et al., 2003)) have been implicated in asymmetric cell division. ML-7 does not allow us to determine which of these Myosins required for Miranda localisation. We therefore sought to re-examine the role of Jaguar in NBs.

4.3. Myosin VI (Jaguar) is not required for Miranda localisation in mitosis.

Previous work identified Jaguar, (*jar*) as being a key player in Miranda localisation during mitosis. Jar was interesting as it is an unconventional Myosin which moves towards the minus end of actin filaments, compared to conventional myosins which move towards the plus end (Wells et al., 1999). This functions due to a sequence inserted into the heavy chain, unique among myosins which redirects the movement of the "lever arm", thereby facilitating reverse movement (Ménétrey et al., 2005). Co-immunoprecipitation of Miranda from embryonic

lysates, coupled to Mass Spectrometry Analysis identified Jar as being a binding partner of Mira. Embryos homozygous for the mutant *jar*^{322} displayed Miranda as being localised in the cytoplasm through mitosis (Petritsch et al., 2003).

However, since publication the *jar*^{322} allele was shown to also contain a deletion of the neighbouring phenyl-alanine tRNA synthetase. A different allelic combination (*jar*^{322}/*crb*$^{87-5}$,**Fig. 4-2A**) was shown to result in no Jaguar RNA or protein to be produced, but not result in a full deletion of the neighbouring genes (Morrison and Miller, 2008). Flies carrying this allelic combination were shown to live to adulthood (contrary to *jar*^{322} homozygotes which die as early larvae). This called into question previous results, including those in NBs. We therefore re-examined the phenotype of Jar deletion in *Drosophila* larval NBs.

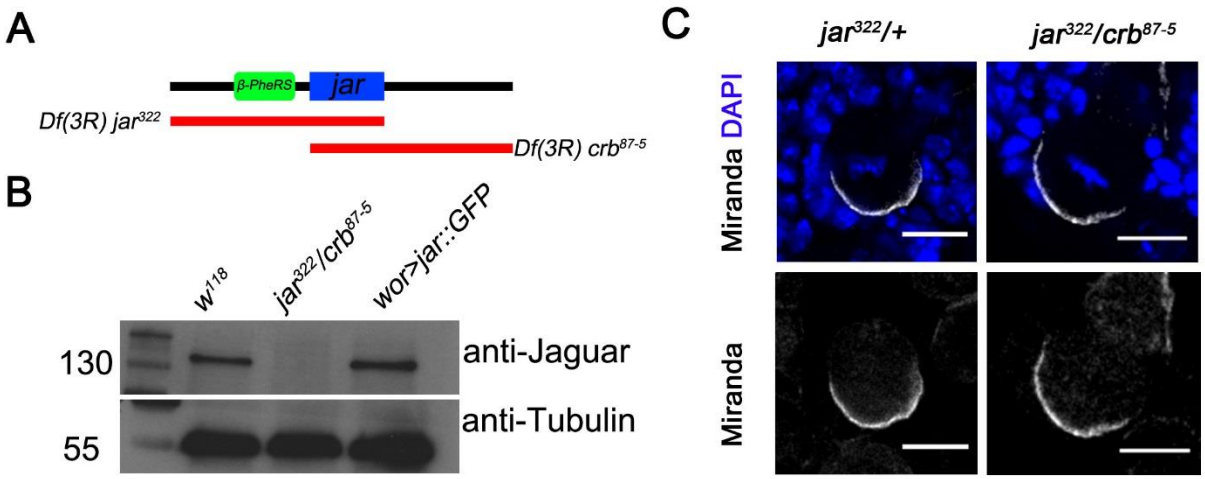

Figure 4-2 - Jaguar is not required for Miranda asymmetric localisation in larval neuroblasts. A) Schematic showing sites of deficiencies used relative to the *jar* locus **B)** Western blot against *jar* in stated genetic backgrounds. No Jar was detectable in lysates made from brains of transheterozygous *Df(3R) jar*^{322}*/Df(3R) crb*$^{87.5}$ larvae. Tubulin was included as a loading control. Mw – molecular weight (kDa). Predicted Jar molecular weight: 140kDa. Images are representative of two biological replicates. Jar-GFP was not detected, only the endogenous Jaguar. **C)** Fixed NBs of labelled genotypes. Despite the absence of Jar, Miranda (grey) localisation was unaffected in metaphase NBs. DNA was stained with DAPI (blue). Scale bar: 5µM

Firstly, we confirmed that the *jar*^{322}/*crb*$^{-87-5}$ allelic combination resulted in loss of Jar protein by western blotting (**Fig. 4-2B**). Brains from trans-heterozygous mutants were fixed and stained for Mira. Contrary to previous reports, both interphase and mitotic localisation of Mira protein is independent of Myosin VI Jaguar (**Fig. 4-2C**, 100% NBs, n=5 brains).

It therefore seems likely that the anchor for Mira at the basal pole is dependent on Myosin II however, this was difficult to study directly due to the pleiotropic functions of Myosin II in the cell, for example its role in cytokinesis (Edwards and Kiehart, 1996).

4.4. Low doses of the ROCK inhibitior Y-27632 causes an enlargement of the Miranda domain, prior to NEB, independently of aPKC inhibition.

It is clear that aPKC plays a crucial role in polarising the cell cortex by clearing Miranda from the interphase plasma membrane. Furthermore, our results suggest that the mitotic basal crescent of Miranda depends upon the actin cytoskeleton to localise. However, we do not know whether aPKC plays a role in maintaining asymmetric Miranda localisation after NEB. To assay this we needed to temporally control the inactivation of aPKC. Previously, a temperature sensitive allele was generated (Guilgur et al., 2012) however it did not faithfully reproduce the *apkc* mutant phenotypes previously described (Rolls et al., 2003). Therefore, we must use small molecule inhibitors. Although no specific inhibitors of *Drosophila* aPKC are published and commercially available, the Rho kinase (Rock) inhibitor Y-27632 (Uehata et al., 1997) has previously been shown to result in Miranda localisation defects similar to genetic perturbation of *apkc* (Barros et al., 2003; Erben et al., 2008). Although these studies attributed this

phenotype to myosin II inhibition, more recent work demonstrated that Y-27632 inhibited aPKC *in vitro* with an IC50 of ~10µM (Atwood and Prehoda, 2009). We sought to utilise this tool to try and understand whether aPKC was required after NEB.

NBs expressing Baz::GFP and Mira::mCherry^{BAC} were arrested in C-metaphase and then treated with 50 µM Y-27632. Interestingly, after 1 hour in the presence of Y-27632, there were no changes in Miranda crescent size (**Fig. 4-3A**; n=22), which we would expect if aPKC was continuously phosphorylating apically localised Miranda to exclude it from the cell cortex. We then wanted to check if Y-27632 had an effect on polarity establishment. Interestingly, when we add half the dose (25µM) to cycling NBs, the cells were able to polarise but Miranda domain size was enlarged, resulting in a loss of the gap between the apical and basal domain (**Fig. 4-3B**; n=12). Interestingly, this appeared to be coupled to an enlargement of the daughter cell size relative to NB size. To quantify this further we utilised the fact that nuclear volume is proportional to cell size in *Drosophila* NBs (Homem et al., 2013). After addition of Y-27632 to NBs expressing NLS::GFP, GMC:NB size ratio significantly increase (~2x, p=0.0001, n=39). However, upon washout of Y-27632 in the next division the nuclear size ratio was similar to the control division prior to drug treatment (**Fig. 4-3C**).

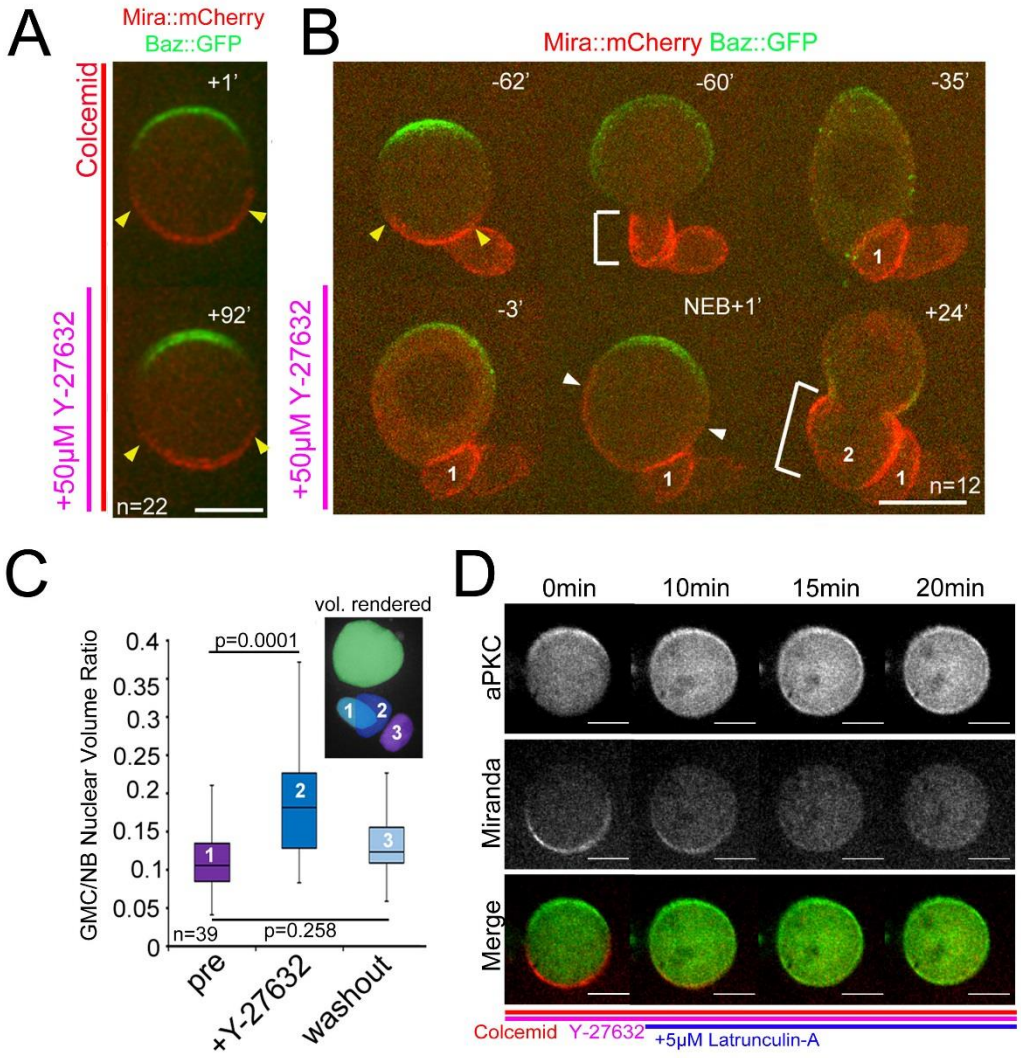

Figure 4-3 - **Y-27632 causes enlarged Miranda crescent size and corresponding daughter cell size. A)** Example of an Isolated NB expressing Baz::GFP (green) and Mira::mCherry^{BAC} (red), arrested with Colcemid. Addition of 50µM Y-27632 did not cause a change in Mira localisation after 92 minutes (n=22). **B)** Example of an isolated, cycling NB expressing Baz::GFP (green) and Mira::mCherry^{BAC} (red). Top row: Prior to Y-27632 addition Mira forms a basal crescent as described already. Bottom Row: Following Y-27632 addition, Mira forms and enlarged basal crescent (NEB+1, white arrows) and as the cell divides GMC size increases (+24). **C)** Isolated NBs expressing NLS::GFP were imaged over three consecutive divisions. GMC/NB nuclear volume ratio was then measured as a proxy for cell size. Following Y-27632 treatment, size asymmetry is significantly disrupted. This is rescued upon washout of the inhibitor. Inset: example Nuclei with GMC labelled corresponding to graph. P values derived from pair wise comparison following kruskal-wallis non-parametric test. **D)** Arrested, isolated NB expressing Mira::mCherry^{BAC} (red) and aPKC::GFP^{BAC} (green). Following Y-27632 treatment, enlarged crescents are sensitive to 5µM Lat-A treatment. Scale bar: 10µM

Previously, it was shown that aPKC also effects size asymmetry in NB divisions. We therefore wanted to know whether the phenotype observed after Y-27632 treatment was indeed due to aPKC inhibition, or whether it was in fact due to ROCK inhibition. To discriminate between these two possibilities we took advantage of the insensivity of Miranda to Lat-A treatment when aPKC activity is perturbed. We would predict that if aPKC was inhibited, Miranda would redistribute until it was uniformly cortical. Instead, Miranda fell into the cytoplasm as we observed in control NBs (**Fig. 4-3D**; n=10). This demonstrated that aPKC function was not inhibited to a level that could explain the observed phenotype.

4.5. Y-27632 inhibits cortical Myosin II accumulation

We therefore decided to check to see if Y-27632 affected myosin dynamics in NBs. To this end we cultured NBs in which the endogenous Zipper locus had been tagged with GFP (Zip::GFP, (Buszczak et al., 2006)). Interestingly, in these NBs shortly prior to NEB, Zip::GFP became very dynamic at the cell cortex. Then just before NEB it stabilised apically before distributing uniformly to the cortex as previously described (Cabernard et al., 2010). In the next cell cycle 25µM Y-27632 was added, this almost completely blocked Zip::GFP recruitment to the cell cortex (**Fig. 4-4;** n=13). Zip::GFP localisation was recovered on washout of the inhibitor and was able to localise prior to the following division at levels similar to the control. We therefore concluded that 25µM Y-27632 impairs myosin dynamics, probably via Rock inhibition. Recent work has observed a similar phenotype in *rock* mutants (Tsankova et al., 2017).

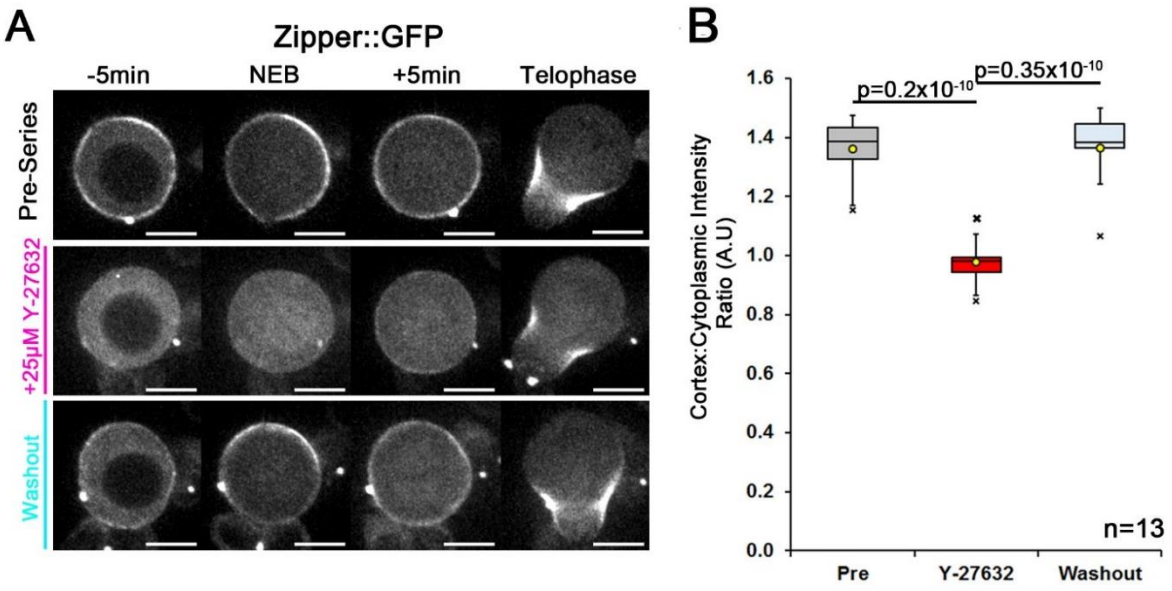

Figure 4-4 - Zipper dynamics are altered upon Y-27632 treatment. A) Isolated NB expressing Zipper::GFP. Zipper localises to the cell cortex shortly before NEB. Upon NEB it briefly accumulates apically before becoming uniformly cortical. At telophase it becomes restricted to the cleavage furrow. Upon Y-27632 treatment, zipper cortical accumulation is reduced, only becoming apparent at the cleavage furrow. Washout of Y-27632 rescues Zipper localisation defects. **B)** Quantification of Zipper::GFP fluorescence intensity as a ratio of cortex to the cytoplasm. Upon Y-27632 this is significantly reduced. Yellow Circle = mean. Asterisk = Outliers. (n=13). Scale bar: 10µm.

4.6. High concentrations of Y-27632 inhibit aPKC

To understand the role of aPKC after NEB we decided to titrate the concentration of Y-27632 until we observed the aPKC phenotype in cycling cells. Treatment with 200µM Y-27632 resulted in uniformly cortical Miranda (**Fig. 4-5A**; n=12) which was insensitive to Lat-A treatment (**Fig. 4-5B, B'**; n=12). Therefore, high concentrations of Y-27632 result in a similar failure to asymmetrically segregate

Miranda as observed in *apkc* loss of function mutants. This is likely to be due to its direct but unspecific inhibition of aPKC.

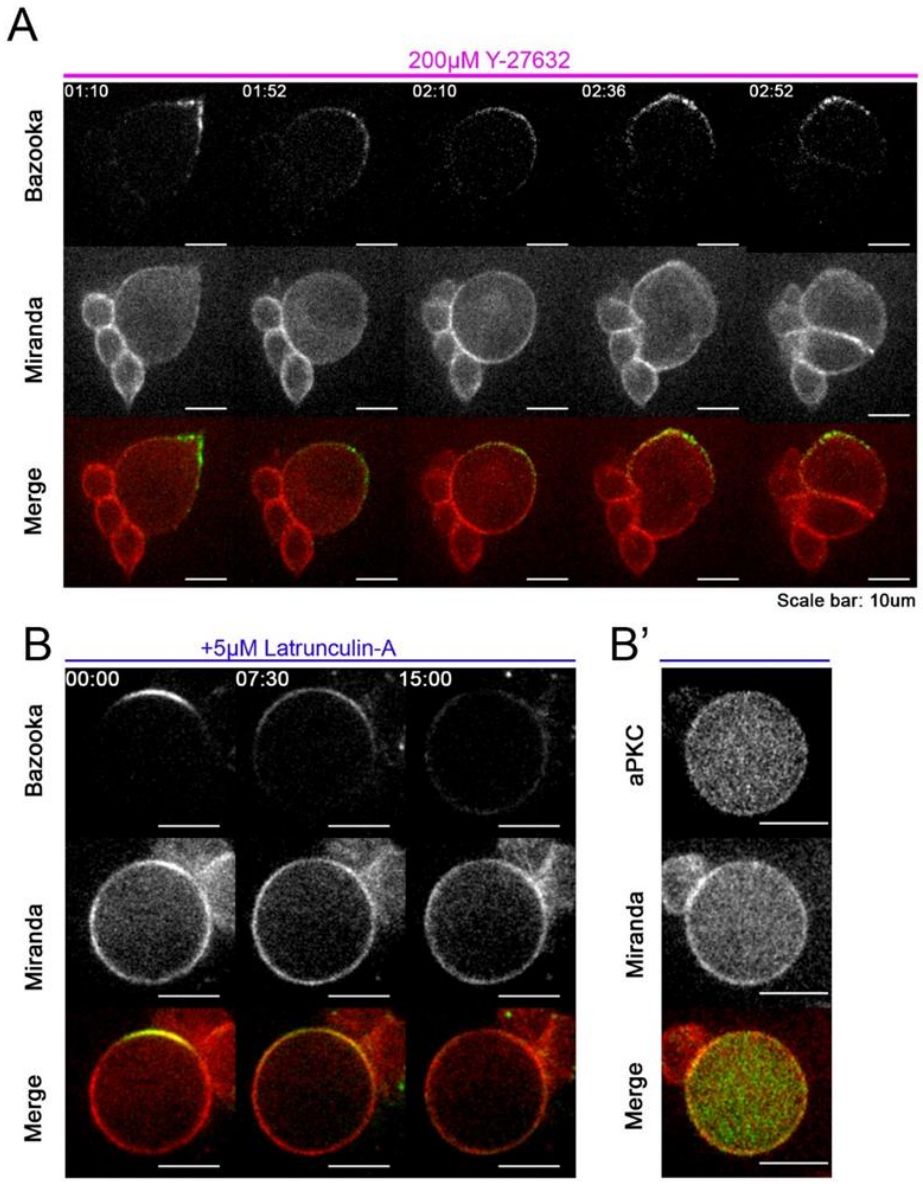

Figure 4-5 - High concentrations of Y-27632 result in the *apkc* phenotype. A) Example isolated NB expressing Baz::GFP (green), Mira::mCherry^{BAC} (red). Cycling in the presence of 200µM Y-27632 results in Miranda localising uniformly to the mitotic NB cortex (2:10). Upon mitosis, size asymmetry is severely altered and Miranda is segregated symmetrically (n=12, 02:36-02:52). **B)** Example isolated colcemid arrested NB expressing Baz::GFP (green) and Mira::mCherry^{BAC} (red). Prior to colcemid arrest NB was cycling in 200µM Y-27632 Uniformly cortical Miranda is insensitive to Lat-A treatment (n=12/12). **B')** aPKC::GFP, Mira::mCherry^{BAC} expressing NB also showing Miranda is insensitive to Lat-A treatment despite aPKC becoming uniformly cortical, similar to Baz. Scale bars: 10um Time stamps: hh:mm

To assay whether aPKC activity was required to maintain cortical polarity we treated Colcemid arrested NBs with 200µM Y-27632. We argued that if aPKC was continuously excluding Miranda from the apical pole, Miranda would spread laterally until it became uniformly cortical. Instead, after ~1hour Miranda began to accumulate uniformly around the cortex, However, most of the protein was still asymmetrically localised (**Fig. 4-6**; n=15).

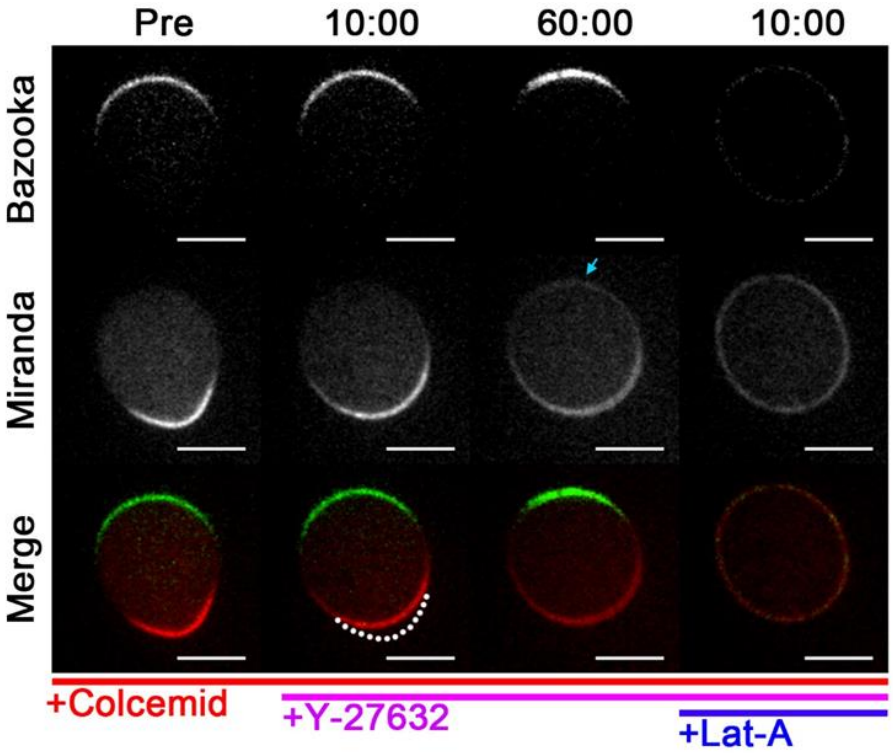

Figure 4-6 - High concentrations of Y-27632 do not result in uniformly cortical Miranda localisation in arrested NBs. Repesentative example of an isolated arrested NB expressing Baz::GFP (green) and Mira::mCherry^{BAC} (red). After the addition of 200µM Y-27632 the cells rounded up (10:00, indicated by white dotted line in the merge). After extended time in Y-27632, faint Miranda signal was detected apically (blue arrow, 60:00), however, asymmetric localisation persisted. Addition of 5µM Lat-A caused Miranda to become uniformly cortical (10:00). Time indicated minutes after addition of Y-27632 or Lat-A. Scale bar: 10µm.

To test whether aPKC was inhibited NBs were treated with Lat-A. This caused the Miranda which was basally localised to spread laterally until it was uniformly

cortical (**Fig. 4-6, 10:00,** n=15). This demonstrates that aPKC appears to be required throughout mitosis to block Miranda localising to the plasma membrane, however, this appears to occur in parallel with the mechanisms localising Miranda to the basal pole, as despite aPKC inhibition, Miranda was enriched at the basal domain. An important caveat of this experiment is that we are inhibiting multiple kinases, so although we have achieved some temporal control of aPKC activity, we have not achieved specificity.

To further investigate the possibility of two, differently regulating binding modes, we set out to generate a *miranda* mutant with which we could separate the interphase and mitotic localisations.

4.7. The BH motif of Miranda is required for localisation in interphase and mitosis

Due to our evidence that Miranda may exhibit two binding modes, one in interphase where it is bound independently of the cytoskeleton and one in mitosis where it is bound in an acto-myosin dependent manner. We hypothesised that mutation of the membrane binding BH motif would block Miranda cortical localisation specifically in interphase.

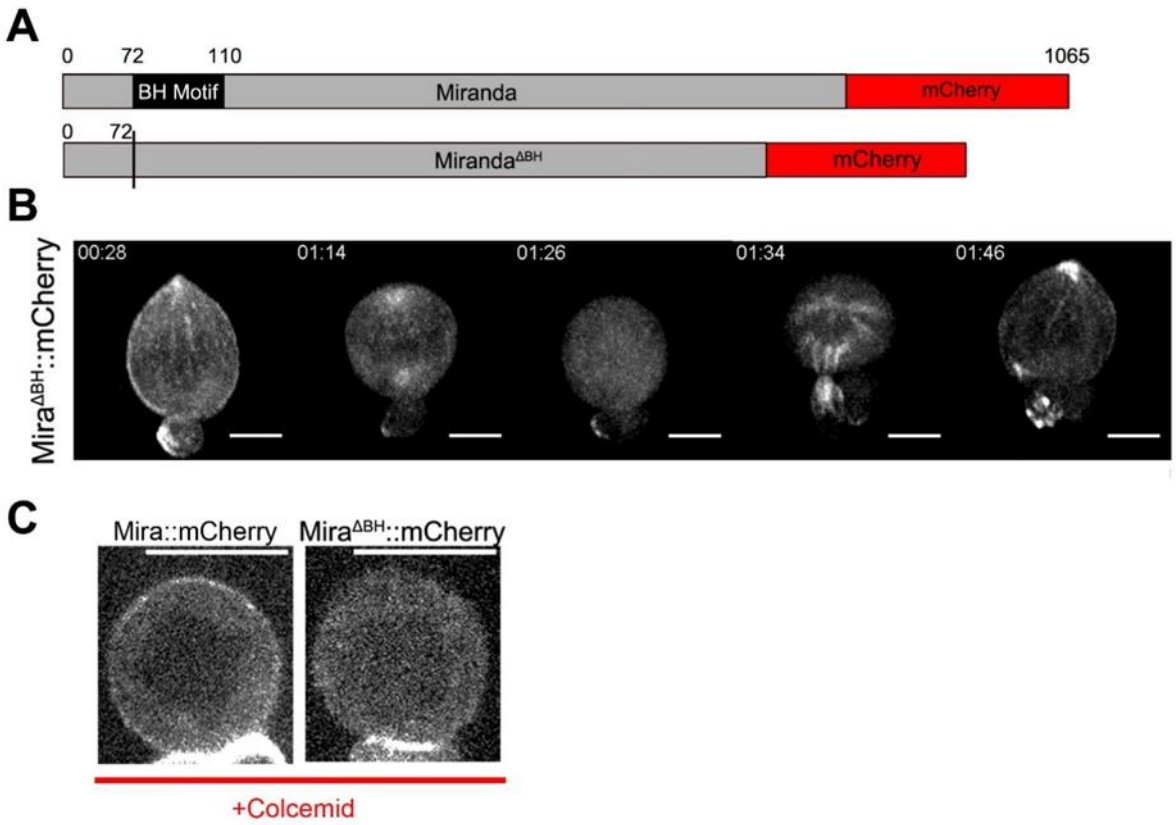

Figure 4-7 - Deletion of Miranda BH motif prevents cortical localisation in NBs. A) Schematic of Miranda gene showing the region coding for the BH motif (aa:72-110, black) To generate *miranda$^{\Delta BH}$::mcherry* these amino acids were deleted and the gene was tagged with mCherry at the C terminus. This variant was then knocked into the Miranda locus. **B)** Example of an isolated NB heterozygous for *mira$^{\Delta BH}$::mcherry*. In interphase (00:28) Mira$^{\Delta BH}$ localised to the microtubule network. Upon NEB the protein was removed from the microtobules and is cytoplasmic (01:26). At telophase it reassociated with the microtubule network (01:34). **C)** Isolated NBs expressing either wild type Mira::mCherry (left) or Mira$^{\Delta BH}$::mCherry (right) were treated with Colcemid to confirm that Mira$^{\Delta BH}$ was bound to the microtubule network. Scale bars: 10µm, time stamp: hh:mm.

Therefore, we utilised the *mira^{attpKO}* (**Fig. 2-1,** (Ramat et al., 2017)) to knock-in *miranda$^{\Delta BH}$::mCherry* containing the previously described deletion of amino acids 72-110 known to be required for membrane interaction (Bailey and Prehoda, 2015) (**Fig. 4-7A**). Live imaging of primary neuroblast cultures heterozygous for *mira$^{\Delta BH}$::mcherry* revealed that during interphase Mira$^{\Delta BH}$::mCherry was localised to the microtubule network (55/55NBs). After NEB, Miranda became cytoplasmic

(55/55 NBs) before re-localising to the microtubules in telophase (**Fig. 4-7B**). This experiment confirmed that the Basic and Hydrophobic motif was required for membrane binding in interphase, however, it was also required for cortical attachment in mitosis. We confirmed that Miranda$^{\Delta BH}$::mCherry was bound to microtubules in interphase by treating cells with Colcemid. In 15/19 cells, cortical signal was lost and Miranda$^{\Delta BH}$::mCherry was cytoplasmic (**Fig. 4-7C**).

4.8. Phospho-mimetic mutation of Serine 96 within the BH motif prevents interphase membrane association of Miranda, but does not prevent basal crescent formation.

To further understand whether Miranda is able to localise to the basal pole independently of mitotic aPKC phosphorylation, we generated a phospho-mimetic mutation in serine 96 of Miranda which was previously shown to be phosphorylated by aPKC and be important for membrane binding (Atwood and Prehoda, 2009; Bailey and Prehoda, 2015) (**Fig. 4-8A**). We hypothesised that Miranda^{S96D}::mCherry would be unable to localise in interphase, due to the loss of Miranda-Membrane binding, however, would be able to localise in mitosis due to binding to the acto-myosin cytoskeleton in the already established Basal domain. This was indeed what we observed. In interphase NBs heterozygous for *mira^{S96D}::mcherry,* Miranda^{S96D} was localised to the cortical microtubules (**Fig. 4-8B, 00:00**; 33/36NBs), similarly to the Miranda$^{\Delta BH}$ mutant, demonstrated by sensitivity to colcemid (**Fig. 4-8D**; 13/20 NBs). In mitosis however, Miranda^{S96D} was still able to form a basal crescent (**Fig. 4-8B, 01:12**; 31/31 NBs).Thus it appeared that we could separate the two binding modes.

Finally, we wanted to test whether the basal localisation of Miranda^{S96D} in mitosis was dependent upon an intact actin network, similar to the wild type protein.

Interestingly, after treatment with 5µM Lat-A, Miranda^{S96D} spread laterally from the basal crescent until it was uniformly cortical (**Fig. 4-8C**; 38/45 NBs). This demonstrates that an intact actin network is required to maintain Miranda^{S96D} in the basal domain, but in the absence of both microtubules and an actin network the mutant is still able to associate with the plasma membrane.

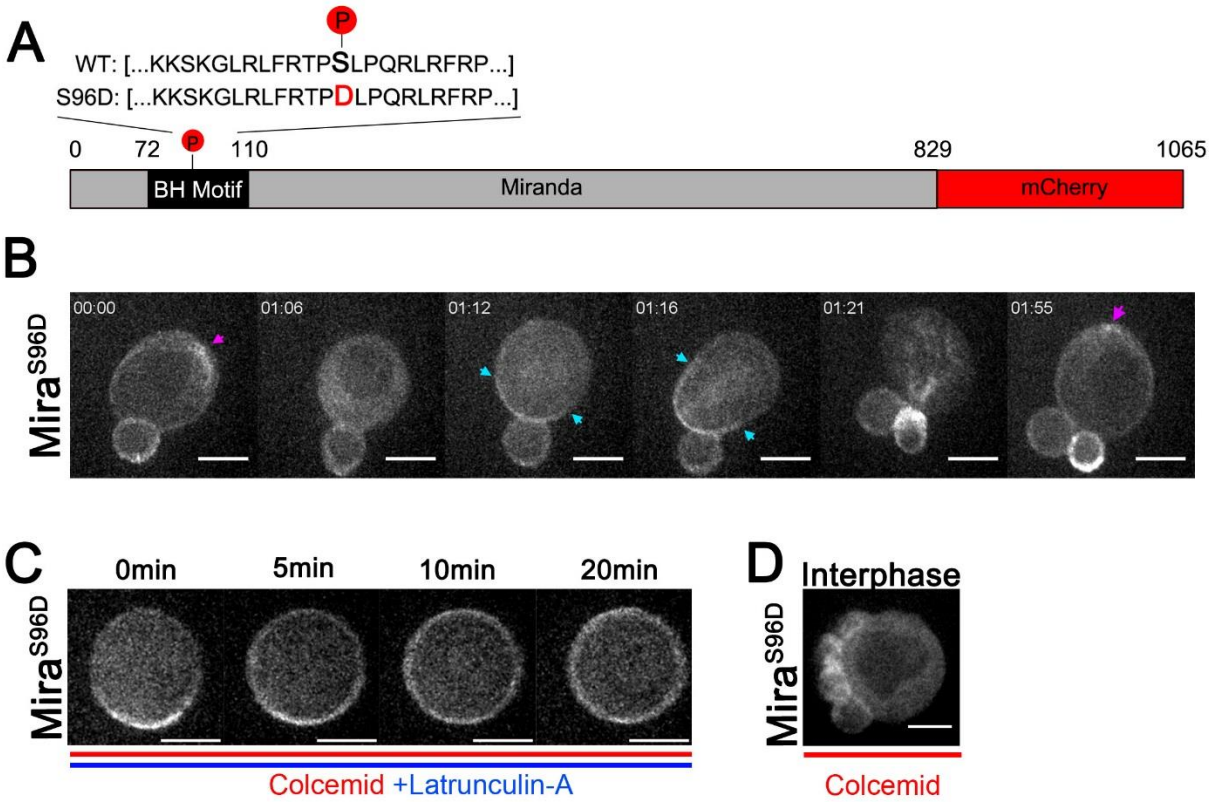

Figure 4-8 - Phospho-mimetic mutation of the BH motif does not prevent mitotic mira crescent formation. A) Schematic showing the site of the Serine to Aspartic Acid mutation in the Mira BH motif. This was tagged with mCherry and knocked into the endogenous locus. **B)** Example image of an isolated NB heterozygous for *mira^{S96D}::mcherry*. Mira^{S96D} localises to the interphase microtubule network (00:00, purple arrow, n=33/36). At NEB it becomes cytoplasmic before forming a basal crescent (01:12, 01:16 blue arrow, n=31/31). Miranda is then asymmetrically segregated, though becomes localised to the microtubule network again at telophase (01:21). **C)** Miranda^{S96D} is still able to bind to the PM in mitosis. Isolated Colcemid arrested NB expressing Mira^{S96D}::mCherry Depolymerisation of F-Actin by Lat-A causes redistribution of Mira^{S96D} from the basal crescent to uniformly cortical localisation (n=38/45). **D)** Image of an isolated NB expressing Mira^{S96D}::mCherry. Interphase localisation of MiraS96D is sensitive to Colcemid (n=13/20). Scale bars 10µm. Time stamp: hh:mm.

These results together demonstrate that the basic and hydrophobic motif is required for localisation of Miranda in interphase and mitosis at the cell cortex. Mimicking phosphorylation of serine96 by the substitution of the serine with an aspartic acid blocked membrane interaction in interphase. However, this mutation did not prevent basal crescent formation. The basal crescent was actin dependent, however, Miranda^{S96D}::mCherry was still able to bind to the plasma membrane in the absence of it.

4.9. MirandaS96D does not rescue aPKC loss of function.

Interestingly, Miranda^{S96D}::mCherry was able to localise to the basal half of the cell in mitosis. We then asked whether the introduction of a negative charge (either by phosphorylation or the aspartic acid mutation) was sufficient to target Miranda to the basal side of the cell in NBs deficient for aPKC activity.

To this end we expressed either aPKC^{RNAi} or Lgl^{3A} along in a background heterozygous for *miranda^{S96D}::mcherry* and assayed for the localisation of Miranda. We speculated that if the introduction of a negative charge to the BH motif of Mira was sufficient to target Miranda to the basal pole of the cell, then Miranda would likely form a basal crescent in the majority of cells, instead of the uniform cortical localisation normally observed in aPKC perturbed cells (Atwood and Prehoda, 2009; Rolls et al., 2003).

However, the S96D mutation resulted in a mild enhancement of uniformly cortical localisation when compared to wild type Miranda::mCherry in Lgl^{3A} expressing NBs (**Fig. 4-9**; WT=12/36, 33%, S96D=11/25, 44%). When aPKC^{RNAi} was used to deplete aPKC, the same trend was observed (**Fig. 4-9**; WT=9/28, 32%, S96D 22/38, 57%). Interestingly, in both control and aPKC perturbed conditions,

Mira^{S96D} signal was higher in the cytoplasm compared to wild type Miranda. This suggests that Mira^{S96D} is both able to interact with the membrane, and the actin dependent basal domain less efficiently than wild type Miranda.

We therefore concluded that the addition of a negative charge to the BH motif of Miranda was alone not sufficient to induce Basal localisation. This demonstrates that aPKC activity is also required for Miranda localisation independently of BH motif phosphorylation. This could occur through two means. It is possible that other aPKC phosphorylation sites outside of the BH motif are required for basal targeting (Atwood and Prehoda, 2009). Alternatively, aPKC could be involved in patterning the cell cortex to generate the basal affinity zone to which Miranda binds. Interestingly, Lgl and Zipper have been shown to interact genetically (Ohshiro et al., 2000; Peng et al., 2000), furthermore, the expression of Lg^{l3A} was shown to reduce Zipper cortical localisation (Barros et al., 2003)

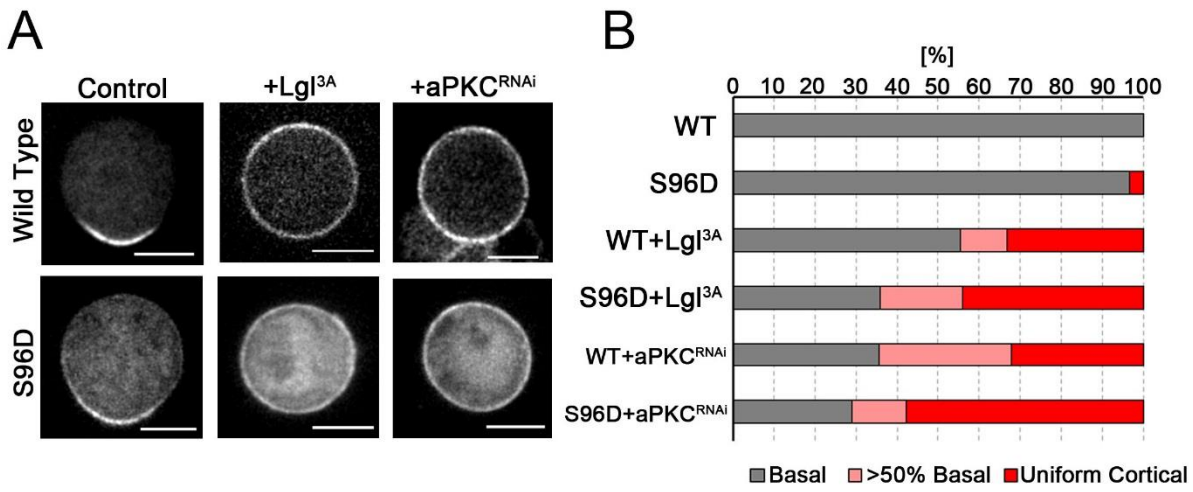

Figure 4-9 - Mira^{S96D} mutation does not rescue aPKC perturbation. A) Representative examples of Colcemid-arrested NBs expressing the indicated UAS transgenes. Miranda localisation was assessed upon aPKC inhibition (+Lgl^{3A}) or knock down (+aPKC^{RNAi}). Expression of Lgl^{3A} and aPKC^{RNAi} results in the uniformly cortical localisation of both wild type Mira::mCherry and MiraS96D::mCherry. **B)** Quantification of phenotypes described in **A**. S96D mutation caused a slight enhancement in the percentage of cells showing uniform cortical localisation of Miranda (red) compared to the control condition. Scale bar: 10µm.

4.10. Phosphorylation of sites outside the BH motif.

The phosphorylation status of Serine 96 is clearly key to regulating the association of Miranda with the plasma membrane via the BH motif. However, previously it was described that Miranda was phosphorylated *in vitro* on four additional residues (194, 195, 205, 206) outside the BH motif (Atwood and Prehoda, 2009) in the predicted coiled coil region of the protein (Shen et al., 1997). It is not known what function these other sites have in regulating Miranda localisation in NBs.

To investigate their potential function, we generated a further three phospho-mimetic knock in mutations for Miranda all tagged with mCherry (**Fig. 4-10A**) which were all analysed as heterozygotes. We mutated these residues as pairs to aspartic acid residues to generate *miranda*^{194195DD}*::mcherry and miranda*^{205206DD}*::mcherry*. Firstly, the localisation of Miranda^{194195DD}::mCherry was analysed (**Fig. 4-10B**; n=22), preventing phosphorylation of this site had previously been implicated in regulating membrane binding in S2 cells (Atwood and Prehoda, 2009). However, our knock in mutation localised as the wild type protein. Secondly, the localisation of Miranda^{205206DD}::mCherry was analysed. Mutation of these sites did not affect Miranda localisation in Interphase or Mitosis (**Fig. 4-10C**; n=24). These data compared to the 96D mutation suggest that although these residues can be phosphorylated *in vitro* they are likely to not be major contributors to Miranda localisation. Although, point mutations in which phosphorylation is prevented at these residues are still to be generated and analysed.

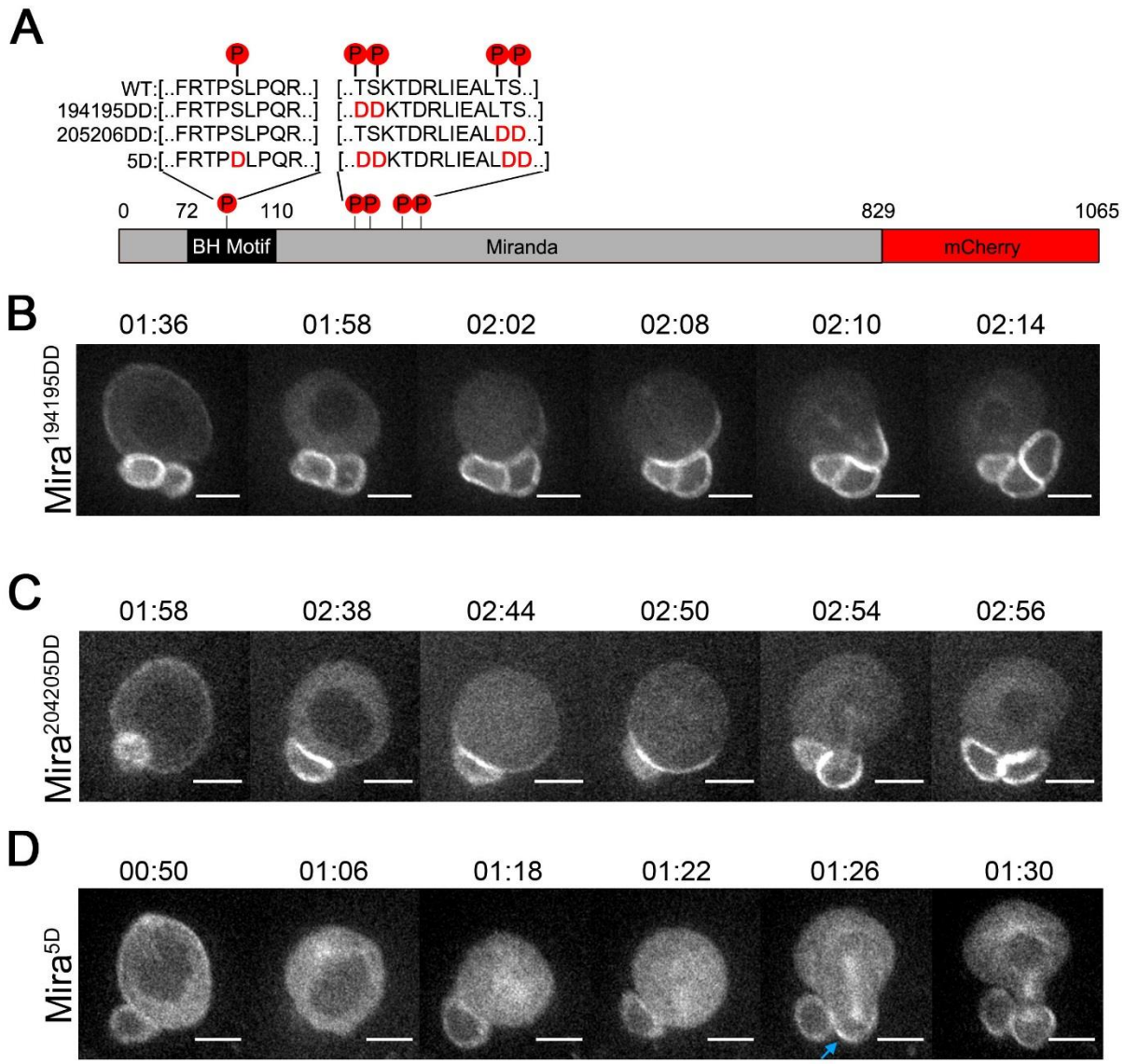

Figure 4-10 - Mutating all aPKC phosphorylation sites in Miranda prevents cortical localisation. A) Schematic showing sites of the phospho-mimetic knock-in proteins coded from the endogenous locus. **B)** Example of a cycling isolated NB expressing Mira^{194195DD}::mCherry. This mutation does not affect Miranda localisation in interphase or mitosis (n=22). **C)** Example of a cycling isolated NB expressing Mira^{205206DD}::mCherry, this mutation does not affect Miranda localisation in interphase or mitosis (n=24). **D)** Example of a cycling isolated NB expressing Mira^{5D}::mCherry. Mira5D localises to the interphase microtubule network (00:50, n=15). Upon NEB it localises in the cytoplasm and to the spindle (01:22, n=15). At telophase it remains on the spindle and localises to the basal pole (blue arrow, 01:26, n=15). Scale bar: 10µm. Time: hh:mm. All mutations were heterozygous.

Finally, we mutated all five described aPKC phosphorylation sites within Miranda to aspartic acid (*miranda^{5D}::mcherry*). This protein had defective localisation in interphase and mitosis (**Fig. 4-10D**; n=15) with Miranda^{5D}::mCherry being localised to the microtubules in interphase and the cytoplasm in mitosis. However, upon telophase Miranda localisation is rescued, localising to the cell cortex of the presumptive GMC and is then asymmetrically segregated, similar to the overexpression of constitutively active aPKC$^{\Delta N}$, suggesting that this mutation represents a situation in which Miranda is ectopically phosphorylated, a scenario not normally achieved *in vivo*. This demonstrates that balancing the phosphorylation of sites within Miranda is essential for ensuring proper Miranda localisation.

4.11. Mislocalisation of aPKC in interphase and mitosis did not prevent basal Miranda localisation.

Lacking a functional method to specifically inhibit aPKC in mitosis, it became necessary to approach the problem of whether aPKC was required once the cell was polarised, from another direction. To this end we decided to conduct an experiment to assay whether the Miranda that localises to the basal cortex in mitosis is sensitive to phosphorylation by aPKC. A recent study generated a series of tools for the mislocalisation of GFP tagged proteins to the apical or basal cell cortex in sensory organ precursor cells (Derivery et al., 2015). This method uses the GFP binding protein (GBP) fused to localisation signals. Partner of numb (pon) is required for the timely localisation of Numb to the basal neuroblast cortex (Lu et al., 1998). By fusing GBP to the localisation domain of Pon it is possible to direct GFP tagged molecules to the basal domain independently of Miranda localisation. We decided to utilise this approach in NBs to specifically mislocalise

a functional aPKC::GFP protein to the basal pole in mitosis. We expected that If Miranda localisation at mitosis is sensitive to phosphorylation, then Miranda should be unable to localise to the basal pole in mitosis. Conversely, if Miranda is insensitive to phosphorylation by aPKC, then we would expect co-localisaiton of Miranda and aPKC at the basal cell cortex (**Fig. 4-11A**).

To test whether this approach works, we first fixed and stained isolated NBs that were either expressing aPKC::GFP alone (control) or aPKC::GFP with GBP::Pon. We observed that both aPKC and its activator Par-6 were mislocalised in mitosis, though still retained an apical bias (**Fig. 4-11B**), likely to be due to the two untagged copies of aPKC still present in this genetic background, which cannot be mislocalised. To assay the effect on Miranda, isolated NBs expressing aPKC::GFP with Mira::mCherry^{BAC} were imaged live once again with and without GBP::Pon. Contrary to control NBs (**Fig. 4-11C**), in 13/14 NBs expressing GBP::Pon (**Fig. 4-11D**), aPKC::GFP was ectopically localised to the apical pole during interphase. This was expected as previously the GBP::Pon localisation domain was shown to be apically enriched in interphase (Derivery et al., 2015). During mitosis, aPKC::GFP was present at the basal pole (although in a lower quantity than at the apical pole) and co-localised with Miranda::mCherry^{BAC} suggesting that at this time point Miranda was insensitive to aPKC::GFP (**Fig. 4-11D**) thought it was possible that the mislocalised aPKC::GFP was inactive.

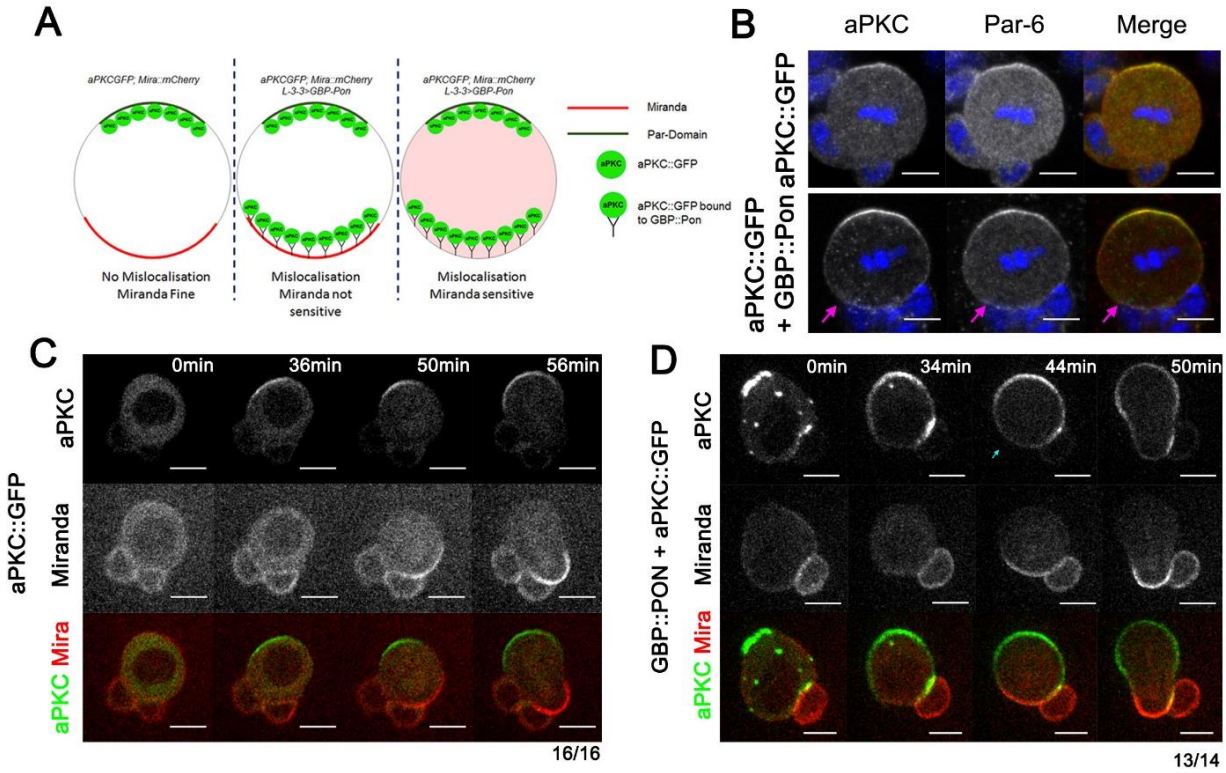

Figure 4-11 - Mislocalisation of aPKC in mitosis does not inhibit Miranda crescent maintenance. A) Schematic of experimental design. Nanobodies are used to mislocalise aPKC::GFP^{BAC} to the basal cell cortex, via the Pon localisation domain fused to GFP binding protein (GBP::Pon). **B)** Representative, fixed isolated metaphase NBs. Immunofluorescence against Par-6 (red) and aPKC (green) demonstrate that an apical bias remains, but both are mislocalised to the basal pole (pink arrow). DAPI was used to label DNA (blue). **C)** Isolated control NB expressing aPKC::GFP^{BAC} and Mira::mCherry^{BAC}. aPKC is apical in mitosis and Miranda is cleared from the membrane at prophase (36min) and forms a basal crescent in mitosis (50min, 16/16 cells). **D)** Isolated NBs expressing aPKC::GFP^{BAC} (green), Mira::mCherry^{BAC} (red) and GBP::Pon. aPKC is mislocalised in interphase, forming an apical cap (0min). In mitosis, aPKC localises all around the cell cortex (blue arrow, 44min), with an apical bias, but Miranda crescents are unaffected (13/14 cells). Scale bars: 10µm.

Previously, localising aPKC to the entire plasma membrane by tagging it with a CAAX prenylation motif (Sotillos et al., 2004) resulted in recognisable phenotypes. Namely, Miranda was cytoplasmic and the brains experienced

tumour like overgrowth and ectopic NB number (Lee et al., 2005). To control for aPKC::GFP activity when mislocalised with GBP, we wanted to test whether mislocalisation of aPKC::GFP to the entire plasma membrane with a CAAX motif (+GBP::CAAX) would replicated the phenotypes observed with aPKC::CAAX overexpression.

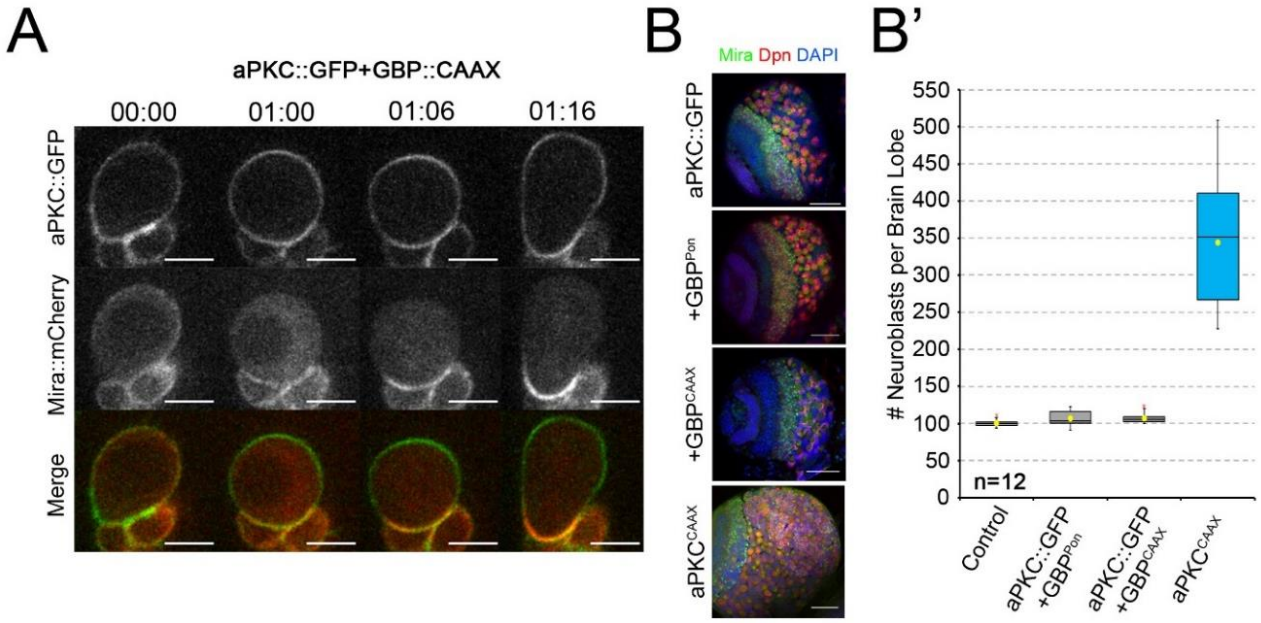

Figure 4-12 - Mislocalisation of aPKC throughout the cell cycle does not affect Miranda Basal crescent formation – A) Example of an isolated NB expressing aPKC::GFP^{BAC} (green), Mira::mCherry^{BAC} (red) and GBP::CAAX. aPKC::GFP^{BAC} was found uniformly dsitributed around the cell cortex throughout the cell cycle. Miranda still localises at the cortex in interphase, then prior to NEB is found in the cytoplasm (01:00). After NEB Miranda forms a basal crescent (01:06). Time: hh:mm, Scale: bar 10µm **B)** Representative images of fixed brain lobes of indicated genotypes stained for Miranda (green), Deadpan (red) and DAPI (Blue). Mislocalisation of aPKC::GFP^{BAC} by either GBP::Pon or GBP::CAAX does not cause altered brain morphology or NB number. aPKC^{CAAX} overexpression however causes tumour like overgrowth of the brain and ectopic NBs. Scale bar: 50µm **B')** Quantification of phenotype described in **B**. NB number was estimated based upon Miranda and Deadpan staining. aPKC::CAAX expression results in a ~4 fold increase in NB number when compared to controls and NBs in which aPKC::GFP was mislocalised by GBP::Pon or GBP::CAAX. 12 lobes were analysed per genotype.

However, isolated NBs expressing GBP::CAAX with aPKC::GFP^{BAC}, and Mira::mCherry^{BAC} did not exhibit defects in Miranda localisation despite aPKC::GFP being efficiently mislocalised (**Fig. 4-12A,** 12/12 NBs). Furthermore, immunofluorescence against the NB markers Deadpan (Dpn) and Miranda revealed that the mislocalisation of aPKC::GFP to the entire cell cortex did not cause overgrowth of the brain or ectopic NBs, though expressing aPKC::CAAX via the same driver did cause a ~four-fold increase in NB number (**Fig. 4-12B B'**, n=12). This suggested that the aPKC::GFP^{BAC} was not active when it was mislocalised. Alternatively, the two remaining wild type copies of aPKC may be masking any observable phenotype caused by the mislocalisation.

4.12. Conclusions

In this chapter we have examined the mechanisms required for retaining Miranda at the basal pole in mitosis. Interestingly, inhibition of Myosin activity by ML-7 treatment resulted in the loss of Miranda from the basal cortex in mitosis, confirming our evidence that Acto-Myosin activity is required for retaining Miranda localisation in mitosis, but not in interphase. It is likely that this is dependent upon the function of Myosin II as we were unable to replicate the *jar* mutant phenotype previously described (Petritsch et al., 2003). Furthermore, phospho-mimetic mutation of Serine96 within the basic and hydrophobic motif, prevented localisation of Miranda in interphase, but not mitosis. These data support our hypothesis that aPKC phosphorylation of Miranda is predominantly required to clear Miranda from the cortex prior to nuclear envelope breakdown and may not be directly involved in regulating Miranda localisation in mitosis.

5. Discussion

5.1. Introduction

Drosophila neuroblasts (NBs) polarise along the apical to basal axis to segregate fate determinants into one of two daughter cells upon cell division. This cell, known as the GMC then goes on to differentiate. Despite being studied for over two decades, how these fate determinants become asymmetrically localised throughout mitosis is still not understood. Improper segregation of fate determinants can lead to tumour like overgrowth of the tissue.

In this study we reinvestigated *in vivo* the polarisation of the cell cortex in *Drosophila* NBs. The most widely accepted model known as the phospho-relay model focussed on the direct phosphorylation of a Basic and Hydrophobic (BH) membrane binding motif by the serine/threonine kinase aPKC (Atwood and Prehoda, 2009; Bailey and Prehoda, 2015). Due the restriction of aPKC to the apical cortex as part of the par-complex, aPKC excludes Miranda and Numb from the apical cortex, thereby resulting in their basal localisation. This would therefore result in a similar mechanism as that used in the *C. elegans* zygote (Goehring et al., 2011a).

An early observation that we made was that while in the *C. elegans* zygote the anterior and posterior domains are maintained by their mutual inhibition resulting in an overlapping boundary region (Goehring et al., 2011a), in the NB there appeared to be a sizeable gap between the apical and basal domain (**Fig 3-1**). It is important to note that a difference in fluorescent intensity profile alone does not constitute a difference in the regulation of these protein complexes. Indeed, one of the main limiting factors of fluorescent microscopy is the limit to what number

of fluorescent molecules are able to be detected. It is possible that a low number of proteins are present at the cell cortex which we have specified as being a gap between the apical and basal domain which we cannot observe over the population present in the cytoplasm. If such a low level of protein is present at the cell cortex it could change the results such that a model similar to the *C.elegans* embryo is likely to be present.

However, it is important to note that there is one key differences between the *Drosophila* NB and the *C. elegans* zygote. In *C. elegans* mutual inhibition between the anterior and posterior par-proteins is required to maintain the anterior-posterior boundary. However, in *Drosophila* NBs, no regulatory interaction from the basal protein complexes to the apical has been identified.

Furthermore, previous work has demonstrated that the actomyosin cytoskeleton is essential for the asymmetric localisation of these proteins (Barros et al., 2003; Broadus and Doe, 1998), a feature not integrated into the BH motif phospho-relay model (Atwood and Prehoda, 2009; Bailey and Prehoda, 2015). We therefore re-examined the contributions of aPKC and the acto-myosin cytoskeleton in a temporally precise manner using the live imaging of endogenous fluorescent polarity reporters.

5.2. The localisation of BH-motif containing proteins in interphase and mitosis is not conducive to a phospho-relay model of polarity establishment and maintenance.

Interestingly, three proteins involved in NB polarity contain a BH motif which is known to be phosphorylated by aPKC. These are Miranda, Numb and Lethal Giant Larvae (Lgl) (Bailey and Prehoda, 2015; Dong et al., 2015). However, all

three localise to different patterns in mitosis: Miranda forms a broad crescent, the intensity of which plateaus, Numb forms a narrower crescent (**Fig. 5-1)**, and Lgl localises to the cytoplasm (Bell et al., 2015). This alone demonstrates that further regulatory mechanisms are required to specify their localisation. For Lgl this is quite well understood. As well as being phosphorylated by aPKC, Lgl is also phosphorylated by Aurora A (Brain, 2015). This phosphorylation by Aurora-A results in cytoplasmic Lgl through mitosis, while in interphase it localises uniformly to the cell cortex (Bell et al., 2015).

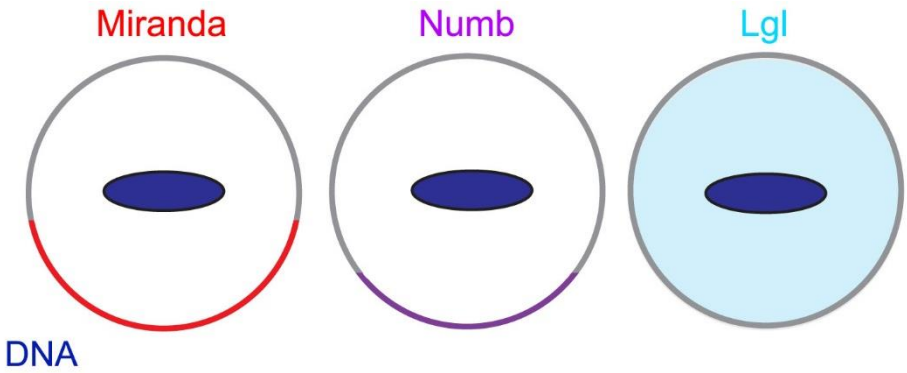

Figure 5-1 – BH motif containing proteins all localise differently in mitotic neuroblasts. Despite being all targets of aPKC phosphorylation, Miranda, Numb and Lgl show different localisation patterns. More specifically, Miranda (Red) forms a broad basal crescent, dependent upon the actin cytoskeleton. Numb (Magenta) forms a narrow basal crescent, also dependent upon Partner of Numb (Pon, not depicted). Lgl (Blue) is cytoplasmic due to the activity of Aurora-A kinase.

Numb and Miranda also utilise different mechanisms to localise basally. Numb binds to an adaptor protein known as Partner of Numb (Pon (Lu et al., 1998)). Pon is not essential for Numb asymmetric localisation, as mutation of Pon only results in a delay in the localisation of Numb to a basal crescent (Lu et al., 1998). Pon mutation has no effect on the localisation of Miranda (Lu et al., 1998). Furthermore, the mitotic kinase Aurora-A has been shown to be required for the asymmetric localisation of Numb, but not Miranda. This is particularly interesting,

as in the *aurora-a* mutant background observed, aPKC was also mislocalised, with no apparent effect on Miranda localisation (Wang et al., 2006).

Miranda relies upon the activity of the Protein phosphatase 4 (PP4) complex for timely localisation in *Drosophila* NBs. Mutation in this complex only delays Miranda basal localisation and does not affect Numb localisation (Sousa-Nunes et al., 2009). This was shown to revolve around the regulation of threonine 591, the function of which is not known, but is independent of aPKC (Zhang et al., 2015).

A further level of Miranda protein regulation has recently been identified to be conferred by the localisation of its mRNA. *mira* mRNA was recently shown by smFISH and MS2-MCPGFP live imaging to co-localise with Miranda protein at the basal pole in NBs. Importantly, co-immunopreciptation experiments demonstrated that there was an interaction between the Miranda protein complex and *mira* mRNA. Finally, genetic studies confirmed that Miranda protein was required for *mira* mRNA localisation, however, the mislocalisation of the mRNA to the apical pole resulted in Miranda protein becoming uniformly cortical (Ramat et al., 2017).

How does *mira* mRNA regulate the localisation of the protein? It is possible that localised translation contributes. However, interestingly in a heteroallelic background, *mira* mRNA was able to interact with the protein encoded by the other allele. Demonstrating that this interaction occurs *in trans* (Ramat et al., 2017). This suggested that a positive feedback loop may exist in which Miranda protein and *mira* mRNA interact with each other to maintain a stable complex at the basal pole. An interesting avenue for further investigation is whether the mRNA is able to link multiple Miranda protein complexes at the basal pole, in a

manner that is not strong enough to detect by immunoprecipitation. These kind of molecular complex assembly could result in the stable localisation of a much larger Miranda complex than we are currently aware of too the basal pole. Alternatively, the recruitment of translational machinery couple to the localised translation of Miranda protein could be contributing to stable Miranda protein localisation at the basal cell cortex.The mechanistic differences between Miranda and Numb are likely reflected in the difference in localisation of Miranda and Numb we observed in isolated mitotic NBs (**Fig. 3-1**).

These differences in localisation demonstrate that localisation is more complicated than the elegant phospho-relay model which has been generated predominantly through the use of *Drosophila* S2 cells which are not asymmetrically dividing and therefore are likely to be a valuable, simplified model but one which will not allow the complete understanding of asymmetric cell division (Atwood and Prehoda, 2009; Bailey and Prehoda, 2015; Zhang et al., 2015).

To gain a better understanding of how NBs polarise, we focussed on the localisation of Miranda and utilised live cell imaging to image isolated NBs polarising with fluorescent reporters for Bazooka, Miranda and aPKC. Interestingly, we observed what appeared to be two stages in Miranda localisation. Miranda was almost completely removed from the interphase plasma membrane during prophase, before returning to form a basal crescent after NEB (**Fig. 3-2**). This was not what we expected, instead we expected Miranda to be cleared from the apical side of the cell cortex as aPKC localised, and then restricted to the basal half. However, given that Miranda is completely cleared, and then returns, with no overlap between the domains, this suggests that before

and after NEB there are properties of Miranda cortical association that are different. Indeed, FRAP analysis confirmed that Miranda in control mitotic cells is much less dynamic than in interphase, quantitatively demonstrating a difference in regulation (**Fig. 3-11**).

5.3. Differential Requirement of the F-Actin network in interphase and mitosis

Previously, the actin cytoskeleton was shown to be key for Miranda cortical localisation in mitosis (Broadus and Doe, 1998; Shen et al., 1997). We asked whether the requirement of the actin cytoskeleton was different between interphase and mitosis. Interestingly, we found that the clearance of Miranda from the interphase cortex at prophase was independent of F-Actin. However, Miranda fails to form a basal crescent at metaphase. Furthermore, the addition of Lat-A to arrested NBs demonstrated that maintenance of the basal crescent is dependent upon an intact F-Actin network.

Previously, Miranda has been shown to directly interact with the actomyosin cytoskeleton (Petritsch et al., 2003; Sousa-Nunes et al., 2009). Furthermore, mutations for the myosin regulatory light chain (*spaghetti squash, sqh*) resulted in Miranda localising to the mitotic spindle and failure to correctly polarise in embryonic NBs (Barros et al., 2003). We observed the same when we treated cells with the myosin light chain kinase inhibitor ML-7 (**Fig. 4-1**). ML-7 caused a failure to establish the basal domain, but did not affect clearance dynamics. It also caused loss of basal Miranda localisation in already polarised cells similar to Lat-A depletion of the actin cytoskeleton (**Fig. 3-4**). Interestingly, this is the opposite to what is observed in *C. elegans* where the acto-myosin cytoskeleton

is required to establish asymmetry, but is dispensable for its maintenance (Goehring et al., 2011a; Hill and Strome, 1988).

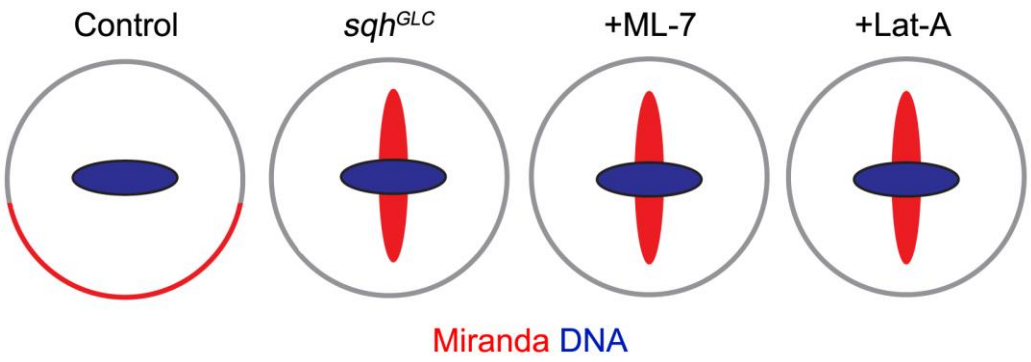

Figure 5-2 - Disruption of the acto-myosin cytoskeleton consistently results in Miranda mislocalisation during mitosis. In control cells Miranda (red) localises to a basal crescent at metaphase (wild type). However, following mutation (*sqh*^{GLC}) or inhibition of activity (+ML-7) of the Myosin regulatory light chain, or following loss of the F-Actin cytoskeleton (+LatA), Miranda becomes mislocalised to the mitotic spindle (Barros et al., 2003).

It is possible that the loss of Miranda upon Latrunculin-A treatment could be due to the spread of the Par-complex, resulting in aPKC being able to phosphorylate Miranda at the basal pole. Importantly however, careful analysis demonstrated that Miranda is lost uniformly, contrary to the expected pattern of loss if aPKC was phosphorylating Miranda as it spread from the apical side to the basal side (**Fig. 3-4**). Furthermore, following ML-7 treatment, although Miranda is lost from the cortex the Par complex remains at the apical pole (**Fig. 4-1**).

5.4. Functions of aPKC after Nuclear Envelope Breakdown

So what of the role for aPKC. *apkc* mutants result in the uniform cortical localisation of Miranda in mitosis (Rolls et al., 2003). This phenotype is also observed in mutants which prevent the phosphorylation of the Miranda BH motif

demonstrating that the direct phosphorylation of Miranda by aPKC is required to establish cortical polarity (**Fig. 3-5**, (Atwood and Prehoda, 2009). The dynamics of how Miranda becomes uniformly cortical was not previously understood. We revealed that this phenotype is due to a failure to remove Miranda from the interphase plasma membrane. In *apkc* mutant NBs, Miranda was never cleared from the interphase cortex at prophase (**Fig**. **3-5**), this is likely due to a lack of direct phosphorylation of the BH motif, as mutating the phosphorylated Serine96 (Ser96) in Miranda's BH motif, to an alanine resulted in a failure to clear Miranda as well (**Fig. 3-9**).

To demonstrate that *apkc* mutants resulted in a continuation of Miranda's interphase binding mode, we demonstrated that in NBs expressing $aPKC^{RNAi}$, Miranda is not removed from the cortex upon Lat-A treatment. The same was observed following the inhibition of aPKC by Lgl^{3A} overexpression (Betschinger et al., 2003), with one key difference. Many NBs expressing Lgl^{3A} had asymmetric Miranda localisation in mitosis (**Fig. 3-8**). However, following Lat-A treatment, rather than being removed from the cell cortex, Miranda is able to spread laterally and occupy the entire plasma membrane. This demonstrates two points of interest. Firstly, F-Actin appears to play a key role in retaining Miranda within the basal crescent. Secondly, in a hypomorphic situation in which Miranda phosphorylation is reduced but not abolished, Miranda is still asymmetrically distributed but remains able to bind the plasma membrane.

The importance for aPKC in establishing cortical polarity is indisputable, but it was not known how important it was in maintaining Miranda asymmetry. Unfortunately a clean method to inhibit aPKC is not yet available. A temperature sensitive allele exists, but does not replicate many of the *apkc* loss of function

phenotypes (Guilgur et al., 2012). Furthermore, experiments involving a temperature shift during live imaging are difficult to control. Therefore, we decided to use the small molecule Y-27632 which typically is used as a Rho kinase (Rock) inhibitor (Uehata et al., 1997), but was previously shown to inhibit aPKC activity *in vitro* (Atwood and Prehoda, 2009). At low concentrations Y-27632 did not affect the maintenance of polarity, but did affect its establishment, resulting in an enlarged basal crescent (**Fig. 4-3**). Furthermore, cell size asymmetry was also affected, with an enlarged GMC cell size. This is interesting, previously placement of cleavage furrow was reported to be myosin dependent and driven by the asymmetric expansion of the apical cell cortex (Cabernard et al., 2010; Connell et al., 2011). However, our evidence suggests that the positioning of the cleavage furrow is linked to basal domain size, and this is structurally encoded prior to NEB. Indeed, recent work has demonstrated that Rho kinase becomes apically enriched at the onset of mitosis (Tsankova et al., 2017).

We wanted to understand whether the enlarged crescent size was due to Myosin inhibition or aPKC inhibition. To test this we examined the dependency of the enlarged Miranda crescent on the F-Actin cytoskeleton. Following Latrunculin-A treatment, Miranda fell off the cortex, suggesting that aPKC was not inhibited by low concentrations of Y-27632 (**Fig. 4-3**). Furthermore, we did affect Myosin dynamics with a reduction in Myosin cortical recruitment (**Fig. 4-4**). A concern with this was that the phenotypes on Miranda were different between Y-27632 and ML-7. Y-27632 resulted in an expansion of the basal domain, while ML-7 resulted in a loss of basal Miranda localisation.

We are not the first to observe different phenotypic outcomes between these two inhibitors. It is possible that these differences arise due to other substrates which

are inhibited. Rock for example has been described in mammalian cells to phosphorylate a whole range of substrates including cell cycle regulators, and actin regulators (Amin et al., 2013). Furthermore, it could be due to differences in the temporal requirement of either kinase in regulating myosin activity.

Previous biochemical analysis showed that Y-27632 treatment resulted in more severe reduction of Myosin regulatory light chain (MRLC) phosphorylation than following ML-7 treatment (Prahalad et al., 2003; Watanabe et al., 2006). This is likely to be due to the activity of Rock in phosphorylating MRLC as well as antagonising the myosin phosphatase (MLCP, (Kimura et al., 1996)**,Fig. 5-3**).

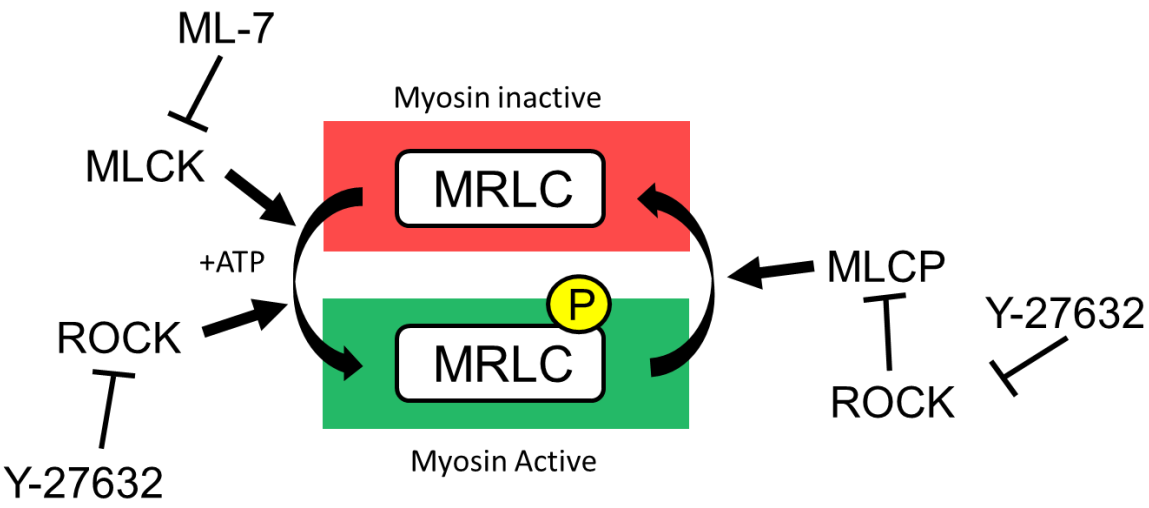

Figure 5-3 - MLCK and ROCK affect Myosin activity through different pathways. MRLC is phosphorylated on two residues to activate Myosin II. These residues can be directly phosphorylated by ROCK and MLCK. Furthermore, Rock antagonises the Myosin phosphatase, therefore promoting the accumulation of phosphorylated MRLC. ML-7 inhibits MLCK thereby inhibiting MRLC phosphorylation. Y-27632 inhibits ROCK, therefore it inhibits phosphorylation of the Myosin Light Chain while also driving dephosphorylation of MRLC by preventing Rock antagonising the MLCP. MRCL = Myosin Regulatory Light Chain, MLCK = Myosin Light Chain Kinase, ROCK = Rho Kinase, MLCP = MLCP, P = Phosphate.

This in itself though is not sufficient to explain the difference in localisation observed. Other work on migratory cell types also encountered a difference in the

contribution of Rock and Myosin Light chain kinase (MLCK) to myosin activity. MLCK inhibition results in more severe defects in cell migration and cell protrusions by blocking phospho-myosin accumulation at the leading edge of migrating cells, which Rock inhibition did not (Totsukawa et al., 2004). This was explained by a spatial difference in the pools of Myosin phosphorylated by these respective kinases (Totsukawa et al., 2000). The authors proposed that ROCK was functioning in the centre of the cell while MLCK was functioning at the cell cortex. Indeed, MLCK localised prominently to the cell cortex. A similar phenomena was observed in zebrafish migratory cells (Lou et al., 2015).

It is possible that a similar phenomenon is occurring in *Drosophila*. In *Drosophila* NBs it is not known what the different contributions are of Rock and MLCK to NB polarity. Recently, the role of Rock in NBs has been investigated as it was observed to accumulate apically at prophase in a manner dependent on the apically localised Partner of Inscuteable (Pins). The apical accumulation of Rock generated an apical bias in the accumulation of phospho-myosin through NEB. However, throughout metaphase this resulted in a gradient of cortical tension which was measured by a sensor taking advantage of Förster resonance energy transfer (FRET) (Tsankova et al., 2017).

FRET can be used to assay how close together two fluorescent proteins are, by measuring a ratio of the intensity of a donor fluorophore and an acceptor fluorophore. The donor fluorophore contributes energy to the excitation of the acceptor, therefore resulting in increased signal of the latter when the donor and acceptor are closer together. This work utilised two actin binding domains couple to mTFP (monomeric turquoise fluorescent protein) and Venus, linked by a flexible series of amino acids. When the sensor is bound to F-Actin at both ends,

and the actin is dense suggesting cortical tension, then the fluorescent proteins are pushed together, resulting in increased FRET signal (Hochreiter et al., 2015; Tsankova et al., 2017).

Measurements of cortical tension through this sensor revealed that following Y-27632 treatment to inhibit Rock, there was a decrease in the cortical tension apically, however it was not largely effected elsewhere (Tsankova et al., 2017). This could explain the difference in phenotypes observed between ML-7 and Rock treatment and would be an interesting direction for further study. Given that ML-7 treatment copies the phenotype previously observed in *sqh* germ line clones (Barros et al., 2003) and can be partially rescued by the over-expression of phospho-mimetic sqh^{EE} we are confident that the effects of ML-7 and Y-27632 are both due to Myosin inhibition, but it likely that this is under temporal and spatial control.

Previously 1mM Y-27632 was shown to result in the *apkc* phenotype of uniformly cortical Mira (Barros et al., 2003; Erben et al., 2008). We wanted to see whether we could take advantage of Y-27632 to test the requirement for aPKC before and after NEB. Indeed, 200µM of Y-27632 resulted in uniformly cortical Mira localisation in mitosis, which is insensitive to Lat-A treatment (**Fig. 4-5**). It is important to note that this phenotype represents both a loss of Myosin function and a loss of aPKC function (as well as likely other kinases due to the unspecific nature of kinase inhibitors).

To investigate the role of aPKC after nuclear envelope breakdown, we arrested the cells and then added 200µM Y-27632. Interestingly, after an hour Mira was not uniformly cortical and was still asymmetrically localised, however, addition of Lat-A then resulted in the spread of Mira to the apical pole, this was remarkably

similar to the effect of Lat-A on Lgl^{3A} expressing cells (**Fig. 3-8, 4-6**). Therefore, when aPKC activity is reduced in mitosis, Miranda can still be asymmetric due the activity of the F-Actin network.

5.5. Role of the BH motif in interphase and mitosis.

The observation that high concentrations of Y-27632 did not cause Miranda to become symmetric after NEB suggested that the BH motif may not be important for mitotic Mira localisation. This is interesting as previous structure-function analysis of Mira demonstrated that the N- terminus of Mira is not sufficient for robust cortical localisation in mitosis (Fuerstenberg et al., 1999), likewise the BH motif is not sufficient for robust cortical localisation in S2 cells (Bailey and Prehoda, 2015). To examine the role of the BH motif in NBs, we generated a deletion of the BH motif and this variant of Mira was found to be bound to the microtubules through interphase and in the cytoplasm through mitosis (**Fig. 4-7**), demonstrating that the BH motif is required for membrane localisation in interphase, and actin-dependent localisation in mitosis. Therefore membrane interaction is possibly important for both localisation modes. Alternatively, the BH motif may be necessary for the direct interaction of Miranda with the actomyosin cytoskeleton (Sousa nunes et al., 2008, Petritsch et al., 2003).

We next analysed the dynamics of a phospho-mimetic Mira mutant for serine 96 ($Mira^{S96D}$). Mira was unable to localise to the interphase plasma membrane, while in mitosis, Mira was still able to form a basal crescent. This appeared to be a separation of function allele, suggesting that phosphorylation by aPKC was not preventing Mira localisation to the basal crescent. However, upon Lat-A treatment, $Mira^{S96D}$ localised to the entire plasma membrane, demonstrating that membrane binding in mitosis was not inhibited (**Fig. 4-8**).

Why did we observe increased affinity for the membrane in mitosis than in interphase? This could be due to a multitude of reasons, but it is possible that the answer lies in the dimerization of Mira. Mira is predicted to form a homodimer through its coiled-coil domain. However, *in vivo* evidence for dimerization is not clear, *in vitro* it is known that the coiled-coil region alone can dimerize (Jia et al., 2015; Yousef et al., 2008). This dimerization could result in an increase in the affinity of the complex for the plasma membrane. Furthermore, it is likely that the S96D mutation does not faithfully replicate the full effect of aPKC phosphorylation. By definition a phosphate provides two negative charges, while an aspartic acid only provides one.

This reduced negative charge of the BH motif perhaps explains why, similar to NBs expressing Lgl^{3A} and those treated with 200µM Y-27632, the actin network is still able to retain Mira at the basal pole (**Fig 5-4**). It is possible that a low level of aPKC activity is required to ensure basal Miranda localisation by increasing Mira's affinity for the basal domain specified by actin-myosin activity compared to the rest of the plasma membrane. Only when the actin cytoskeleton is depleted, is Mira affinity for the plasma membrane visualised by uniform localisation.

Serine 96 is not the only phosphorylation site identified on Miranda. There are four other phosphorylation sites outside of the BH motif which were identified to be phosphorylated by aPKC *in vitro* (Atwood and Prehoda, 2009). Phospho-mimetic mutation of these sites individually did not result in a phenotype on Mira localisation. However, phospho-mimetic mutation of all five did result in Mira mislocalisation (**Fig. 4-10**) in both interphase and mitosis. The same phenotype was observed when a constitutively active form of aPKC is over-expressed (**Fig.**

3-6). Therefore, when all aPKC sites are phosphorylated Mira is unable to localise.

Is this due to a change in binding affinity to the PM? It is possible but interestingly the other four phosphorylation sites are not in the BH motif. The other four phosphorylation sites are found in the region predicted to form a coiled coil (Shen et al., 1997). There is some evidence that phosphorylation can cause a loss of stability in alpha-helices (Szilák et al., 1997). It is possible therefore that phosphorylating all of these residues affects other aspects of the Miranda protein which we do not understand. Unfortunately, to fully understand the role of Mira phosphorylation *in vivo* it is important to understand which of these phosphorylation sites are actually phosphorylated *in vivo* and in which combination. Targeted mutagenesis will then enable the detailed functional analysis of these sites. We attempted to generate a phospho-specific antibody for serine 96, which would have enabled us to conclude whether serine96 phosphorylation prevented basal localisation, however, these attempts were unsuccessful.

It is fascinating that even following reduced aPKC activity or BH motif phosphorylation, Miranda is still asymmetrically localised in a manner dependent upon the actin cytoskeleton (**FIG 5-4)**. This demonstrates that there is a structural element in determining where Miranda is able to localise following NEB, however very little is known about this. To better understand the regulation of the basal domain, we perturbed aPKC activity through RNAi depletion or Lgl^{3A} overexpression in NBs expressing $Mira^{S96D}$. We were interested to see whether in this context, $Mira^{S96D}$ was able to form a basal crescent. Interestingly, it did not. Instead, the S96D mutant was localised uniformly at the cell cortex. aPKC kinase

activity therefore remains important, independently of BH motif phosphorylation. We are unable to specify whether this is due to phosphorylation of the other sites on Mira being important, or whether aPKC acts through another pathway to form the zone to which Miranda binds at the basal pole.

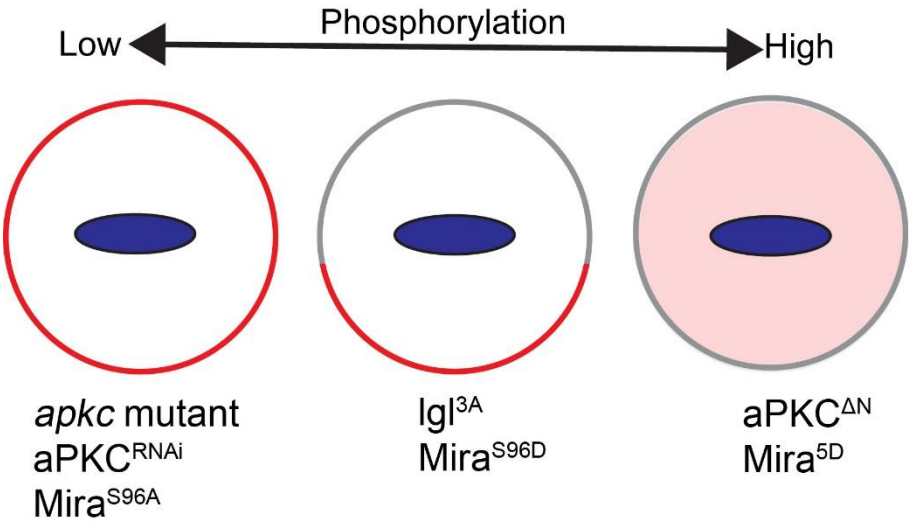

Figure 5-4 - Phosphorylation must be carefully balanced to facilitate asymmetric Miranda localisation. In the absence of any aPKC phosphorylation of serine 96 (*aPKC* loss of function or Mira^{S96A} mutation), Miranda is uniformly cortical in mitosis. This localisation pattern is a continuation of the interphase binding mode, due to the failure to clear Miranda from the cell cortex. Ectopic phosphorylation of Miranda (aPKC$^{\Delta N}$ and Mira^{5D}) results in the loss of Miranda from the cell cortex altogether in metaphase. Medium levels of phosphorylation do not prevent localisation of Miranda to the basal pole (Lgl^{3A}, Mira^{S96D}).

It is possible that phosphorylation of the other sites is important to maintain asymmetry. However, preventing phosphorylation of ser96 (Mira^{S96A}, **Fig. 3-9**) was alone sufficient to prevent Miranda asymmetry. Furthermore, aspartic acid mutation of Ser96 was the only site which alone prevented interphase membrane interaction. Therefore, ser96 is demonstrably the key phosphorylation site regulating Miranda localisation. It is unfortunate that the 96D mutation is still able to bind to the membrane in mitosis, as this prevents us from observing whether

the uniformly cortical localisation in mitosis is due to decreased phosphorylation of the other sites, or whether it is due to the actin dependent binding mode never being established.

Therefore, in the complete absence of aPKC phosphorylation of Miranda, Miranda is localised uniformly to the plasma membrane. Upon phosphorylation, the affinity for the plasma membrane decreases, relative to the acto-myosin dependent affinity to the basal crescent. Upon ectopic phosphorylation, Miranda is unable to localise to the cortex at all.

An interesting observation was that when interphase cortical localisation is affected by deletion of the BH motif, or mutation of Ser96 to aspartic acid, Miranda localises to the microtubule network. Miranda has previously been described to interact with microtubules (Mollinari and Lange, 2002). This is likely mediated by homology observed between the N-terminus of Miranda and the microtubule associated protein receptor for hyaluronan-mediated motility (RHAMM, (Chang et al., 2011)). It is possible that microtubules provides a rescue function when Miranda interphase localisation is ectopically affected.

It is important to note that these Miranda mutants were all analysed as heterozygotes. To be sure that the wild type copy is not rescuing the localisation of the mutant Miranda we would need to conduct clonal analysis due to these mutations being embryonic lethal as homozygotes. However, it is unlikely there is significant rescue by dimerization with the wild type copy as $Mira^{S96A}$, $Mira^{\Delta BH}$ and $Mira^{5D}$ did not form basal crescents.

5.6. aPKC regulation of the cytoskeleton

Has aPKC activity been linked to regulating the cytoskeleton before? Certainly. In *Drosophila* NBs one of the key regulators of aPKC is Lgl. Lg^{l3A} expression has previously been shown to effect Myosin II localisation (Barros et al., 2003). Furthermore, Lgl is known to share a genetic interaction with *zipper* (Ohshiro et al., 2000; Peng et al., 2000). *apkc* mutation is also known to affect cell size asymmetry (Rolls et al., 2003) a feature which is clearly under structural control. In other systems aPKC has also been linked to cytoskeletal regulation. In the preimplantation mouse embryo, as cortical domains establish, aPKC antagonises the accumulation of phosphorylated myosin regulatory light chain. This causes asymmetry of cortical tension at the cell cortex (Maître et al., 2016).

It is likely that aPKC regulates p-myosin accumulation through Lgl. Certainly, Lgl has been shown to directly interact with Myosin II (Strand et al., 1994). Furthermore, phosphorylation of Lgl inhibits the interaction of Lgl with Myosin II (Betschinger et al., 2005). This interaction is known to result in cytoskeletal regulation. Work investigating actin microridges in the apical compartment of zebrafish epithelial cells showed that these microridges were longer when aPKC was depleted. These elongated microridges were dependent upon Lgl and Myosin activity. Indeed, in *apkc* mutants there were elevated levels of p-Myosin in the apical compartment of the epithelia, dependent upon Lgl (Raman et al., 2016).

A clear link between aPKC and the cytoskeleton is through its interaction with Cdc42 (Atwood et al., 2007). In NBs Cdc42 interacts with the Par-complex and mutation in *cdc42* causes a phenotype of striking similarity to that observed in *apkc* mutants. However this was accounted for by failure to correctly localise

aPKC. It is possible that Cdc42 plays a secondary role to structurally compartmentalise the cell cortex. Cdc42 is known to regulate the cytoskeleton through its downstream effectors Arp2/3 and WASP (Nobes and Hall, 1995; Rohatgi et al., 2000; Rohatgi et al., 1999) .

The function of Cdc42 in cytoskeletal polarity has been addressed in other systems. During Meiosis in the mouse oocyte, an actin cap forms in a Cdc42 dependent manner (Zhang et al., 2017). Interestingly, this apical actin enrichment was dependent upon intersectin2. Knockdown of intersectin-2 caused a loss of actin asymmetry. However, this was rescued by constitutively active Cdc42. In *Drosophila*, intersectin is encoded by the gene *dynamin associated protein 160 (dap160).* Mutation in *dap160* causes mislocalisation of the Par-complex and enlarged Miranda crescent size (Chabu and Doe, 2008). This was largely attributed to the regulation of aPKC kinase activity *in vitro* however detailed analysis of aPKC binding sites *in vivo* were not conducted. Due to the role of Cdc42 in regulating aPKC activity, it is challenging to assay whether its function as an actin cytoskeleton regulator is also important for NB asymmetry.

5.7. Role of aPKCs apical localisation before and after NEB.

Due to limitations in our experiments we were unable to conclusively describe the role for aPKC after NEB. Y-27632 although it inhibits aPKC, is not specific and MiraS96D was still able to interact with the plasma membrane. Previously, one of the main bodies of evidence that aPKC excludes Miranda from the cortex is the observation that targeting aPKC uniformly to the cell cortex with a CAAX prenylation motif (Sotillos et al., 2004), results in tissue overgrowth and loss of Miranda cortical localisation (Lee et al., 2005). However, this does not distinguish

between an effect of mislocalising aPKC before, or after nuclear envelope breakdown.

Therefore, we wanted to re-examine the effects of aPKC mislocalisation on Miranda. Specifically, we wanted to bring aPKC to the basal pole, in mitosis. To achieve this we took advantage of the GFP binding protein (GBP) coupled to the localisation domain of the basally localised protein Pon (Derivery et al., 2015). This tool appears to work as we observed both aPKC and Par-6 were mislocalised in mitosis. However, in mitosis Miranda localisation was unaffected (**Fig. 4-11**). Unfortunately, it is unclear whether the aPKC that we have moved to the basal pole is active. To test this we decided to mislocalise aPKC by targeting it uniformly to the membrane using a GBP::CAAX fusion protein. This was successful in mislocalsing aPKC uniformly to the cortex throughout the cell cycle, however, Miranda was still unaffected (**Fig. 4-12**). Furthermore, we did not observe the overgrowth of the brains that is observed following over-expression of aPKC::CAAX (Lee et al., 2005). Therefore, we cannot conclude that mislocalising aPKC::GFP does not have an effect because Miranda is insensitive to its mislocalisation. It could be that the aPKC we mislocalise is just inactive. Furthermore, it could be that the wild type aPKC protein in the background is rescueing any polarity defects we would normally observe.

A second possibility is that the aPKC::CAAX protein upon binding to the membrane causes a change in aPKC conformation. aPKC is normally inhibited by its pseudosubstrate motif (Graybill et al., 2012), it has not yet been tested whether the aPKC::CAAX is actually constitutively active. Clearly, mislocalising an over-expressed, potentially constitutively active protein to the entire cell cortex, is not the same as mislocalising the regulatable protein at near

endogenous levels of expression. Because of this, it would be interesting to repeat these aPKC::GFP mislocalisation experiments in an *apkc* mutant background.

5.8. Controlling the switch between interphase and mitosis

An interesting question is what regulates the switch in binding mode of Miranda at NEB. Previously, the phosphatase PP4 and its interactor Phosphotyrosol phosphatase activator (PTPA) have been implicated in regulating the asymmetric localisation of Miranda in a manner independent of aPKC phosphorylation (Sousa-Nunes et al., 2009; Zhang et al., 2015). It was demonstrated that the PP4/PTPA complex dephosphorylates Miranda on Threonine 591 (T591) in the cargo binding region of the coiled coil structure (Jia et al., 2015; Zhang et al., 2015).

As the PP4/PTPA complex is released from the nucleus upon NEB, phosphatase signalling presented an interesting candidate to explain the switch in binding mode (Sousa-Nunes et al., 2009). To test this we mutated threonine591 to generate a phospho-null ($Mira^{591A}$) and phospho-mimetic ($Mira^{591D}$) construct. We expected the phospho-mimetic to be able to bind to the interphase plasma membrane, but unable to interact with the basal crescent based upon experiments described in the literature (Zhang et al., 2015). Instead, $Mira^{591D}$ was able to localise normally throughout the cell cycle (**Fig. 3-13**). These results

challenge the interpretation of the experiments conducted by Zhang et al., (2015) which relied upon over-expression of mutant transgenes.

The function of T591 phosphorylation was not previously known. Interestingly, Mira^{591A} (which cannot be phosphorylated) exhibited nuclear localisation in interphase. But localised normally in mitosis. To understand this in more detail we need to generate some untagged mutants to examine any developmental phenotypes. This is due to the mCherry tag alone causing lethality at the pupal stage. Furthermore, it would be interesting to look for other threonine kinases which have not yet been described to phosphorylate Miranda.

On the basis of genetic evidence it is still likely that dephosphorylation events by the PP4 complex, independently of aPKC activity, regulates Mira localisation and is key to the switch in binding mode. However, it is not clear whether this is due to a direct effect on Mira or a combination of de-phosphorylation events of multiple proteins which could be downstream of the same phosphatase families. Furthermore, this could act in concert with mitotic kinases of which a series have been implicated in asymmetric cell division, such as Aurora-A, Cdk1 and Polo kinase (Lee et al., 2006a; Tio et al., 2001; Wang et al., 2006; Wang et al., 2007).

5.9. Model of Cortical Asymmetry

From out data we can show that in interphase Miranda is bound uniformly to the cell cortex. This localisation is dependent upon direct interaction with the membrane by Miras BH motif, as described by Bailey and Prehoda (2015). During prophase, the Par-complex assembles at the apical side of the cell. Coincident with this, aPKC becomes active and phosphorylates the BH motif of Miranda. Miranda is then removed from the cell cortex. Prior to NEB, the acto-myosin cell

cortex is also remodelled, defining the zone to which Miranda will localise. This is likely to occur via an asymmetry in Acto-myosin structure, observed through a sensor for cortical tension (Tsankova et al., 2017). This step is also important in determining the size of the GMC.

Upon NEB, Miranda is able to interact with the basal affinity zone, which stabilises the protein basally. Binding of Miranda to the basal affinity zone is likely to be independent of a low level of phosphorylation, but dependent upon the acto-myosin network, which ensures the stable retention of Miranda in the basal crescent (**Fig. 5-5**).

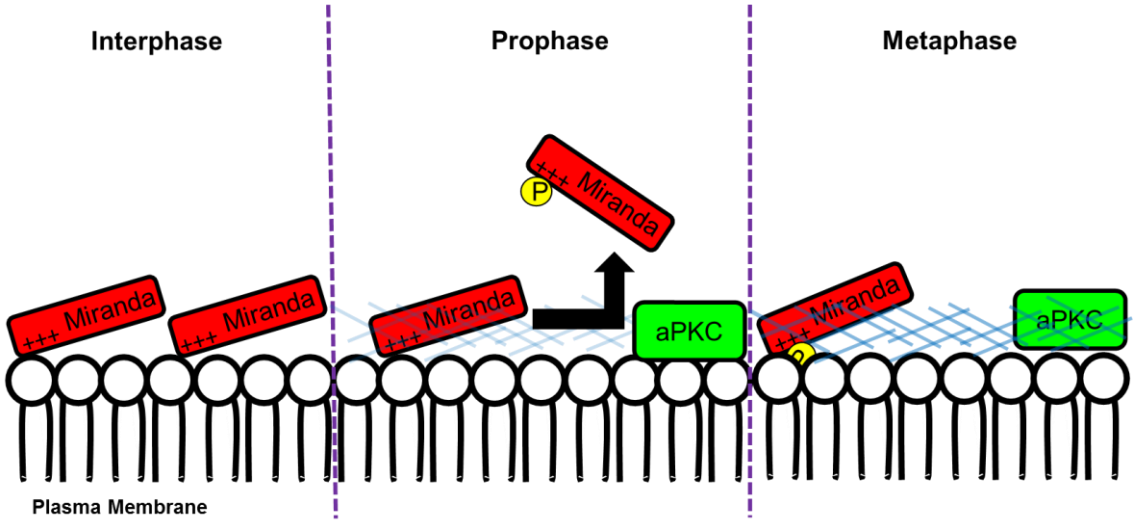

Figure 5-5 - Model for asymmetric localisation of Miranda in mitosis. In interphase, Miranda (red) binds uniformly to the plasma membrane via its BH motif (+++). At the onset of prophase, Miranda becomes phosphorylated (yellow, P) by aPKC (green), preventing the interaction between the BH motif and the phospholipids of the plasma membrane. Concurrently, the acto-myosin cytoskeleton (blue) begins to be remodelled. Following NEB at the onset of Metephase, Miranda is able to localise to the cell cortex again, in a manner dependent upon the acto-myosin cytoskeleton (blue).

5.10. Perspectives and future work

5.10.1. What is the role of interphase Miranda localisation?

Why does this complicated mechanism to control Miranda localisation exist? It is unknown how the NB protects itself from the fate determinants it produces to then segregate into the GMC. Nuclear Prospero (Pros) localisation for example can cause differentiation and cell cycle exit (Lai and Doe, 2014; Maurange et al., 2008). It is possible that Miranda at the interphase cortex is able to sequester these fate determinants, restricting them from functioning in the NB.

The mechanism by which Prospero is prevented from entering the nucleus is unclear. In embryonic NBs, loss of Miranda results in Pros within the nucleus (Ikeshima-Kataoka et al., 1997; Matsuzaki et al., 1998). The activity of Hedgehog signalling and the temporal cascade of transcription factors, particularly grainy head are also required (Chai et al., 2013; Maurange et al., 2008). However, the cell biology underpinning this signalling activity is not clear. It has been suggested that RanGEFBJ1 promotes Prospero nuclear exclusion, but this has not been shown to be a direct effect (Joy et al., 2014).

To better understand the relationship between Miranda and Prospero localisation we can examine the localisation of Prospero in mutants in which Miranda is unable to localise to the cell cortex in interphase. Furthermore, we would expect these mutants to show increased sensitivity to the over-expression of Pros. Clonal analysis of lineage size provides a useful readout for the importance of Miranda interphase cortical localisation.

5.10.2. Is membrane binding important for Miranda localisation in mitosis?

It is yet to be shown that membrane binding is essential for Miranda localisation in mitosis, although it is likely. Structure-function experiments concluded that the N-terminal fragment containing the BH motif is essential for Miranda localisation (Bailey and Prehoda, 2015; Fuerstenberg et al., 1999). Furthermore, deletion of the BH motif results in a loss of Miranda cortical association in interphase and mitosis (**Fig. 4-7**). These together suggest that membrane binding is important. However, the S96D mutant is able to bind to the membrane, yet is still asymmetric, suggesting an alternative binding mode in the basal crescent (**Fig. 4-8**). It is possible that the phenotype observed in the ΔBH mutant is due to loss of interaction with other binding partners.

To address the requirement of membrane binding in mitosis, it is possible to make a less severe mutation, in which the BH motif is neutralised by mutating the basic amino acids to ones of neutral charge. This has previously been done in a study investigating the regulation of Lgl (Dong et al., 2015).

Interaction between the BH motif and the plasma membrane is dependent upon phosphoinositide signalling. Screening regulators of lipid phosphorylation may enable us to further address this question. However, this is likely to effect the integrity of the Par-complex as well due to Bazookas direct interaction with phospholipids (Krahn et al., 2010), therefore it would be difficult to identify how direct the effect is on Miranda localisation.

It may also be beneficial to use small molecules which disrupt membrane charge, and assay the effect this has on cycling and mitotic arrested NBs on Miranda localisation. Ionomycin for example can activate phospholipase C, resulting in a

decrease in membrane phospholipids (Várnai and Balla, 1998) while Phenylarsine oxide specifically depletes PI4P (Hammond et al., 2012). Both of these inhibitors resulted in mislocalisation of Lgl in epithelial cells (Dong et al., 2015). Interestingly, recent work has demonstrated that PI signalling is a key feature of epithelial polarity (Claret et al., 2014).

5.10.3. What is the role for aPKC after NEB

To fully understand the role of aPKC in a temporal manner, we must be able to inhibit the kinase specifically in mitosis. Thus far, a selective inhibitor of aPKC is not commercially available. In this thesis, we attempted to get around this problem by using Y-27632. A major limitation of these experiments though is that Y-27632 is very unspecific.

One way to specifically inhibit a kinase of interest is to sensitize the kinase to enlarged ATP-competitive PP1 analogs. This is known as the gatekeeper strategy (Bishop *et al.,* 2000). Essentially the kinase of interest is mutated to result in an enlarged ATP binding pocket. This approach generates a kinase still able to process ATP, but an enlarged PP1-analog can enter the binding pocket and specifically inhibit the mutated kinase, as it is not able to enter the ATP binding pockets of the other, wild type kinases in the cell (**Fig. 5-6**, (Bishop et al., 2000)).

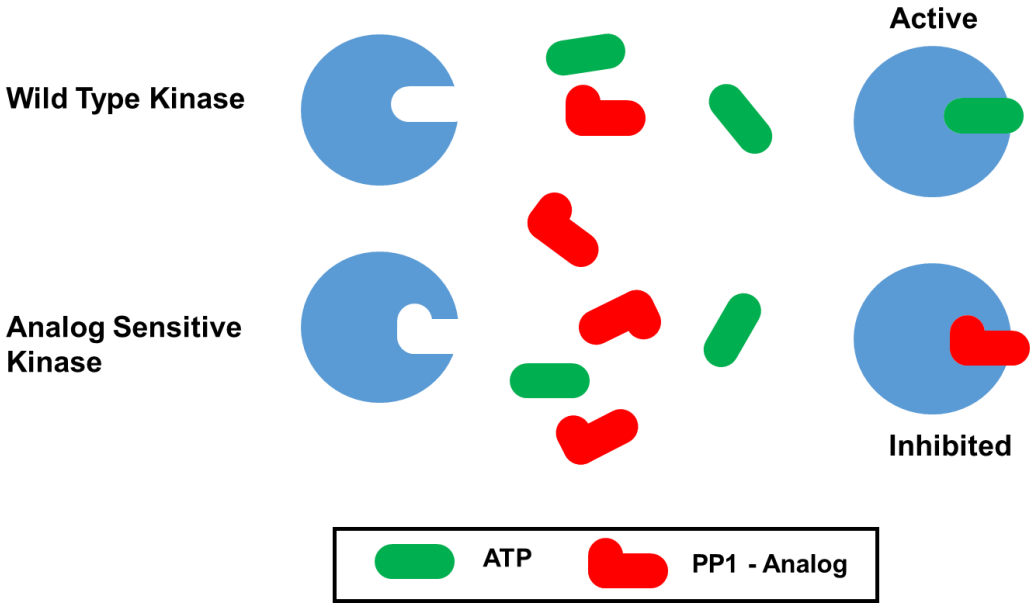

Figure 5-6 - The gatekeeper strategy for inhibiting protein kinases. The mutation of the conserved gatekeeper residue to a smaller amino acid (Isoleucine or Methionine to an alanine or glycine) can cause an enlargement of the ATP binding pocket which enables it to be inhibited by an ATP (green) competitive PP1 analog (red). Due to other kinases smaller ATP binding pockets they should not be inhibited. This can be controlled by comparing the phenotype observed following inhibitor treatment of the analog sensitive kinase, with the phenotype observed following inhibitor treatment of the wild type kinase.

This approach has been widely used in yeast to mutate a range of kinases as well as in mice (Lopez et al., 2014), however has thus far not been used in *Drosophila*. Generating an analog sensitive *apkc* mutant (*apkc*^{AS}) by CRISPR/CAS9 would enable us to answer the question of when aPKC activity is required for cortical polarity.

5.10.4. Temporal Regulation of Cortical Asymmetry

One interesting question is why the cortex polarises during mitosis rather than before. It is thus far unknown what the trigger is for the Par-complex to assemble at the apical pole. Genetic screens have identified a series of mitotic kinases involved in NB polarity including: Cdk1 (Tio et al., 2001), Polo (Wang et al., 2007) and Aurora-A (Lee et al., 2006a; Wang et al., 2006). However, the relative contributions of these kinases to polarising the cell cortex is unclear, most likely because this analysis has been conducted on fixed cells.

To better understand the contribution of these kinases, live cell imaging of isolated NBs expressing polarity markers at endogenous levels, coupled to temporally controlled, small molecule inhibition of these kinases, could allow us to piece together a temporal map of the regulation of asymmetric cell division.

6. Concluding Remarks

In this thesis I have re-examined the relative contributions of the acto-myosin cytoskeleton and the kinase aPKC in the establishment and maintenance of Miranda at the basal pole. I reveal that this process is much more dynamic than thought in the current model. First Miranda is symmetrically localised at the interphase cortex, it is then cleared by the activity of aPKC independently of the actin cytoskeleton. Upon NEB, Miranda localises to a basal crescent in a manner dependent on the actin myosin cytoskeleton, both for regulating the size of the basal domain, and the stabilisation of Miranda at the cell cortex. Therefore, the establishment and maintenance of cortical asymmetry in *Drosophila* neuroblasts are two distinct phases, both temporally and molecularly.

The main impact of this thesis is that it demonstrates the importance of examining the dynamics of how polarity proteins become localised to the patterns then observed in metaphase, as too much information is lost when this is inferred purely from the metaphase phenotype. It also demonstrates that although *Drosophila* S2 cells are a good, simplified, model for understanding the biochemistry of polarity protein interactions, they cannot replace asymmetrically dividing cells themselves.

In summary, *Drosophila* neuroblasts polarise their cell cortex via a highly dynamic mechanism relying upon the combination of aPKC removal from the plasma membrane, and acto-myosin mediated stabilisation of proteins at the basal pole. This is more complex than the existing phospho-relay model, but takes into account important evidence that the current model does not address.

7. References

Albertson, R., Chabu, C., Sheehan, A. and Doe, C. Q. (2004). Scribble protein domain mapping reveals a multistep localization mechanism and domains necessary for establishing cortical polarity. *J Cell Sci* **117**, 6061–6070.

Amin, E., Dubey, B. N., Zhang, S.-C., Gremer, L., Dvorsky, R., Moll, J. M., Taha, M. S., Nagel-Steger, L., Piekorz, R. P., Somlyo, A. V., et al. (2013). Rho-kinase: regulation, (dys)function, and inhibition. *Biol Chem* **394**, 1399–1410.

Arama, E., Dickman, D., Kimchie, Z., Shearn, A. and Lev, Z. (2000). Mutations in the beta-propeller domain of the Drosophila brain tumor (brat) protein induce neoplasm in the larval brain. *Oncogene* **19**, 3706–3716.

Atwood, S. X. and Prehoda, K. E. (2009). aPKC phosphorylates Miranda to polarize fate determinants during neuroblast asymmetric cell division. *Curr Biol* **19**, 723–729.

Atwood, S. X., Chabu, C., Penkert, R. R., Doe, C. Q. and Prehoda, K. E. (2007). Cdc42 acts downstream of Bazooka to regulate neuroblast polarity through Par-6 aPKC. *J Cell Sci* **120**, 3200–3206.

Aughey, G. N. and Southall, T. D. (2015). Dam it's good! DamID profiling of protein-DNA interactions. *Wiley Interdiscip Rev Dev Biol* **5**, 25–37.

Axelrod, D., Koppel, D. E., Schlessinger, J., Elson, E. and Webb, W. W. (1976). Mobility measurement by analysis of fluorescence photobleaching recovery kinetics. *Biophys J* **16**, 1055–1069.

Baena-Lopez, L. A., Alexandre, C., Mitchell, A., Pasakarnis, L. and Vincent, J.-P. (2013). Accelerated homologous recombination and subsequent genome modification in Drosophila. *Development* **140**, 4818–4825.

Bailey, M. J. and Prehoda, K. E. (2015). Establishment of Par-Polarized Cortical Domains via Phosphoregulated Membrane Motifs. *Dev Cell* **35**, 199–210.

Bain, J., McLauchlan, H., Elliott, M. and Cohen, P. (2003). The specificities of protein kinase inhibitors: an update. *Biochem J* **371**, 199–204.

Bajaj, J., Zimdahl, B. and Reya, T. (2015). Fearful symmetry: subversion of asymmetric division in cancer development and progression. *Cancer Res* **75**, 792–797.

Barros, C. S., Phelps, C. B. and Brand, A. H. (2003). Drosophila nonmuscle myosin II promotes the asymmetric segregation of cell fate determinants by cortical exclusion rather than active transport. *Dev Cell* **5**, 829–840.

Beatty, A., Morton, D. and Kemphues, K. (2010). The C. elegans homolog of Drosophila Lethal giant larvae functions redundantly with PAR-2 to maintain polarity in the early embryo. *Development* **137**, 3995–4004.

Bell, G.P., Fletcher, G.C., Brain, R. and Thompson, B.J. (2015). Aurora Kinases Phosphorylate Lgl to Induce Mitotic Spindle Orientation in Drosophila Epithelia. *Curr Biol* **25**, 61.

Bello, B., Reichert, H. and Hirth, F. (2006). The brain tumor gene negatively regulates neural progenitor cell proliferation in the larval central brain of Drosophila. *Development* **133**, 2639–2648.

Besson, C., Bernard, F., Corson, F., Rouault, H., Reynaud, E., Keder, A., Mazouni, K. and Schweisguth, F. (2015). Planar Cell Polarity Breaks the Symmetry of PAR Protein Distribution prior to Mitosis in Drosophila Sensory Organ Precursor Cells. *Curr Biol* **25**, 1104–1110.

Betschinger, J., Eisenhaber, F. and Knoblich, J. A. (2005). Phosphorylation-induced autoinhibition regulates the cytoskeletal protein Lethal (2) giant larvae. *Curr Biol* **15**, 276–282.

Betschinger, J., Mechtler, K. and Knoblich, J. A. (2006). Asymmetric segregation of the tumor suppressor brat regulates self-renewal in Drosophila neural stem cells. *Cell* **124**, 1241–1253.

Betschinger, J., Mechtler, K. and Knoblich, J. A. (2003). The Par complex directs asymmetric cell division by phosphorylating the cytoskeletal protein Lgl. *Nature* **422**, 326–330.

Bishop, A. C., Ubersax, J. A., Petsch, D. T., Matheos, D. P., Gray, N. S., Blethrow, J., Shimizu, E., Tsien, J. Z., Schultz, P. G., Rose, M. D., et al. (2000). A chemical switch for inhibitor-sensitive alleles of any protein kinase. *Nature* **407**, 395–401.

Bondar, T. and Medzhitov, R. (2010). p53-mediated hematopoietic stem and progenitor cell competition. *Cell stem cell* **6**, 309-322.

Bray, S. J. (2016). Notch signalling in context. *Nat Rev Mol Cell Biol* **17**, 722–735.

Broadus, J. and Doe, C. Q. (1998). Extrinsic cues, intrinsic cues and microfilaments regulate asymmetric protein localization in Drosophila neuroblasts. *Curr Biol* **7**, 827–835.

Broadus, J., Fuerstenberg, S. and Doe, C. Q. (1998). Staufen-dependent localization of prospero mRNA contributes to neuroblast daughter-cell fate. *Nature* **391**, 792–795.

Bultje, R. S., Castaneda-Castellanos, D. R., Jan, L. Y., Kriegstein, A. R. and Shi, S.-H. (2009). Mammalian Par3 regulates progenitor cell asymmetric division via notch signaling in the developing neocortex. *Neuron* **63**, 189–202.

Buszczak, M., Paterno, S., Lighthouse, D., Bachman, J., Planck, J., Owen, S., Skora, A. D., Nystul, T. G., Ohlstein, B., Allen, A., et al. (2006). The carnegie protein trap library: a versatile tool for Drosophila developmental studies. *Development* **175**, 1505–1531.

Cabernard, C., Prehoda, K. E. and Doe, C. Q. (2010). A spindle-independent cleavage furrow positioning pathway. *Nature* **467**, 91–94.

Cai, Y., Yu, F., Lin, S., Chia, W. and Yang, X. (2003). Apical complex genes control mitotic spindle geometry and relative size of daughter cells in Drosophila neuroblast and pI asymmetric divisions. *Cell* **112**, 51–62.

Campos-Ortega, J. A. and Hartenstein, V. (1997). *The Embryonic Development of Drosophila Melanogaster*. Springer Verlag.

Casali, A. and Batlle, E. (2009). Intestinal stem cells in mammals and Drosophila. *Cell Stem Cell* **4**, 124–127.

Caussinus, E. and Gonzalez, C. (2005). Induction of tumor growth by altered stem-cell asymmetric division in Drosophila melanogaster. *Nat Genet* **37**, 1125–1129.

Chabu, C. and Doe, C. Q. (2008). Dap160/intersectin binds and activates aPKC to regulate cell polarity and cell cycle progression. *Development* **135**, 2739–2746.

Chabu, C. and Doe, C. Q. (2009). Twins/PP2A regulates aPKC to control neuroblast cell polarity and self-renewal. *Dev Biol* **330**, 399–405.

Chai, P. C., Liu, Z., Chia, W. and Cai, Y. (2013). Hedgehog signaling acts with the temporal cascade to promote neuroblast cell cycle exit. *PLoS Biol* **11**, e1001494.

Chalmers, A.D., Pambos, M., Mason, J., Lang, S., Wylie, C., Papalopulu, N. (2005). aPKC, Crumbs3 and Lgl2 control apicobasal polarity in early vertebrate development. *Development* **132**, 977-986.

Chang, C.-W., Nashchekin, D., Wheatley, L., Irion, U., Dahlgaard, K., Montague, T. G., Hall, J. and Johnston, D. S. (2011). Anterior-posterior axis specification in Drosophila oocytes: identification of novel bicoid and oskar mRNA localization factors. *Development* **188**, 883–896.

Cheng, N. (1988). Identification of genes required for cytoplasmic localization in early C. elegans embryos. *Cell* **52**, 311.

Chenn, A. and McConnell, S. K. (1995). Cleavage orientation and the asymmetric inheritance of Notch1 immunoreactivity in mammalian neurogenesis. *Cell* **82**, 631–641.

Choksi, S. P., Southall, T. D., Bossing, T., Edoff, K., de Wit, E., Fischer, B. E., van Steensel, B., Micklem, G. and Brand, A. H. (2006). Prospero acts as a binary switch between self-renewal and differentiation in Drosophila neural stem cells. *Dev Cell* **11**, 775–789.

Cicalese, A., Bonizzi, G., Pasi, C. E., Faretta, M., Ronzoni, S., Giulini, B., Brisken, C., Minucci, S., Di Fiore, P. P. and Pelicci, P. G. (2009). The tumor suppressor p53 regulates polarity of self-renewing divisions in mammary stem cells. *Cell* **138**, 1083–1095.

Claret, S., Jouette, J., Benoit, B., Legent, K. and Guichet, A. (2014). PI(4,5)P2 produced by the PI4P5K SKTL controls apical size by tethering PAR-3 in Drosophila epithelial cells. *Curr Biol* **24**, 1071–1079.

Colaluca, I. N., Tosoni, D., Nuciforo, P., Senic-Matuglia, F., Galimberti, V., Viale, G., Pece, S. and Di Fiore, P. P. (2008). NUMB controls p53 tumour suppressor activity. *Nature* **451**, 76–80.

Connell, M., Cabernard, C., Ricketson, D., Doe, C. Q. and Prehoda, K. E. (2011). Asymmetric cortical extension shifts cleavage furrow position in Drosophila neuroblasts. *Mol Biol Cell* **22**, 4220–4226.

Cuenca, A. A., Schetter, A., Aceto, D., Kemphues, K. and Seydoux, G. (2003). Polarization of the C. elegans zygote proceeds via distinct establishment and maintenance phases. *Development* **130**, 1255–1265.

Das, R. M. and Storey, K. G. (2014). Apical abscission alters cell polarity and dismantles the primary cilium during neurogenesis. *Science* **343**, 200–204.

Derivery, E., Seum, C., Daeden, A., Loubéry, S., Holtzer, L., Jülicher, F. and Gonzalez-Gaitan, M. (2015). Polarized endosome dynamics by spindle asymmetry during asymmetric cell division. *Nature* **528**, 280–285.

Doe, C. Q., Chu-LaGraff, Q., Wright, D. M. and Scott, M. P. (1991). The prospero gene specifies cell fates in the Drosophila central nervous system. *Cell* **65**, 451–464.

Dong, W., Zhang, X., Liu, W., Chen, Y.-J., Huang, J., Austin, E., Celotto, A. M., Jiang, W. Z., Palladino, M. J., Jiang, Y., et al. (2015). A conserved polybasic domain mediates plasma membrane targeting of Lgl and its regulation by hypoxia. *J Cell Biol* **211**, 273–286.

Edwards, K. A. and Kiehart, D. P. (1996). Drosophila nonmuscle myosin II has multiple essential roles in imaginal disc and egg chamber morphogenesis. *Dev Biol* **122**, 1499–1511.

El-Hashash, A. H. K. and Warburton, D. (2012). Numb expression and asymmetric versus symmetric cell division in distal embryonic lung epithelium. *J Histochem Cytochem* **60**, 675–682.

Elsir, T., Smits, A., Lindström, M. S. and Nistér, M. (2012). Transcription factor PROX1: its role in development and cancer. *Cancer Metastasis Rev* **31**, 793–805.

Erben, V., Waldhuber, M., Langer, D., Fetka, I., Jansen, R. P. and Petritsch, C. (2008). Asymmetric localization of the adaptor protein Miranda in neuroblasts is achieved by diffusion and sequential interaction of Myosin II and VI. *J Cell Sci* **121**, 1403–1414.

Fuerstenberg, S., Peng, C. Y., Alvarez-Ortiz, P., Hor, T. and Doe, C. Q. (1999). Identification of Miranda protein domains regulating asymmetric cortical localization, cargo binding, and cortical release. *Mol Cell Neurosci* **12**, 325–339.

Fuse, N., Hisata, K., Katzen, A. L. and Matsuzaki, F. (2003). Heterotrimeric G proteins regulate daughter cell size asymmetry in Drosophila neuroblast divisions. *Curr Biol* **13**, 947–954.

Gallagher, P. J., Herring, B. P. and Stull, J. T. (1997). Myosin light chain kinases. *J Muscle Res Cell Motil* **18**, 1–16.

Gateff, E. (1978). Malignant neoplasms of genetic origin in Drosophila melanogaster. *Science* **200**, 1448–1459.

Gibson, D. G., Young, L., Chuang, R.-Y., Venter, J. C., Hutchison, C. A. and Smith, H. O. (2009). Enzymatic assembly of DNA molecules up to several hundred kilobases. *Nat Methods* **6**, 343–345.

Goehring, N. W., Hoege, C., Grill, S. W. and Hyman, A. A. (2011a). PAR proteins diffuse freely across the anterior-posterior boundary in polarized C. elegans embryos. *J Cell Biol* **193**, 583–594.

Goehring, N. W., Trong, P. K., Bois, J. S., Chowdhury, D., Nicola, E. M., Hyman, A. A. and Grill, S. W. (2011b). Polarization of PAR proteins by advective triggering of a pattern-forming system. *Science* **334**, 1137–1141.

Goldman, R. D., Spector, D. L. and Masters, B. R. (2006). Live Cell Imaging, A Laboratory Manual. *Journal of Biomedical Optics* **11**, 019901.

Goldstein, B. and Macara, I. G. (2007). The PAR proteins: fundamental players in animal cell polarization. *Dev Cell* **13**, 609–622.

Graybill, C., Wee, B., Atwood, S. X. and Prehoda, K. E. (2012). Partitioning-defective protein 6 (Par-6) activates atypical protein kinase C (aPKC) by pseudosubstrate displacement. *J Biol Chem* **287**, 21003–21011.

Guilgur, L. G., Prudêncio, P., Ferreira, T., Pimenta-Marques, A. R. and Martinho, R. G. (2012). Drosophila aPKC is required for mitotic spindle orientation during symmetric division of epithelial cells. *Development* **139**, 503–513.

Guo, S. and Kemphues, K. J. (1995). par-1, a gene required for establishing polarity in C. elegans embryos, encodes a putative Ser/Thr kinase that is asymmetrically distributed. *Cell* **81**, 611–620.

Hammond, G. R. V., Fischer, M. J., Anderson, K. E., Holdich, J., Koteci, A., Balla, T. and Irvine, R. F. (2012). PI4P and PI(4,5)P2 are essential but independent lipid determinants of membrane identity. *Science* **337**, 727–730.

Hao, Y., Boyd, L. and Seydoux, G. (2006). Stabilization of cell polarity by the C. elegans RING protein PAR-2. *Dev Cell* **10**, 199–208.

Heinemann, F., Vogel, S. K. and Schwille, P. (2013). Lateral membrane diffusion modulated by a minimal actin cortex. *Biophys J* **104**, 1465–1475.

Heissler, S. M., Chinthalapudi, K. and Sellers, J. R. (2015). Kinetic characterization of the sole nonmuscle myosin-2 from the model organism Drosophila melanogaster. *FASEB J* **29**, 1456–1466.

Hill, D. P. and Strome, S. (1988). An analysis of the role of microfilaments in the establishment and maintenance of asymmetry in Caenorhabditis elegans zygotes. *Dev Biol* **125**, 75–84.

Hochreiter, B., Garcia, A. P. and Schmid, J. A. (2015). Fluorescent proteins as genetically encoded FRET biosensors in life sciences. *Sensors (Basel)* **15**, 26281–26314.

Homem, C. C. F., Reichardt, I., Berger, C., Lendl, T. and Knoblich, J. A. (2013). Long-term live cell imaging and automated 4D analysis of drosophila neuroblast lineages. *PLoS ONE* **8**, e79588.

Hope, K. J., Cellot, S., Ting, S. B., MacRae, T., Mayotte, N., Iscove, N. N. and Sauvageau, G. (2010). An RNAi screen identifies Msi2 and Prox1 as having opposite roles in the regulation of hematopoietic stem cell activity. *Cell Stem Cell* **7**, 101–113.

Horvitz, H. R., Sternberg, P. W., Greenwald, I. S., Fixsen, W. and Ellis, H. M. (1983). Mutations that affect neural cell lineages and cell fates during the development of the nematode Caenorhabditis elegans. *Cold Spring Harb Symp Quant Biol* **48 Pt 2**, 453–463.

Hung, T. J. and Kemphues, K. J. (1998). PAR-6 is a conserved PDZ domain-containing protein that colocalizes with PAR-3 in Caenorhabditis elegans embryos. *Development* **126**, 127–135.

Huttner, W. B. and Kosodo, Y. (2005). Symmetric versus asymmetric cell division during neurogenesis in the developing vertebrate central nervous system. *Curr Opin Cell Biol* **17**, 648–657.

Ikeshima-Kataoka, H., Skeath, J. B., Nabeshima, Y., Doe, C. Q. and Matsuzaki, F. (1997). Miranda directs Prospero to a daughter cell during Drosophila asymmetric divisions. *Nature* **390**, 625–629.

Ito, K., Urban, J. and Technau, G. M. (1995). Distribution, classification, and development ofDrosophila glial cells in the late embryonic and early larval ventral nerve cord. *Rouxs Arch Dev Biol* **204**, 284–307.

Ito, T., Kwon, H. Y., Zimdahl, B., Congdon, K. L., Blum, J., Lento, W. E., Zhao, C., Lagoo, A., Gerrard, G., Foroni, L., et al. (2010). Regulation of myeloid leukaemia by the cell-fate determinant Musashi. *Nature* **466**, 765–768.

Jia, M., Shan, Z., Yang, Y., Liu, C., Li, J., Luo, Z.-G., Zhang, M., Cai, Y., Wen, W. and Wang, W. (2015). The structural basis of Miranda-mediated Staufen localization during Drosophila neuroblast asymmetric division. *Nat Commun* **6**, 8381.

Johnston, D. S., Beuchle, D. and Nüsslein-Volhard, C. (1991). Staufen, a gene required to localize maternal RNAs in the Drosophila egg. *Development* **66**, 51–63.

Joshi, P. A., Jackson, H. W., Beristain, A. G., Di Grappa, M. A., Mote, P. A., Clarke, C. L., Stingl, J., Waterhouse, P. D. and Khokha, R. (2010).

Progesterone induces adult mammary stem cell expansion. *Nature* **465**, 803–807.

Joy, T., Hirono, K. and Doe, C. Q. (2014). The RanGEF Bj1 promotes prospero nuclear export and neuroblast self-renewal. *Dev Neurobiol* **75**, 485–493.

Kaltschmidt, J. A., Davidson, C. M., Brown, N. H. and Brand, A. H. (2000). Rotation and asymmetry of the mitotic spindle direct asymmetric cell division in the developing central nervous system. *Nat Cell Biol* **2**, 7–12.

Kim, S., Gailite, I., Moussian, B., Luschnig, S., Goette, M., Fricke, K., Honemann-Capito, M., Grubmüller, H. and Wodarz, A. (2009). Kinase-activity-independent functions of atypical protein kinase C in Drosophila. *J Cell Sci* **122**, 3759–3771.

Kimura, K., Ito, M., Amano, M., Chihara, K., Fukata, Y., Nakafuku, M., Yamamori, B., Feng, J., Nakano, T., Okawa, K., et al. (1996). Regulation of myosin phosphatase by Rho and Rho-associated kinase (Rho-kinase). *Science* **273**, 245–248.

Kleinfeld, R. G. and Sisken, J. E. (1966). Morphological and kinetic aspects of mitotic arrest by and recovery from colcemid. *J Cell Biol* **31**, 369–379.

Knoblich, J. A. (2010). Asymmetric cell division: recent developments and their implications for tumour biology. *Nat Rev Mol Cell Biol* **11**, 849–860.

Knoblich, J. A., Jan, L. Y. and Jan, Y. N. (1995). Asymmetric segregation of Numb and Prospero during cell division. *Nature* **377**, 624–627.

Krahn, M. P., Klopfenstein, D. R., Fischer, N. and Wodarz, A. (2010). Membrane targeting of Bazooka/PAR-3 is mediated by direct binding to phosphoinositide lipids. *Curr Biol* **20**, 636–642.

Kuang, S., Kuroda, K., Le Grand, F. and Rudnicki, M. A. (2007). Asymmetric self-renewal and commitment of satellite stem cells in muscle. *Cell* **129**, 999–1010.

Kuchinke, U., Grawe, F. and Knust, E. (1999). Control of spindle orientation in Drosophila by the Par-3-related PDZ-domain protein Bazooka. *Curr Biol* **8**, 1357–1365.

Kusek, G., Campbell, M., Doyle, F., Tenenbaum, S. A., Kiebler, M. and Temple, S. (2012). Asymmetric segregation of the double-stranded RNA binding protein Staufen2 during mammalian neural stem cell divisions promotes lineage progression. *Cell Stem Cell* **11**, 505–516.

Lai, S.-L. and Doe, C. Q. (2014). Transient nuclear Prospero induces neural progenitor quiescence. *Elife* **3**.

Lee, C.-Y., Andersen, R. O., Cabernard, C., Manning, L., Tran, K. D., Lanskey, M. J., Bashirullah, A. and Doe, C. Q. (2006a). Drosophila Aurora-A kinase inhibits neuroblast self-renewal by regulating aPKC/Numb cortical polarity and spindle orientation. *Genes Dev* **20**, 3464–3474.

Lee, C.-Y., Robinson, K. J. and Doe, C. Q. (2005). Lgl, Pins and aPKC regulate neuroblast self-renewal versus differentiation. *Nature* **439**, 594–598.

Lee, C.-Y., Wilkinson, B. D., Siegrist, S. E., Wharton, R. P. and Doe, C. Q. (2006b). Brat is a Miranda cargo protein that promotes neuronal differentiation and inhibits neuroblast self-renewal. *Dev Cell* **10**, 441–449.

Lee, T. and Luo, L. (1999). Mosaic analysis with a repressible cell marker for studies of gene function in neuronal morphogenesis. *Neuron* **22**, 451–461.

Li, P., Yang, X., Wasser, M., Cai, Y. and Chia, W. (1997). Inscuteable and Staufen mediate asymmetric localization and segregation of prospero RNA during Drosophila neuroblast cell divisions. *Cell* **90**, 437–447.

Lopez, M. S., Kliegman, J. I. and Shokat, K. M. (2014). The logic and design of analog-sensitive kinases and their small molecule inhibitors. *Meth Enzymol* **548**, 189–213.

Lou, S. S., Diz-Muñoz, A., Weiner, O. D., Fletcher, D. A. and Theriot, J. A. (2015). Myosin light chain kinase regulates cell polarization independently of membrane tension or Rho kinase. *J Cell Biol* **209**, 275–288.

Lu, B., Ackerman, L., Jan, L. Y. and Jan, Y. N. (2000). Modes of protein movement that lead to the asymmetric localization of partner of Numb during Drosophila neuroblast division. *Mol Cell* **4**, 883–891.

Lu, B., Rothenberg, M., Jan, L. Y. and Jan, Y. N. (1998). Partner of Numb colocalizes with Numb during mitosis and directs Numb asymmetric localization in Drosophila neural and muscle progenitors. *Cell* **95**, 225–235.

Matsuzaki, F., Ohshiro, T., Ikeshima-Kataoka, H. and Izumi, H. (1998). miranda localizes staufen and prospero asymmetrically in mitotic neuroblasts and epithelial cells in early Drosophila embryogenesis. *Development* **125**, 4089–4098.

Maurange, C., Cheng, L. and Gould, A. P. (2008). Temporal Transcription Factors and Their Targets Schedule the End of Neural Proliferation in Drosophila. *Cell* **133**, 891.

Mavrakis, M., Rikhy, R. and Lippincott-Schwartz, J. (2009). Plasma membrane polarity and compartmentalization are established before cellularization in the fly embryo. *Dev Cell* **16**, 93–104.

Maître, J.-L., Turlier, H., Illukkumbura, R., Eismann, B., Niwayama, R., Nédélec, F. and Hiiragi, T. (2016). Asymmetric division of contractile domains couples cell positioning and fate specification. *Nature* **536**, 344–348.

Mollinari, C. and Lange, B. (2002). Miranda, a protein involved in neuroblast asymmetric division, is associated with embryonic centrosomes of Drosophila melanogaster. *Biol Cell* **94**, 1–13.

Morrison, J. K. and Miller, K. G. (2008). Genetic characterization of the Drosophila jaguar322 mutant reveals that complete myosin VI loss of function is not lethal. *Development* **179**, 711–716.

Motegi, F., Zonies, S., Hao, Y., Cuenca, A. A., Griffin, E. and Seydoux, G. (2011). Microtubules induce self-organization of polarized PAR domains in Caenorhabditis elegans zygotes. *Nat Cell Biol* **13**, 1361–1367.

Munro, E., Nance, J. and Priess, J. R. (2004). Cortical flows powered by asymmetrical contraction transport PAR proteins to establish and maintain anterior-posterior polarity in the early C. elegans embryo. *Dev Cell* **7**, 413–424.

Muller H.A. and Wieschaus, E. (1996). armadillo, bazooka, and stardust are critical for early stages in formation of the zonula adherens and maintenance of the polarized blastoderm epithelium in Drosophila. *J Cell Biol* **134**, 149-163

Ménétrey, J., Bahloul, A., Wells, A. L., Yengo, C. M., Morris, C. A., Sweeney, H. L. and Houdusse, A. (2005). The structure of the myosin VI motor reveals the mechanism of directionality reversal. *Nature* **435**, 779–785.

Nobes, C. D. and Hall, A. (1995). Rho, rac, and cdc42 GTPases regulate the assembly of multimolecular focal complexes associated with actin stress fibers, lamellipodia, and filopodia. *Cell* **81**, 53–62.

Noctor, S. C., Martínez-Cerdeño, V., Ivic, L. and Kriegstein, A. R. (2004). Cortical neurons arise in symmetric and asymmetric division zones and migrate through specific phases. *Nat Neurosci* **7**, 136–144.

O'Connor-Giles, K.M. and Skeath, J.B. (2003). Numb Inhibits Membrane Localization of Sanpodo, a Four-Pass Transmembrane Protein, to Promote Asymmetric Divisions in Drosophila. **5**, 231-243.

Ogawa, H., Ohta, N., Moon, W. and Matsuzaki, F. (2009). Protein phosphatase 2A negatively regulates aPKC signaling by modulating phosphorylation of Par-6 in Drosophila neuroblast asymmetric divisions. *J Cell Sci* **122**, 3242–3249.

Ohshiro, T., Yagami, T., Zhang, C. and Matsuzaki, F. (2000). Role of cortical tumour-suppressor proteins in asymmetric division of Drosophila neuroblast. *Nature* **408**, 593–596.

Orkin, S. H. and Zon, L. I. (2008). Hematopoiesis: an evolving paradigm for stem cell biology. *Cell* **132**, 631–644.

Pampalona, J., Januschke, J., Sampaio, P. and Gonzalez, C. (2015). Time-lapse recording of centrosomes and other organelles in Drosophila neuroblasts. *Methods Cell Biol* **129**, 301–315.

Pece, S., Serresi, M., Santolini, E., Capra, M., Hulleman, E., Galimberti, V., Zurrida, S., Maisonneuve, P., Viale, G. and Di Fiore, P. P. (2004). Loss of negative regulation by Numb over Notch is relevant to human breast carcinogenesis. *J Cell Biol* **167**, 215–221.

Peng, C. Y., Manning, L., Albertson, R. and Doe, C. Q. (2000). The tumour-suppressor genes lgl and dlg regulate basal protein targeting in Drosophila neuroblasts. *Nature* **408**, 596–600.

Petritsch, C., Tavosanis, G., Turck, C. W., Jan, L. Y. and Jan, Y. N. (2003). The Drosophila myosin VI Jaguar is required for basal protein targeting and correct spindle orientation in mitotic neuroblasts. *Dev Cell* **4**, 273–281.

Petronczki, M. and Knoblich, J. A. (2001). DmPAR-6 directs epithelial polarity and asymmetric cell division of neuroblasts in Drosophila. *Nat Cell Biol* **3**, 43–49.

Prahalad, P., Calvo, I., Waechter, H., Matthews, J. B., Zuk, A. and Matlin, K. S. (2003). Regulation of MDCK cell-substratum adhesion by RhoA and myosin light chain kinase after ATP depletion. *Am J Physiol, Cell Physiol* **286**, C693–707.

Qian, X., Goderie, S. K., Shen, Q., Stern, J. H. and Temple, S. (1998). Intrinsic programs of patterned cell lineages in isolated vertebrate CNS ventricular zone cells. *Development* **125**, 3143–3152.

Raman, R., Damle, I., Rote, R., Banerjee, S., Dingare, C. and Sonawane, M. (2016). aPKC regulates apical localization of Lgl to restrict elongation of microridges in developing zebrafish epidermis. *Nat Commun* **7**, 11643.

Ramat, A., Hannaford, M. and Januschke, J. (2017). Maintenance of Miranda Localization in Drosophila Neuroblasts Involves Interaction with the Cognate mRNA. *Curr Biol*.

Rapsomaniki, M. A., Kotsantis, P., Symeonidou, I.-E., Giakoumakis, N.-N., Taraviras, S. and Lygerou, Z. (2012). easyFRAP: an interactive, easy-to-use tool for qualitative and quantitative analysis of FRAP data. *Bioinformatics* **28**, 1800–1801.

Rennstam, K., McMichael, N., Berglund, P., Honeth, G., Hegardt, C., Rydén, L., Luts, L., Bendahl, P.-O. and Hedenfalk, I. (2009). Numb protein expression correlates with a basal-like phenotype and cancer stem cell markers in primary breast cancer. *Breast Cancer Res Treat* **122**, 315–324.

Reya, T., Morrison, S. J., Clarke, M. F. and Weissman, I. L. (2001). Stem cells, cancer, and cancer stem cells. *Nature* **414**, 105–111.

Rodriguez, J., Peglion, F., Martin, J., Hubatsch, L., Reich, J., Hirana, N., Gubieda, A.G., Roffey, J., Riberio Fernandes, A., St Johnston, D., Ahringer, J., Goehring, N.W. (2017). aPKC Cycle between Functionally Distinct PAR Protein Assemblies to Drive Cell Polarity. *Developmental Cell*. **42**, 400-415.

Rohatgi, R., Ho, H. Y. and Kirschner, M. W. (2000). Mechanism of N-WASP activation by CDC42 and phosphatidylinositol 4, 5-bisphosphate. *J Cell Biol* **150**, 1299–1310.

Rohatgi, R., Ma, L., Miki, H., Lopez, M., Kirchhausen, T., Takenawa, T. and Kirschner, M. W. (1999). The interaction between N-WASP and the Arp2/3 complex links Cdc42-dependent signals to actin assembly. *Cell* **97**, 221–231.

Rolls, M. M., Albertson, R., Shih, H.-P., Lee, C.-Y. and Doe, C. Q. (2003). Drosophila aPKC regulates cell polarity and cell proliferation in neuroblasts and epithelia. *J Cell Biol* **163**, 1089–1098.

Roth, M., Roubinet, C., Iffländer, N., Ferrand, A. and Cabernard, C. (2015). Asymmetrically dividing Drosophila neuroblasts utilize two spatially and temporally independent cytokinesis pathways. *Nat Commun* **6**, 6551.

Saitoh, M., Ishikawa, T., Matsushima, S., Naka, M. and Hidaka, H. (1987). Selective inhibition of catalytic activity of smooth muscle myosin light chain kinase. *J Biol Chem* **262**, 7796–7801.

Santoro, A., Vlachou, T., Carminati, M., Pelicci, P. G. and Mapelli, M. (2016). Molecular mechanisms of asymmetric divisions in mammary stem cells. *EMBO Rep* **17**, 1700–1720.

Sato, T., van Es, J.H., Snippert, H.J., Strange, D.E., Vries, R.G., van den Born, M., Barker, N., Shoryer, N.F., van de Wetering, M. and Clevers, H. (2011). Paneth cell constitute the niche for Lgr5 stem cells in intestinal crypts. *Nature* **469**, 415-418.

Savoian, M. S. and Rieder, C. L. (2002). Mitosis in primary cultures of Drosophila melanogaster larval neuroblasts. *J Cell Sci* **115**, 3061–3072.

Schaefer, M., Petronczki, M., Dorner, D., Forte, M. and Knoblich, J. A. (2001). Heterotrimeric G proteins direct two modes of asymmetric cell division in the Drosophila nervous system. *Cell* **107**, 183–194.

Schindelin, J., Arganda-Carreras, I., Frise, E., Kaynig, V., Longair, M., Pietzsch, T., Preibisch, S., Rueden, C., Saalfeld, S., Schmid, B., et al. (2012). Fiji: an open-source platform for biological-image analysis. *Nat Methods* **9**, 676–682.

Schober, M., Schaefer, M. and Knoblich, J. A. (1999). Bazooka recruits Inscuteable to orient asymmetric cell divisions in Drosophila neuroblasts. *Nature* **402**, 548–551.

Schuldt, A. J., Adams, J. H., Davidson, C. M., Micklem, D. R., Haseloff, J., Johnston, D. S. and Brand, A. H. (1998). Miranda mediates asymmetric protein and RNA localization in the developing nervous system. *Genes Dev* **12**, 1847–1857.

Schwamborn, J. C., Berezikov, E. and Knoblich, J. A. (2009). The TRIM-NHL protein TRIM32 activates microRNAs and prevents self-renewal in mouse neural progenitors. *Cell* **136**, 913–925.

Sengupta, A., Duran, A., Ishikawa, E., Florian, M. C., Dunn, S. K., Ficker, A. M., Leitges, M., Geiger, H., Diaz-Meco, M., Moscat, J., et al. (2011). Atypical protein kinase C (aPKCzeta and aPKClambda) is dispensable for mammalian hematopoietic stem cell activity and blood formation. *Proc Natl Acad Sci USA* **108**, 9957–9962.

Shen, C. P., Jan, L. Y. and Jan, Y. N. (1997). Miranda is required for the asymmetric localization of Prospero during mitosis in Drosophila. *Cell* **90**, 449–458.

Shen, C. P., Knoblich, J. A., Chan, Y. M., Jiang, M. M., Jan, L. Y. and Jan, Y. N. (1998). Miranda as a multidomain adapter linking apically localized Inscuteable and basally localized Staufen and Prospero during asymmetric cell division in Drosophila. *Genes Dev* **12**, 1837–1846.

Slack, C., Overton, P. M., Tuxworth, R. I. and Chia, W. (2007). Asymmetric localisation of Miranda and its cargo proteins during neuroblast division requires the anaphase-promoting complex/cyclosome. *Development* **134**, 3781–3787.

Smith, C. A., Lau, K. M., Rahmani, Z., Dho, S. E., Brothers, G., She, Y. M., Berry, D. M., Bonneil, E., Thibault, P., Schweisguth, F., et al. (2007). aPKC-mediated phosphorylation regulates asymmetric membrane localization of the cell fate determinant Numb. *EMBO J* **26**, 468–480.

Sonoda, J. and Wharton, R. P. (2001). Drosophila Brain Tumor is a translational repressor. *Genes Dev* **15**, 762–773.

Sotillos, S., Díaz-Meco, M. T., Caminero, E., Moscat, J. and Campuzano, S. (2004). DaPKC-dependent phosphorylation of Crumbs is required for epithelial cell polarity in Drosophila. *J Cell Biol* **166**, 549–557.

Sousa-Nunes, R. and Somers, W. G. (2013). Mechanisms of asymmetric progenitor divisions in the Drosophila central nervous system. *Adv Exp Med Biol* **786**, 79–102.

Sousa-Nunes, R. and Somers, W. G. (2010). Phosphorylation and dephosphorylation events allow for rapid segregation of fate determinants during Drosophila neuroblast asymmetric divisions. *Commun Integr Biol* **3**, 46–49.

Sousa-Nunes, R., Chia, W. and Somers, W. G. (2009). Protein phosphatase 4 mediates localization of the Miranda complex during Drosophila neuroblast asymmetric divisions. *Genes Dev* **23**, 359–372.

Spana, E. P. and Doe, C. Q. (1995). The prospero transcription factor is asymmetrically localized to the cell cortex during neuroblast mitosis in Drosophila. *Development* **121**, 3187–3195.

Sprague, B. L., Pego, R. L., Stavreva, D. A. and McNally, J. G. (2004). Analysis of binding reactions by fluorescence recovery after photobleaching. *Biophys J* **86**, 3473–3495.

Stine, R.R. and Matunis, E.L. (2013). Stem Cell Competition: finding balance in the niche. *Trends in Cell Biology*. **23**, 357-364.

Strand, D., Jakobs, R., Merdes, G., Neumann, B., Kalmes, A., Heid, H. W., Husmann, I. and Mechler, B. M. (1994). The Drosophila lethal(2)giant larvae tumor suppressor protein forms homo-oligomers and is associated with nonmuscle myosin II heavy chain. *J Cell Biol* **127**, 1361–1373.

Szilák, L., Moitra, J., Krylov, D. and Vinson, C. (1997). Phosphorylation destabilizes alpha-helices. *Nat Struct Biol* **4**, 112–114.

Tabuse, Y., Izumi, Y., Piano, F., Kemphues, K. J., Miwa, J. and Ohno, S. (1998). Atypical protein kinase C cooperates with PAR-3 to establish embryonic polarity in Caenorhabditis elegans. *Development* **125**, 3607–3614.

Tio, M., Udolph, G., Yang, X. and Chia, W. (2001). cdc2 links the Drosophila cell cycle and asymmetric division machineries. *Nature* **409**, 1063–1067.

Tomasetti, C. and Vogelstein, B. (2015). Cancer etiology. Variation in cancer risk among tissues can be explained by the number of stem cell divisions. *Science* **347**, 78–81.

Tomasetti, C., Li, L. and Vogelstein, B. (2017). Stem cell divisions, somatic mutations, cancer etiology, and cancer prevention. *Science* **355**, 1330–1334.

Tosoni, D., Zecchini, S., Coazzoli, M., Colaluca, I., Mazzarol, G., Rubio, A., Caccia, M., Villa, E., Zilian, O., Di Fiore, P. P., et al. (2015). The Numb/p53 circuitry couples replicative self-renewal and tumor suppression in mammary epithelial cells. *J Cell Biol* **211**, 845–862.

Totsukawa, G., Wu, Y., Sasaki, Y., Hartshorne, D. J., Yamakita, Y., Yamashiro, S. and Matsumura, F. (2004). Distinct roles of MLCK and ROCK in the regulation of membrane protrusions and focal adhesion dynamics during cell migration of fibroblasts. *J Cell Biol* **164**, 427–439.

Totsukawa, G., Yamakita, Y., Yamashiro, S., Hartshorne, D. J., Sasaki, Y. and Matsumura, F. (2000). Distinct roles of ROCK (Rho-kinase) and MLCK in spatial regulation of MLC phosphorylation for assembly of stress fibers and focal adhesions in 3T3 fibroblasts. *J Cell Biol* **150**, 797–806.

Tsankova, A., Pham, T. T., Garcia, D. S., Otte, F. and Cabernard, C. (2017). Cell Polarity Regulates Biased Myosin Activity and Dynamics during Asymmetric Cell Division via Drosophila Rho Kinase and Protein Kinase N. *Dev Cell*.

Uehata, M., Ishizaki, T., Satoh, H., Ono, T., Kawahara, T., Morishita, T., Tamakawa, H., Yamagami, K., Inui, J., Maekawa, M., et al. (1997). Calcium sensitization of smooth muscle mediated by a Rho-associated protein kinase in hypertension. *Nature* **389**, 990–994.

Uemura, T., Shepherd, S., Ackerman, L., Jan, L. Y. and Jan, Y. N. (1989). numb, a gene required in determination of cell fate during sensory organ formation in Drosophila embryos. *Cell* **58**, 349–360.

Updike, D. and Strome, S. (2009). P granule assembly and function in Caenorhabditis elegans germ cells. *J Androl* **31**, 53–60.

Vessey, J. P., Amadei, G., Burns, S. E., Kiebler, M. A., Kaplan, D. R. and Miller, F. D. (2012). An asymmetrically localized Staufen2-dependent RNA complex regulates maintenance of mammalian neural stem cells. *Cell Stem Cell* **11**, 517–528.

Várnai, P. and Balla, T. (1998). Visualization of phosphoinositides that bind pleckstrin homology domains: calcium- and agonist-induced dynamic changes and relationship to myo-[3H]inositol-labeled phosphoinositide pools. *J Cell Biol* **143**, 501–510.

del Valle Rodríguez, A., Didiano, D. and Desplan, C. (2011). Power tools for gene expression and clonal analysis in Drosophila. *Nat Methods* **9**, 47–55

Wang, C., Chang, K. C., Somers, G., Virshup, D., Ang, B. T., Tang, C., Yu, F. and Wang, H. (2009). Protein phosphatase 2A regulates self-renewal of Drosophila neural stem cells. *Development* **136**, 2287–2296.

Wang, H., Ouyang, Y., Somers, W. G., Chia, W. and Lu, B. (2007). Polo inhibits progenitor self-renewal and regulates Numb asymmetry by phosphorylating Pon. *Nature* **449**, 96–100.

Wang, H., Somers, G. W., Bashirullah, A., Heberlein, U., Yu, F. and Chia, W. (2006). Aurora-A acts as a tumor suppressor and regulates self-renewal of Drosophila neuroblasts. *Genes Dev* **20**, 3453–3463.

Watanabe, T., Hosoya, H. and Yonemura, S. (2006). Regulation of myosin II dynamics by phosphorylation and dephosphorylation of its light chain in epithelial cells. *Mol Biol Cell* **18**, 605–616.

Wells, A. L., Lin, A. W., Chen, L. Q., Safer, D., Cain, S. M., Hasson, T., Carragher, B. O., Milligan, R. A. and Sweeney, H. L. (1999). Myosin VI is an actin-based motor that moves backwards. *Nature* **401**, 505–508.

Winters, M. J., Lamson, R. E., Nakanishi, H., Neiman, A. M. and Pryciak, P. M. (2005). A membrane binding domain in the ste5 scaffold synergizes with gbetagamma binding to control localization and signaling in pheromone response. *Mol Cell* **20**, 21–32.

Wirtz-Peitz, F., Nishimura, T. and Knoblich, J. A. (2008). Linking cell cycle to asymmetric division: Aurora-A phosphorylates the Par complex to regulate Numb localization. *Cell* **135**, 161–173.

Wodarz, A., Ramrath, A., Grimm, A. and Knust, E. (2000). Drosophila atypical protein kinase C associates with Bazooka and controls polarity of epithelia and neuroblasts. *J Cell Biol* **150**, 1361–1374.

Wodarz, A., Ramrath, A., Kuchinke, U. and Knust, E. (1999). Bazooka provides an apical cue for Inscuteable localization in Drosophila neuroblasts. *Nature* **402**, 544–547.

Wu, J. S. and Luo, L. (2007). A protocol for mosaic analysis with a repressible cell marker (MARCM) in Drosophila. *Nat Protoc* **1**, 2583–2589.

Wu, M., Kwon, H. Y., Rattis, F., Blum, J., Zhao, C., Ashkenazi, R., Jackson, T. L., Gaiano, N., Oliver, T. and Reya, T. (2008). Imaging hematopoietic precursor division in real time. *Cell Stem Cell* **1**, 541–554.

Yousef, M. S., Kamikubo, H., Kataoka, M., Kato, R. and Wakatsuki, S. (2008). Miranda cargo-binding domain forms an elongated coiled-coil homodimer in solution: implications for asymmetric cell division in Drosophila. *Protein Sci* **17**, 908–917.

Yu, F., Cai, Y., Kaushik, R., Yang, X. and Chia, W. (2003). Distinct roles of Galphai and Gbeta13F subunits of the heterotrimeric G protein complex in the mediation of Drosophila neuroblast asymmetric divisions. *J Cell Biol* **162**, 623–633.

Zhang, J., Niu, C., Ye, L., Huang, H., He, X., Tong, W.G., Ross, J., Haug, J., Johnson, T., Feng, J.Q., Harris, S., Wiedemann, L.M., Mishina, Y. and Li, L. (2003). Identification of the haematopoietic stem cell niche and control of the niche size. *Nature* **425.** 836-841.

Zhang, F., Huang, Z.-X., Bao, H., Cong, F., Wang, H., Chai, P. C., Xi, Y., Ge, W., Somers, W. G., Yang, Y., et al. (2015). Phosphotyrosyl phosphatase activator facilitates localization of Miranda through dephosphorylation in dividing neuroblasts. *Development* **143**, 35–44.

Zhang, J., Ma, R., Li, L., Wang, L., Hou, X., Han, L., Ge, J., Li, M. and Wang, Q. (2017). Intersectin 2 controls actin cap formation and meiotic division in mouse oocytes through the Cdc42 pathway. *FASEB J* fj.201700179R.

Zhong, W., Feder, J. N., Jiang, M. M., Jan, L. Y. and Jan, Y. N. (1996). Asymmetric localization of a mammalian numb homolog during mouse cortical neurogenesis. *Neuron* **17**, 43–53.

Zimdahl, B., Ito, T., Blevins, A., Bajaj, J., Konuma, T., Weeks, J., Koechlein, C. S., Kwon, H. Y., Arami, O., Rizzieri, D., et al. (2014). Lis1 regulates asymmetric division in hematopoietic stem cells and in leukemia. *Nat Genet* **46**, 245–252..